Voltage Stability Analysis of a Power System Network Comprising a Nuclear Power Plant

Prepared by:

Dawid John Johannes Boesak

BSKDAW001

Department of Electrical Engineering
University of Cape Town

Prepared for:

Prof. Komla Folly

Faculty of Engineering and the Built Environment
University of Cape Town

September 2018

Submitted to the Department of Electrical Engineering at the University of Cape Town in partial fulfilment of the academic requirements for a Master of Science degree in Nuclear Engineering (Electrical Engineering).

Declaration

1. I know that plagiarism is wrong. Plagiarism is the use of another's work in pretence that it is one's own.

2. I have used the IEEE convention for citation and referencing. Each contribution to, and quotation in, this final year project report from the work(s) of other people has been attributed and has been cited and referenced.

3. This final year project report is my own work.

4. I have not allowed, and will not allow, anyone to copy my work with the intention of passing it off as their own work or part thereof.

5. I know the meaning of plagiarism and declare that all the work in the document, save for that which is properly acknowledged, is my own. This dissertation has been submitted to the Turnitin module (or equivalent similarity and originality checking software) and I confirm that my supervisor has seen my report and any concerns revealed by such have been resolved with my supervisor.

Name: Dawid John Johannes Boesak

Signature: Signed by candidate

Date: 29 January 2019

Acknowledgements

I would like to acknowledge, first and foremost, the will that the Lord Almighty gave me in order to undertake this assignment as part of my journey here one earth; without Him, the completion of this dissertation would not have been possible. Secondly, I would like to thank my wife Bianca and my children Noel and Tyra for the motivation and support they gave me my during the challenging period of my studies.

I would not want to forget my supervisor, Prof. Komla Folly — for whom I have great professional respect, who agreed to take me on as a student. The interactions I had with Prof. Folly really motivated me to look beyond what has been done in the field of power system stability and explore ideas of what I could do differently.

Abstract

As recently as 2016, the performance of South Africa's power utility has shown that it is not resilient enough to withstand the consequences of a power system blackout. Blackouts are defined as being a form of power system instability that can be brought about by a variety of abnormal network scenarios. The most common modes of failure are grouped under the term power system stability. In this dissertation, the different modes of power stability that can affect a nuclear power station will be investigated and discussed. The particular phenomenon that will be focused on, however, is the effect that voltage instability has on the ability of generators and loads to perform their standard functions, thus ensuring a secure power system.

To investigate the effect that voltage instability has on a nuclear power station, this dissertation will look at relevant literature on the topic. In addition, by extracting from common examples of national and international occurrences of voltage stability, this dissertation will record the effects that this phenomenon has on the security of a power system, in particular on nuclear power plants.

To model the network containing a nuclear power plant for the evaluation of voltage stability, the different mathematical models of the generation plant are presented, which include: the automatic voltage regulator, power system stabilizer, governor, nuclear reactor, and excitation system. Also presented are mathematical models of network equipment such as under voltage tap changers and the dynamic loads that are of interest when evaluating voltage stability.

The models used for evaluation of the voltage stability phenomenon affecting a nuclear power plant and the surrounding integrated power system are built in the Digsilent PowerFactory® software. The scenario for evaluation is based on a voltage stability event that occurred around at the Koeberg nuclear power system situated in the Western Cape province on South Africa on 15 October 2003.

It is commonly accepted that voltage stability can be evaluated at a steady state level by performing power versus voltage (PV) analysis to determine the voltage buses vulnerable to voltage collapse, and reactive power versus voltage (QV) analysis to determine the critical reactive devices required to avert a voltage instability event. The scenarios that are evaluated for voltage stability are divided into two sections: i) a PV and QV analysis as per the event that occurred on 15 October 2003 and ii) present-day voltage stability indices for PV and QV if mixed with a generation such as renewable energy sources that include wind, solar, biomass and concentrated solar power (CSPs).

The result reveals the vulnerabilities of the nuclear power plant and the surrounding integrated power system due to a voltage instability event. Some of the solutions proposed include a review of the typical power system protection schemes — such as under and overvoltage detection scheme — that are used. In the study, PV and QV curves provide

good indications of the state of critical busbars and the reactive power reserve margins available before instability can potentially settle in. Simulations confirmed the effectiveness of critical equipment installed in the Western Grid and the effect on their electrical parameters such as torque and the slip on motors.

Key words: Voltage stability, voltage stability indices, PV curves, QV curves, dynamic simulations, integrated power system.

Table of Contents

List of Figures

List of Tables

Chapter 1. Introduction

1.1 Motivation for the study

In recent years, the South African power grid has faced significant operational challenges due to various technical constraints. Adding to the severity of technical challenges has been the persistent expansion of the grid, the addition of power sources such as renewable energy power plants, the nature of the highly interconnected integrated power supply (IPS), and the interdependency this has introduced within the South African generation pool. In considering these factors, one should also take into account the influence of the neighbouring Southern African Development Community on the power utility when considering reactive power requirements and quality of supply indices.

Following widespread load shedding (also referred to as rolling blackouts) in 2008, and more recently in 2014 and 2015, due to a shortage of coal supply to power stations and the unavailability/inability of some power stations to contribute to national needs, a key question that has dominated the public discourse is: To what extent is the current power system robust enough to avoid a total system blackout. In addition, what margins need to be considered at the planning phase and during the day-to-day operations of power plants? Furthermore, prevailing concerns are uncertainty regarding at which stage the power system will not be able to provide the necessary voltage support to keep power activity going and whether or not the system operator is sufficiently capable of determining this critical point. In this dissertation, some of these questions are answered, and the tools for the evaluation of the critical contingencies are demonstrated using a particular contingency event in the Western Cape grid of South Africa.

Globally, it has been recognised that voltage instability has had a considerable impact on the number of incidents that have caused grid instability. This study will thus investigate the phenomena of power system voltage collapses and the triggers thereof as such a collapse can impact a network that has a nuclear power plant.

Voltage instability is mainly associated with "*the inability of the power system to maintain acceptable voltages at all buses in the system under normal conditions and after being subject to disturbances such as gradual load increases or outages of critical lines or generating units"* [9]. The voltage collapse phenomenon is characterised by small changes in the voltage level at different locations after a disturbance, which results in the abrupt decline of the voltage to the point of near collapse. Given this fact, only looking at the voltage is not a sufficient indicator of

voltage instability. A more accurate approach for determining how close the system is to collapse is for the system operator to measure voltage indices in either online or offline modes. This also serves to establish the control actions that are required.

In offline planning activities, computational speed is generally not a problem. However, for online analysis, real-time or even faster than real-time tools are important when monitoring and enhancing the stability of the power system [9]. In this dissertation, an offline test was performed. Such a voltage stability analysis has previous not been undertaken by operational level personnel; this function has typically been performed by the system operator on request. In this dissertation, the Western grid network has been set up in such a way that distribution level staffs are also able to perform voltage stability simulations. Some of the features that have been added to the normal DigSilent PowerFactory® software base case to make this possible include:

- Addition of dynamic mathematical models for relevant power system equipment to allow for dynamic studies to be performed;
- DigSilent PowerFactory® software scripts have been programmed to allow for automation of repetitive tasks, for example for the generation of PV diagrams at different substation busbars;
- And adding load characteristics for all substation loads sourced from power system load capturing databases. This enables the user to study load dynamics for any period of time.

Nuclear power plants (NPPs) in particular are sensitive to voltage fluctuations. This is based on the reality that, given the nuclear physics behind the generation of the heat energy used for electricity generation, a secure means of heat generation absorption is necessary when a nuclear reaction shut down is required. If a secure means of heat generation shut down is not present, nuclear fission products can cause nuclear fuel elements to overheat, which can result in a nuclear fission product release that may in fact be harmful to human life. For this heat ejection, a reliable power system voltage supply on and off-site supply are required. The voltage levels that are observed during quasi-dynamic (long-term studies) and electromagnetic network (EMN)/ root mean square (RMS) studies in the DigSilent PowerFactory® software enable the observation of the effects of network abnormalities on the critical busbars for small signals and steady state scenarios.

1.2 Research Questions

The main questions to be investigated in this study include:

- What are the voltage stability indices that need to be evaluated in order to detect the critical busbars that may lead to a voltage collapse in the power system;

- Which busbars are deemed critical for the full operation of the Western Cape power grid;

- Is the current network future proof with regard to voltage stability given the plans to expand the network and the introduction of renewable resources such as wave energy and small modular nuclear reactors;

- What are the critical contingencies that can affect the NPP house load and the off-site supplies needed to remove decay heat out of the nuclear reactor given the sensitivity to voltage deviation; and

- Are the current network models in the simulation software Digsilent PowerFactory adequate for the evaluation of the voltage stability and dynamic studies to enable reasonable engineering decisions?

1.3 Purpose of the study

Evaluations of the power system's stability with regard to rotor stability and frequency have been well documented [1, 2]. Other daily operational analyses that are widely understood include the calculation of the transfer limit when critical 400kV voltage levels contingency are evaluated for the South African power grid. These tasks are performed by the system operator and not the local distribution operator personnel.

Many of the power system stability studies performed on the South African power grid have not focussed on the voltage collapse phenomenon and the evaluation of the limits of the equipment, which is important to understand given the power and reactive limits of the load, the availability of critical lines, and the ability of reactive devices to influence the risk of voltage collapse, which can lead to a total system blackout.

Having a simulation network that is sensitive to steady and dynamic studies is critical to answering these fundamental questions often posed in the literature when seeking to evaluate a power system's stability. In this study, the following will be done:

- The Western Cape Power Grid will be configured in such a way that it reflects the real time system;

- Steady state studies will be performed to evaluate real power versus voltage (PV curve analysis) and reactive power versus voltage (QV curve analysis) in order to evaluate voltage stability at all busbars.

Such an evaluation will assist network operators in determining:

- Critical busbars on the Western Cape power grid;

- Through analysis, when to introduce reactive devices so as to ensure voltage stability and guarantee the safe operation of the NPP in the Western Cape power grid.

The configuration of the network to present the real-time operational network proved to be challenging mainly due to the very sensitive reactive requirements needed for an IPS. However, these challenges have been successfully addressed by configuring the network as close to the operational network as possible and by making sure all reactive devices are configured as per the online network.

1.4 Objective

The objective of this dissertation is to investigate the voltage stability limits of the Koeberg nuclear power station and the surrounding power system networks under certain network constraints and/ or contingency scenarios. The scenarios to be evaluated will be detailed in the voltage collapse sensitivity evaluation program section to follow, which also includes:

- steady state analysis of critical busbars using bus PV analysis;

- bus QV analysis; and

- dynamic voltage stability analysis.

1.5 Methodology

In this research project, the focus of the investigation is to determine the voltage stability of the Western Cape grid given the presence of a nuclear power station and the effect of a voltage stability event on the plant given a known event. The project further considers the network expansion following the occurrence of a fault.

As such, both dynamic and steady state approaches have been considered using the DigSilent PowerFactory® power system simulation software. This software

allows for steady state analysis, short dynamic simulation (RMS/ EMT simulation), long-dynamic analysis (quasi-dynamic simulation), dynamic modelling of power system components, and the use of script to automate power system analysis functions such as PV and PQ curves for generators.

To perform the simulations, an evaluation of the Western Cape power grid's voltage stability was required given the presence of the NPP. In addition, two network models, case 2003 and case 2017, were created as base cases. In these networks, the grids were configured to model realistic power system networks as they were in 2003 and 2017 respectively. In addition, the power system's equipment was modelled to take into consideration the dynamic characteristics of the equipment, which is discussed in later chapters.

The analysis will be presented in the relevant sections. Further results of the evaluation are presented in Appendices A, B, and C, and the relevant graphics are also provided.

1.6 Plan of development

To follow this introductory chapter, in Chapter 2, a literature review relevant to the research undertaken is presented. In this chapter, the theory of power system stability and the different facets that are attached to it are discussed as per the IEEE definition of power system stability. In particular, Chapter 2 discusses rotor angle, frequency, and voltage stability. The chapter also looks at the overall operation of the NPP, specifically focusing on the process of heat generation through the nuclear fission process and how this particular nuclear quantum event is harnessed to generate steam, which has the ability to move a prime mover or turbine. Turbine movement leads to the generation of useful electricity that can be used to perform work. The protection systems that apply to avert a large-scale voltage collapse are discussed briefly. This section also provides some detail of how a voltage is arrested. To model or present a good approximation of what happens when a voltage instability occurs under steady and small signal stability analysis, the dynamic behaviour of critical equipment — such as loads and under voltage tap changers —need to be modelled as accurately as possible. As such, the different relevant equipment models are discussed.

Chapter 3 contains the voltage stability analysis that was conducted based on the incident that occurred on 15 October 2003, which involved the tripping of the only online NPP. During the time in which this study was conducted, this event had been the only event of its nature to occur in Africa and was thus selected as the base case

for the 2003 study case. For the 2017 case, the 2003 reactive devices configuration and sequence of events of 15 October 2003 were kept the same to allow for a fair analysis on the improvement, or not, of the voltage stability for the two case studies.

For both the case studies, i.e. 2003 and 2017, the dynamic voltage stability is evaluated over a period of 24 hours. In order to gauge how close the system has come to experiencing a voltage collapse, a PV and QV analysis is undertaken at critical busbars. Critical Buses are identified through a network voltage scan of the lowest and highest voltage at the busbars. Those busbars with the lowest margin for reactive loading were also analysed. The evaluation is repeated for a current network configuration (2017).

Chapter 4 outlines the contribution this research study has made to the body of knowledge regarding voltage stability analysis provides concluding remarks and relevant recommendations derived from the evaluation in Chapter 3.

Chapter 2. Literature Review

Transient stability analysis studies have been undertaken for many years as a means of determining generator stability during major grid disturbances [11]. Grid disturbances, *"which can be categorised as the tripping of one or more power system components of the grid"* [16], have resulted in many nuclear power stations being disconnected from the grid and operated in islanding mode. Further to this, "*many reports suggest that network disturbances can operate both network and generator protective devices that eventually could trip the nuclear power station*" [16]. In this chapter, the concept of transient stability is broadened to include other stability phenomenon such as rotor angle stability, frequency stability, and — the topic under evaluation — voltage stability.

A review of the voltage stability events that have been experienced nationally and internationally is presented as well as a discussion of the triggers of these events so as to provide an idea of the type of events than have the potential to initiate events that can lead to a cascading voltage collapse effect.

2.1 Power system stability

The study of power system stability involves the analysis of the behaviour and conditions of power systems, mostly confined to the transmission system type faults and outages, before and after sudden changes in load or generation. Distribution faults at voltage below 66kV have a less significant impact on system stability; as such, they are excluded from studies. How a system reacts to an instability is an indication of the robustness of the system [10]; therefore, knowing the system instability events that are likely to occur means the system can be designed and operated in such a manner that any transient event (such as n-1 contingencies) can be navigated without losing customer supply and synchronism of the grid [10]. The classification of the transients on the power system is based on the time frames of their occurrences [10].

When considering South Africa's power stability problem, concerns have tended to focus on ensuring that the system maintains synchronism during normal or system abnormal conditions (such as a physical disturbance) [1]. More broadly, power system stability can be broken into different categories of stability, thus making the study of different phenomena separate, which adds to the overall understanding of power stability.

The literature contains a vast amount of information on this phenomenon. The Institute of Electrical and Electronics Engineers' classification of power system stability is generally accepted in most literature [2]. The classifications are based on the following considerations:

- *"The **physical nature** of the resulting mode of instability as indicated by the main system variable in which instability can be observed"* [2]. In this dissertation, small signal stability will be performed to verify the model, thus the speed of the generator is seen as a critical variable to determine if the system is functioning normally or abnormally. The other critical variables to be observed are the voltage at critical busbars and variables as per the voltage stability analysis tools, i.e. PV and QV curves;
- "*The **size of the disturbance** considered which influences the method of calculation and prediction of stability*" [2]. To ensure that a thorough power system stability study is performed, small signal and quasi-dynamic studies will be performed to evaluate the different timeframes and the reaction of the critical variables; and
- "*The **devices, processes, and the time span** that must be taken into consideration in order to assess stability"* [2]. Important devices such as under load tap changer and certain particular loads are modelled as non-linear and as constant power loads to observe their behaviour under transient conditions.

The categories with the particular timelines and with events doing the stability classification are shown in figures 2.1 and 2.2. The related voltage stability events are highlighted in red.

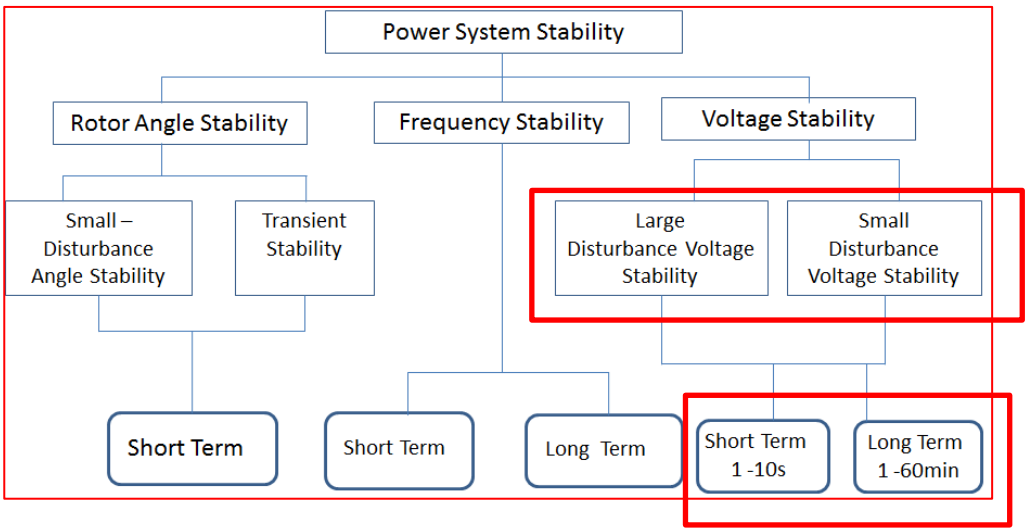

Figure 2.1: The classification of power system stability events with timelines. Related voltage stability events are highlighted in red [2,11]

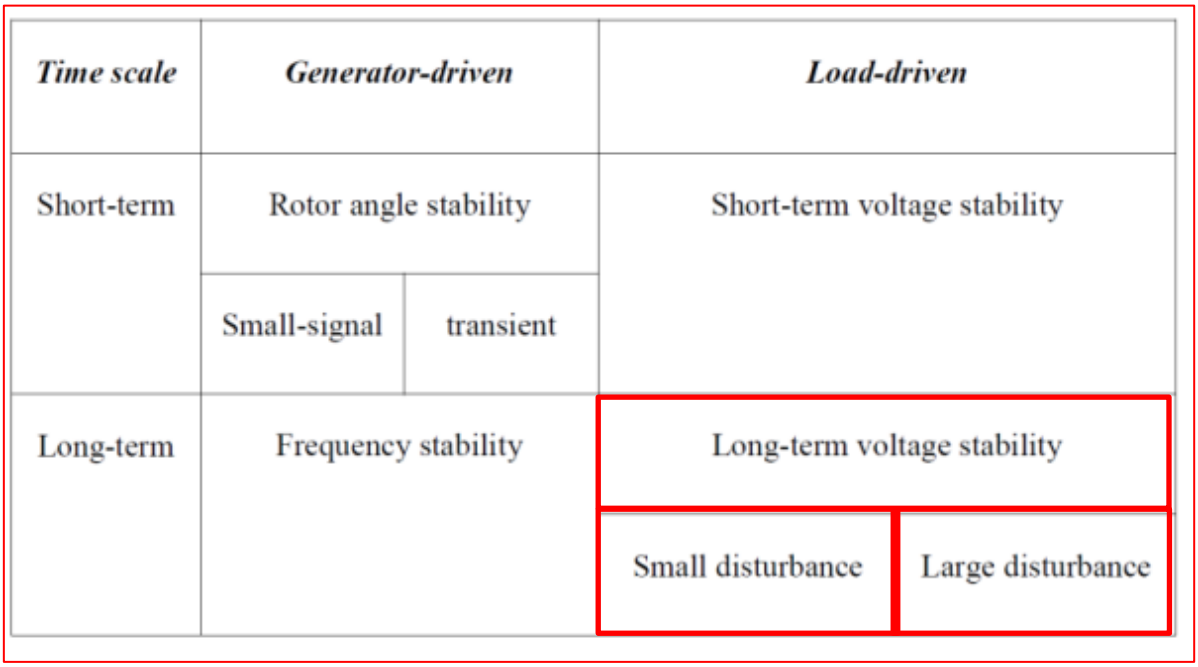

Figure 2.2: The classification of power system stability events with timelines. Related voltage stability events are highlighted in red [2, 11]

As shown in figure 2.1, the classification of transients is based on a time scale as shown below:

- Short-term, or electromagnetic transients;
- Mid-term, or electromechanical transients; and
- Long-term transients [10].

Each of these categories will now be discussed separately. This is a deliberate choice that is intended to provide an introduction to voltage stability and to contextualise the differences noted when evaluating various stability classifications with concern to the voltage stability phenomenon.

2.1.1 Power system rotor angle stability

The term rotor angle stability refers to the study of the electromechanical oscillations that are inherent within the power system. The fundamental question to answer is how the rotor angle changes in relation to a change in the power output, because under normal stable operation:

- The synchronous machines on the network all operate at $2\pi f$ electrical speed;

- The phase angle between the internal electro-magnetic forces of all machines are constant, thus the term synchronism; and

- All mechanical and electromagnetic torques acting on the rotating masses of the synchronous machine are equal.

The main concerns in rotor angle stability studies is to make sure that synchronous generators are in a state of synchronism, the electrical speed of all generators is equal, and adequate damping is available if oscillation occurs. Regarding rotor speed, this is studied so as to determine if there is an imbalance between the mechanical and electromagnetic torques. An imbalance is typical in the event of a disturbance and can lead to the over-speeding of the synchronous machine if not corrected timeously. The reduction of oscillation when a disturbance is present can be achieved through a decrease of active power generation, adding dynamic braking resistance when oversupply of power supply is available, or shedding of a load if a power shortage is present [14].

As briefly discussed above, the control methods required to stabilize a power system for transient or small-signal stability include dynamic resistance braking, excitation, fast valving (i.e., decreasing the mechanical torque as quickly as possible), a power system stabilizer, generation tripping, and load shedding [14].

The typical time scale for rotor angle stability is in accordance to its sub categories:

- Small (signal rotor angle stability): 10 to 20 seconds after the disturbance has been observed. To visualize these effects, the relevant equation (2.1) are given below:

$$\Delta \boldsymbol{T_e} = \boldsymbol{K_s}\Delta\boldsymbol{\delta} + \boldsymbol{K_d}\Delta\boldsymbol{\omega} \qquad \textbf{(2.1)}$$

  where

$$\Delta \boldsymbol{T_e} = \boldsymbol{electromagnetic\ torque}$$

$$\boldsymbol{K_s}\Delta\boldsymbol{\delta} : \boldsymbol{synchronizing\ torque}$$

$$\boldsymbol{K_d}\Delta\boldsymbol{\omega} : \boldsymbol{damping\ torque}$$

  What can be observed during small-signal stability events is a decrease in synchronising torque, that is, the machine moves out of step and/or there is a decrease in damping torque, which can lead to growing oscillations; and

- Large (disturbance rotor angle stability or transient angle stability): 3 to 5 seconds after the disturbance. What can be observed during these events is

that generators that go out of synchronism and large angle swings creating voltage dips can affect voltage sensitive customers.

2.1.2 Power system frequency stability

Power system frequency stability is defined as the ability to maintain a steady frequency even after a system disturbance has taken place. Disturbances have the potential to cause an imbalance between the power generation process and the load. If the system is not robust enough to maintain a balance between the generation and load, frequency swings — which can result in the large-scale tripping of synchronous generators — are inevitable. Typical frequency limits that need to be adhered to are illustrated in figure 2.3. The frequency variations and tripping time considerations are consistent with the South African Grid Code and in particular the Network Code Version 7.07 Section 3.1.6.2 [38]. Beyond 47.0Hz, the system may potentially go into a collapse scenario if not dealt with operationally or through an automated system in real-time system operations.

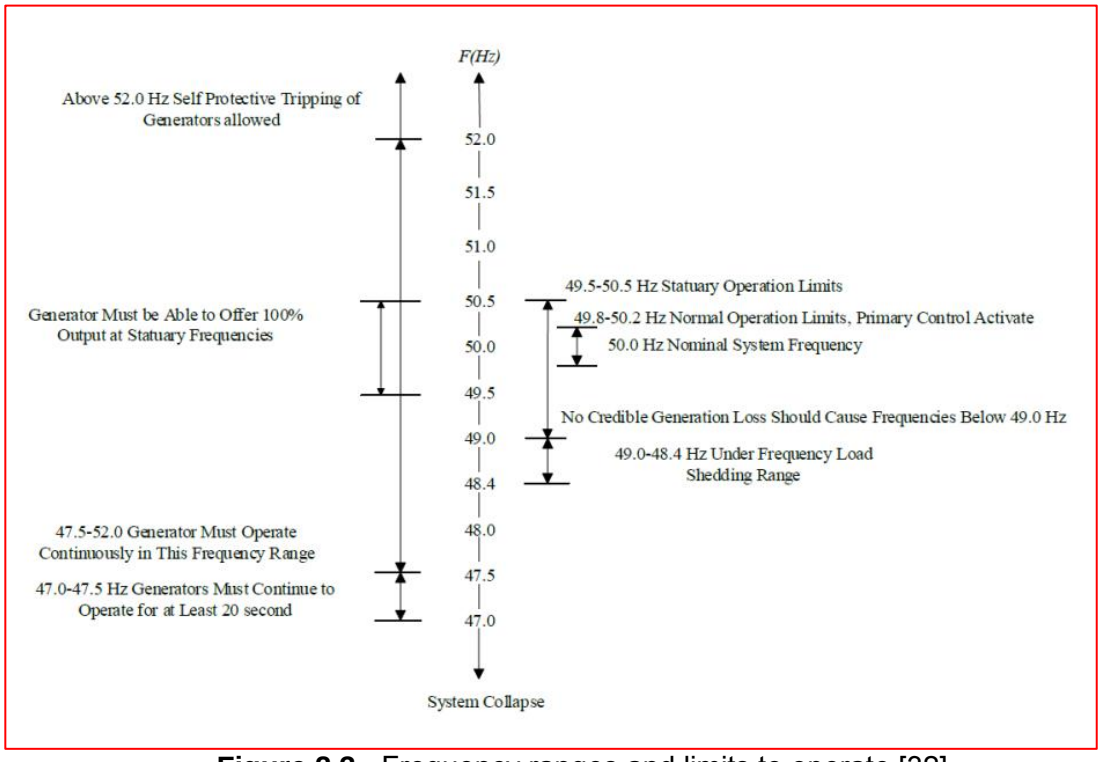

Figure 2.3 : Frequency ranges and limits to operate [32]

The ability of a power system to maintain a steady frequency after a disturbance depends on the characteristics of the load, governors, and automatic generation control (AGC) system. Some loads — such as lightning and heating loads — are not dependent on frequency at all, while others — such as motors — are dependent on frequency. Only the loads that are frequency dependant can aid in the overall system damping process in the event of a system disturbance. In this dissertation, the

behaviour of frequency type load, such as non-linear and motor loads, are included in the observation process when a large system disturbance occurs (for example the tripping of the NPP).

The timeline for a frequency deviation ranges from seconds to several minutes. The deviation depends on the activation of devices such as the under frequency load shedding schemes, the response of generators to frequency excursions, and the response of the under voltage regulators. It can thus be concluded that the frequency stability phenomenon can both be short term or long term.

2.1.3 Power system voltage stability

Voltage stability refers to the ability of a power system to maintain acceptable voltages at all buses both under normal operating conditions and after being subjected to contingency conditions [3-6]. A power system enters a state of voltage instability when a disturbance results in a progressive and uncontrollable voltage decline. The primary cause of this problem could be [5]:

- *"sudden load increase";*
- *"outages of a major generator and transmission line"*, as is the case in the case study reviewed in this dissertation; or
- "*a combination of multiple events*".

In recent decades, the consequence of voltage instability has resulted in several widespread power interruptions in many power systems throughout the world [1, 3, 7]. "*These incidents have caused serious losses in terms of economy and public welfare. Therefore, voltage stability studies have to be incorporated in planning and real time operating studies of modern power systems*" [8].

Voltage stability can be classified as:

- Static voltage stability or long-term voltage stability: In this study, device behaviour of *"under load tap changers, thermostatically controlled loads, and generator current limiters"* should to be monitored [2]. In this dissertation, the relevant loads are modelled and the quasi-dynamic simulation, which provides the option to simulate long-term dynamics, in DigSilent PowerFactory® is used; and

- Dynamic voltage stability or short-term voltage stability: When observing short-term voltage stability phenomenon, fast acting devices such as "*induction motors and electronically controlled loads*" will be used in the simulation [2]. In DigSilent PowerFactory®, the EMT/ RMS simulation is

performed in order to monitor critical parameters that could prompt voltage instability where the short-term voltage instability need to be observed.

2.2 Examples of system disturbances leading to voltage instability

With the increased complexity of the power system driven by the increased power demand over a wide geographical area, the option to expand the existing network has placed major stress on the power system's utilities. In response, utilities have opted, through their planning and operations departments, to load generators and transmission equipment above their nominal operation limits. However, such a strategy can actually lead to an operational scenario in which there are deficiencies in reactive power supplies intended for a power system. This can lead to system voltage failures in contingency scenarios or when large disturbances occur.

To foster a greater appreciation of the voltage stability problem, examples of voltage stability events on a global scale are presented in the table2.1 below. These are summarized based on a presentation by John H. Bickel [34] detailing events in North America involving NPP plants. Thereafter, the leading causes of voltage collapse are discussed.

Table 2.1 : System disturbances in North America where NPPs are present

Date	Name	No.	Events	Cause
November 9, 1965	North east Blackout	1	Power surge causes excess power relay to trip	Incorrect application of protection setting; excess power flow relay set too low
		2	Power transfer to other lines causes overload and overcurrent relays	
		3	<5 minutes overloads occur, causing wide-scale tripping of generators and lines	
		4	Unreliable voltage supply available to loads	
July 5, 1976	Millstone grid under-voltage	1	Millstone 1 boiling water reactor is working at its maximum VAR rating	Millstone 2 pressurised water reactor trips on 20% voltage
		2	Millstone 2 pressurised water reactor trips on 20% voltage	

		3	Voltage dip occurs	
July 13, 1977	New York City blackout	1	Substation connected to NPP trips due to lightning event	Lightning strike in HV yard
		2	Subsequently 2 transmission lines operate leading to loss of load trip at 900MW NPP	
		3	Unable to start peaking gas turbine due to unavailability of personnel	
		4	2 NPPs not designed to cope with full load rejection	
August 1, 1983	Monticello degraded voltage	1	Unit operates at 100% power output	Reduction of generator voltage by 5% due to a slightly loaded system
		2	Grid is slightly loaded	
		3	Reduction in auxiliary safety busses of NPP of 5%	
		4	Large motor start causes voltage dip to 6%	
		5	Under voltage protection operates after 6 seconds	
July 11, 1989	Virgil summer NPP grid under voltage	1	Record high temperatures; excessive VAR requirement	Stator cooling lost
		2	Unit trip on stator cooling lost	
		3	Resultant severe voltage dip in the system	
August 10, 1996	Grid disturbance in Pacific North West	1	Overloaded lines sag and cause short circuits	Higher power demand
		2	Turbines experience major load fluctuations	
		3	Over power trip relay cause the shut down two units	

August 12, 1999	Callaway NPP degraded voltage event	1	The plant was on offsite supply for the cooling system	High temperatures resulting in degraded voltages
		2	Voltages were inadequate to support critical house loads	
July 28, 2003	Substation fault causes grid disturbance	1	Sub synchronous oscillation relays set to sensitive	Human error — grounding switch left closed
		2	No fault ride through	
		3	Reactor cooling pump operates due to sub synchronous oscillation relay operation	
August 14, 2003	North East Blackout	1	NPP affected	System fault causes cascading system trips
June 14, 2004	Substation fault causes grid disturbance	1	Bird droppings cause flashover	Protection malfunction and takes 38s to trip
		2	Cause loss trip of approximately 4000MWe	

In table 2.1, the initiating events were mostly due to external grid triggers and closely relate to the primary causes outlined in section 2.1.4.

For a more local perspective, the significant events affecting the only NPP in Africa (South Africa in particular) between the period 2005 and 2006, according to [35], are summarised below in table 2.2:

Table 2.2: Causes of faults that influenced the only NPP in Africa between 2005 and 2006

No.	Date	Event	Load Lost Shed	Cause
1	11th November 2005	Switching in 400kV yard	1326MW	Switching event in HV yard
		Koeberg unit two trip		

2	12th November 2005	Trip of 765./ 400kV at Hydra substation due to bird nest short out phase conductors		Bird's nest
		cause voltage dip		
		Auxillary power at Koeberg NPP trip causes delay in Koeberg unit 2 start up		
3	16th November 2005	1 x 400kV line in Western Grid trip due to fire under line	1230MW	Fire under line
		Resultant significant system dip		
		Dip caused Koeberg unit 2 to trip		
4	18th February 2006	Under frequency event caused by generator trip caused Koeberg unit 2 to trip	1079MW	Generator trip resulting in under frequency event
		Subsequent load shedding leads to high voltages at transmission substation, thus prompting line trips		
		Line tripping leads to under frequency load shedding operation		
5	28th February 2006	1 x 400kV line in Western Cape Grid trips		Major 400kV line into Western Cape Grid trip
		This creates a Western Grid island situation		
		Attempts to synchronise to the rest of the grid leads to Koeberg unit 2 tripping		

Looking at the listed events, it is noted that a large proportion of the faults are initiated by external grid events and do not emanate for faults on the NPP, thus justifying the need to evaluate the voltage stability of the grid wherein a nuclear power plant is present.

2.2.1 Overall causes of voltage stability problems

In local and international events described above, most of the faults were triggered by a fault situation or a component malfunction [15]. The main components that cause voltage collapses are described below and need to be read in conjunction with Figure 2.4.

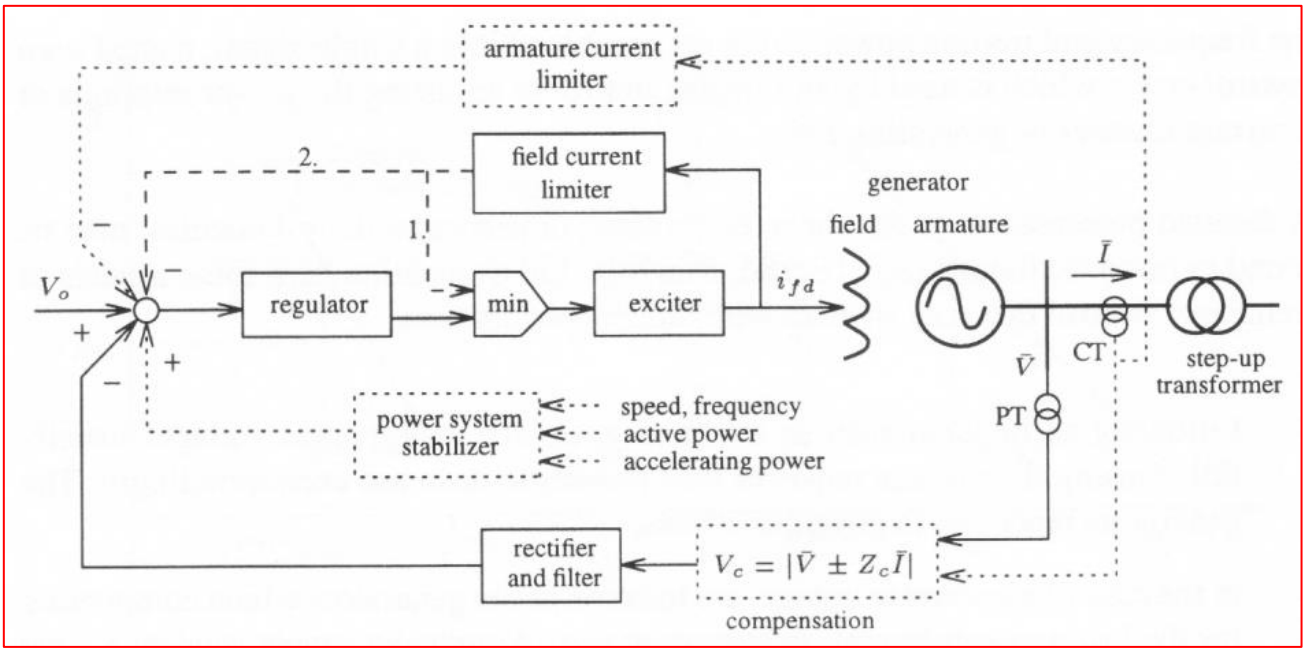

Figure 2.4 : Synchronous machine system showing individual components and the integration point with the power system through the step up transformer [33]

Components that cause voltage collapses:

- Over excitation limiter (OEL), which limits the number of field currents that can be produced;

- On/ under load tap changers that interact and cause low voltages as well as resultant high currents and losses due to the nature of the loads mostly being of constant power type;

- In NPP, generator excitation controllers use armature current limiters that need to be considered in addition to the field current limiters mentioned above [15]. The equation that applies in this case is shown in equation 2.2(below). It is very restrictive when voltages on the network are low and the reactive requirement increases:

$$\boldsymbol{Q = \sqrt{(VI_{max})^2 - P^2}} \qquad \textbf{(2.2)}$$

Where Q is the reactive power, V is the generator voltage and I_{max} is the maximum generator current.

- Field current limiters, which cause the overall reactive output to reduce to the point when field current limiters are activated. A classic example of this is shown in figure 2.5.

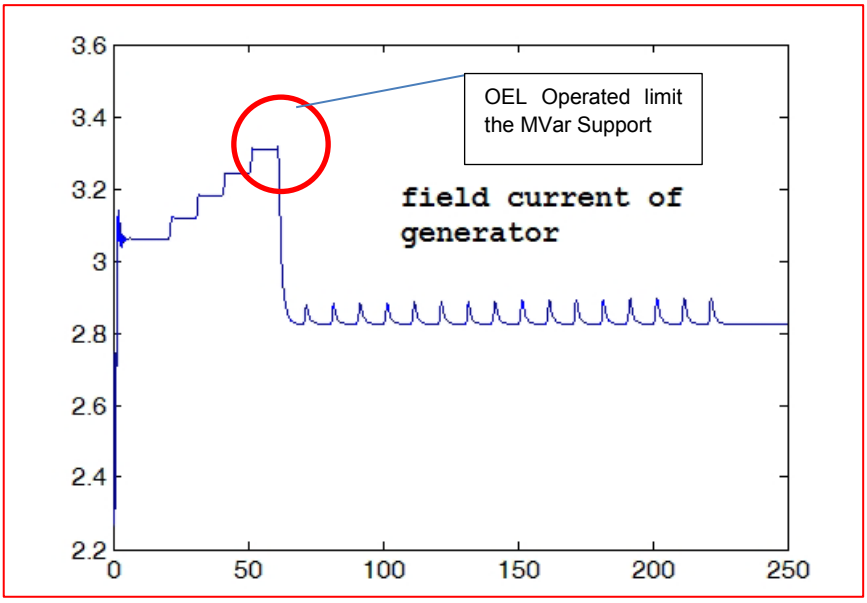

Figure 2.5 : Field current limit reached due to sudden increase in load [33]

In much of the literature reviewed as mentioned by S. B. Bhaladhare, A. S. Telang and P. P. Bedekar in [28] and A. K. Ramasamy, R Verayiah, I.Z. Abidin, S. Gunalan and P. Perumal in [29], an attempt has been made to clarify the mechanism of voltage collapse and how these collapses can be avoided. However, in the majority of the cases, the focus has been on the maximum loading limit using PV and QV curves. This approach of looking at voltage stability is steady state formulation of voltage stability analysis. While this is one way of predicting potential voltage instability, as shown above, the majority of the causes are due to the dynamic reaction of the synchronous generators after a system disturbance.

In the following section, the importance of studying voltage stability effects in the close vicinity of NPP is discussed.

2.3 Effect of grid instability on nuclear power generation

For an NPP to operate in a safe, efficient, secure, and reliable manner, the grid itself must be safe, reliable, efficient, and secure. Most significantly, in the context of the nuclear power station, the grid plays an important safety function through the provision of a reliable source of energy to the plant's cooling system by keeping the fuel cool after the reactor has shut down. This is the first requirement of the nuclear

power plant; nevertheless, it is a stipulation that NPPs have a backup power system and that these backup generators are reliably available.

Cooling requirements place limitations on the voltage and frequency of the grid as well as the power required [24]. This impresses certain technical requirements on the grid's reliability and nuclear safety that are inherited in the design and safety regulations of the power grid. When evaluating the technical requirements for the power grid, the parameters to consider are nuclear safety, the nature of the grid disturbance, safety regulations, and standards of dealing with the NPP grid interface.

Unlike traditional thermal power plants, NPPs will still produce heat energy from fission product decay after being shut down because of the nuclear chain reaction. This rate of decay is shown in figure 2.6. It should be noted that this rate of decay is on a logarithmic scale, which means that a reliable means of power supply for heat removal is required to ensure that the fuel elements do not overheat and cause a release of the fission products.

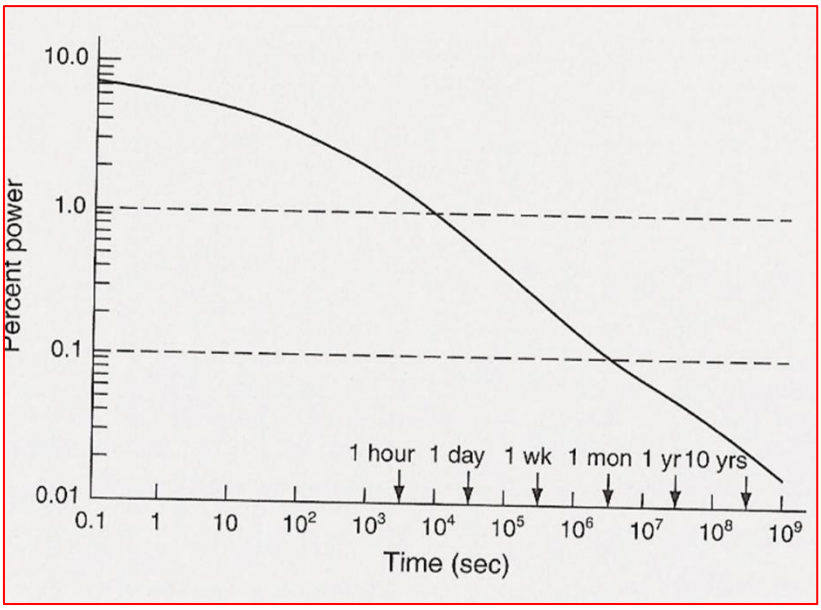

Figure 2.6 : Decay power in percentage versus time [25]

When it comes to the grid's interconnectivity, it is not only the need for redundancy in the transmission and generating resources available that adds to the grid reliability; however, it is also the nature of the grid disturbance. These technical issues include [24]:

- The magnitude and frequency of load rejections and loss of load to the nuclear power station. In this regard, it is worth noting the following definitions:
    - Load rejection is a sudden loss of load, which can be due to an unexpected opening of a circuit breaker that supplies a significant

amount of load in the power system. The power system design makes provision for this sudden rejection of the load through a ride-through mechanism without disconnecting the NPP. A typical range is in the order of 50% of the load, which depends on the reactor, the balance of plant design, and the ability of the NPP to load and unload. This loading and unloading can be in the order of 5% per minute within a specified power band. Typical techniques that are used to change the power output of the NPP include insertion of control rods to reduce the power level of NPPs due to reduced load demand, running back of the steam turbine, and bypassing excess steam around the turbine to the condenser.

- Loss of load refers to 100% rejection of a load, meaning that the entire load that is being supplied by the nuclear power plant has been lost.

- The transients on the grid that involve abnormal voltage or frequency where:
  - The frequency of the power system is contained within a small band to avoid the power system going out of synchronism, thus resulting in a total blackout scenario. The frequency droop is caused by an imbalance between generation and the load. This is shown in figure 2.7.

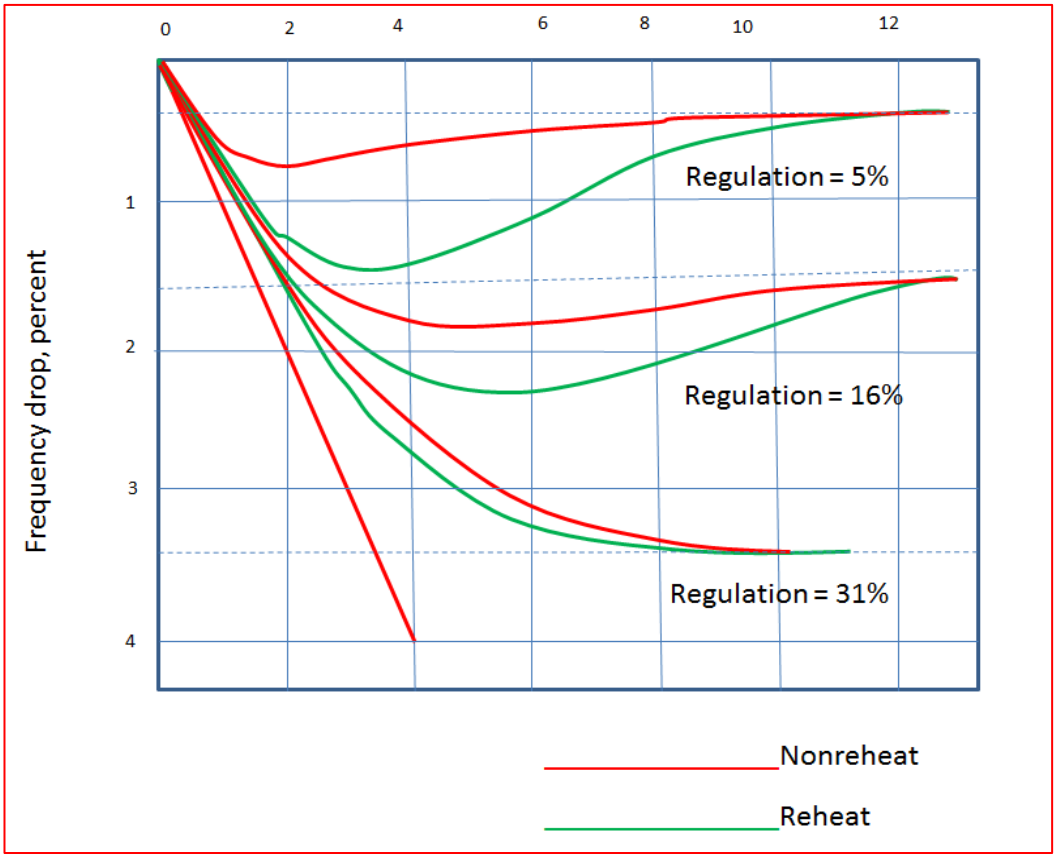

Figure 2.7: Frequency response for a 10% generation loss with different regulation regimes [25]

To control these frequency deviations, the system operator should respond by adding additional peaking generation to the power system. If this is not effective, the next option is to reduce the voltage set points at certain busbars. In the event that the voltage reduction at busbars does not yield the desired result, the automatic frequency load shedding devices will be activated. These will reduce the overall demand in certain predetermined MW blocks at particular frequency points.

- The decay of voltages on the power system: This has previously occurred due to inefficient reactive devices that need to cope with reactance deficiencies [24]. The reason for highlighting the concern of a reduced voltage is because NPPs have system and heat removal equipment that requires stable power to be functional. For example, AC motors that are used in the critical loops of the NPP are directly affected by voltage levels. Therefore, if the voltage is not efficient and/or sufficient, the motors are not able to develop the required torque. If the voltage drops below a certain threshold, the motor will draw large currents that can cause the operation of overcurrent protection relays or protective fuses that could lead to the disconnection of the effected circuits. The narrow band of the critical motors requires the protection of the NPP to avoid separating from the power system until such time that the voltage and frequency are within the desired range. When the NPP disconnects from the system, the critical emergency supplies are drawn from the on-site emergency power sources and batteries.

- The loss of off-site power due to a grid disturbance (*0.85pu on grid is required as a safe offsite voltage limit, if lower than this NPP can trip on loss of coolant [25]*): The unavailability of the off-site supply is mainly caused by external events to the NPP such as line failures and faults brought on by natural events (such as lightning). Such a loss affects supply to pumps and can, in certain nuclear reactor design types, even cause control rods to be inserted into the nuclear core, which can result in a shutdown of the nuclear reaction. Failure of off-site power will also require that on-site emergency supplies be switched on.

- NPP tripping causing a grid disturbance that result in a cascading grid collapse: Cascading causes a major power system event when a large portion of the load is being supplied by a single NPP. To circumvent this, a significant amount of equal generation needs to be brought online to avoid the rapid degradation of voltage and frequency, which can cause loss of the off-site supply and tripping of the NPP to local emergency supplies.

Based on the above, a stable grid supply is essential to ensure that NPPs remain online and are operated in a safe manner. Failure to do so can compromise the technical integrity of the NPP, which can lead to a nuclear fission product release into the atmosphere. To analyse the critical network scenarios that can lead to an abnormal operation of a NPP, the different components of the NPP and the external plant influencing the operational stability of the NPP need to be modelled appropriately so as to evaluate all credible contingency scenarios that can affect the NPP's stability.

2.4 Protection and other systems available to avert the influence of a voltage collapse

Leaving the NPP unprotected against voltage stability can lead to an adverse situation that may compromise the nuclear reactor. In NPPs, several defence in-depth mechanisms are in place to ensure that no nuclear fission elements leave the reactor core. The table 2.3 and 2.4 below details typical fission products released and their corresponding half-life in the event of a nuclear incident being triggered.

Table 2.3: The estimated releases of radio-active isotopes during the Chernobyl incident

Isotope	Half-Life	Type of Radiation	Estimated Release during Accident†
			PBq
Neptunium-239	58 hr	Beta, gamma	95
Molybdenum-99	67 hr	Beta, gamma	>168
Tellurium-132	78 hr	Beta, gamma	1150
Xenon-133	5 days	Beta, gamma	6500
Iodine-131	8 days	Beta, gamma	1760
Barium-140	13 days	Beta, gamma	240
Cerium-141	33 days	Beta, gamma	196
Ruthenium-103	40 days	Beta, gamma	>168
Strontium-89	52 days	Beta	115
Zirconium-95	65 days	Beta, gamma	196
Curium-242	163 days	Alpha	0.9
Cerium-144	285 days	Beta, gamma	116
Ruthenium-106	1 yr	Beta, gamma	>73
Cesium-134	2 yr	Beta	54
Plutonium-241	13 yr	Beta	6
Strontium-90	28 yr	Beta	10
Cesium-137	30 yr	Beta, gamma	85
Plutonium-238	86 yr	Alpha	0.035
Plutonium-240	6,850 yr	Alpha, gamma	0.042
Plutonium-239	24,400 yr	Alpha, gamma	0.030

Table 2.4 : The effective doses radiation when exposed to different radiation sources

Exposure	Effective Dose *mSv*	Estimated Duration of Equivalent Radiation Dose from Natural Background
Medical or nonmedical exposure		
One-way flight from New York to Tokyo[9]	0.07	7 days
Chest radiograph (posteroanterior and lateral)[10]	0.1	10 days
Average annual occupational exposure of crew on commercial airline[11]	2	6 mo
Computed tomography of the chest[10]	7	2 yr
Thallium cardiac stress test[12]	36	12 yr
Annual dose allowed for a U.S. radiation worker during occupational exposure[13]	50	17 yr
Risk of health effects that is either too small to be observed or nonexistent[14]	<100	<34 yr
Three Mile Island exposure[2]		
Average dose to residents within 10 miles of the plant	0.01	1 day
Maximum dose to a person at the plant boundary	1	3 mo
Chernobyl exposure[15]		
Residents in low-contamination areas from 1986 to 2005*	10–20	3–6 yr
Evacuated residents in 1986	>33	>11 yr
Residents in high-contamination areas from 1986 to 2005*	>50	>17 yr
Reactor-site clean-up workers in 1986 and 1987	>100	>34 yr

Thus, it is very important that the protection system ensures the integrity of the NPP. Before applying protection, the time scales of different power system disturbances need to be understood. In figure 2. 8 below, the different time scales that apply to the power system are illustrated.

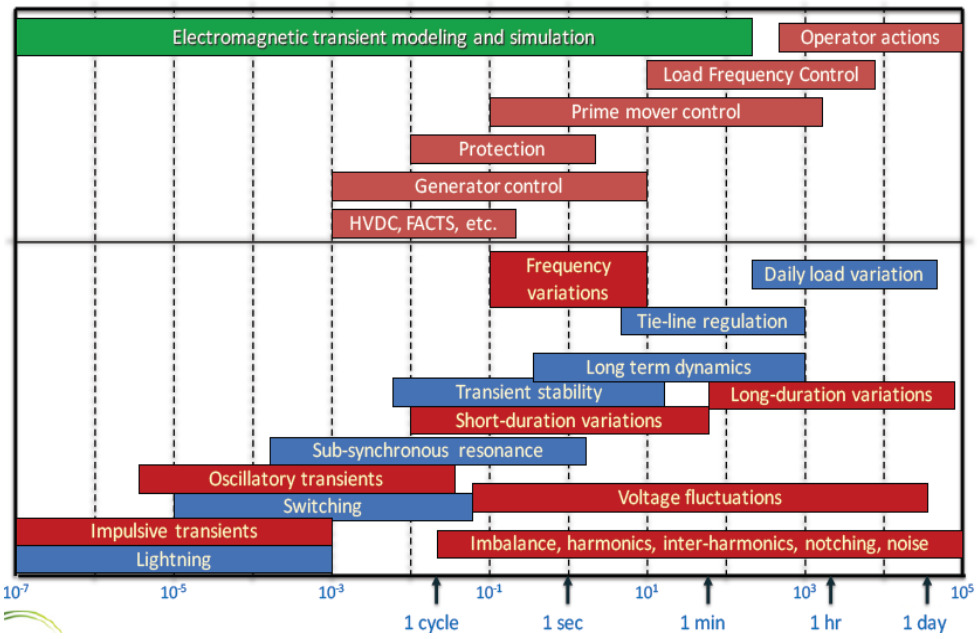

Figure 2.8: Time scales for different power system disturbances (Source: IEEE-PES)

In seeking to avert voltage instability, the main power system equipment influencing the phenomena needs to be identified. Usually, these are the generator field, armature current limiters, under load tap changers, and load types involved in the disturbance. Proper identification means that the correct precautionary measures can be applied according to the time scale of the operation in figure 2.8.

Regarding the generator's limiter, it is important to understand the limiter's behaviour because the voltage support function of the generator may be lost if the limits are reached, and the result of this can be voltage collapse.

During the disturbance, the under load tap changer will try to keep the regulated busbars voltage at a consistent level, potentially requiring a higher current requirement and leading to high current demand on the power system. Not only can this lead to the operation of the overcurrent protection but also further voltage drops on the power system.

Unlike constant loads, dynamic loads have what is called a load recovery, which can lead to a higher power demand on the power system than before the disturbance. The protection responses summarised in figure 2.9 will often try to prevent disturbances that can lead to voltage instability include, but these include:

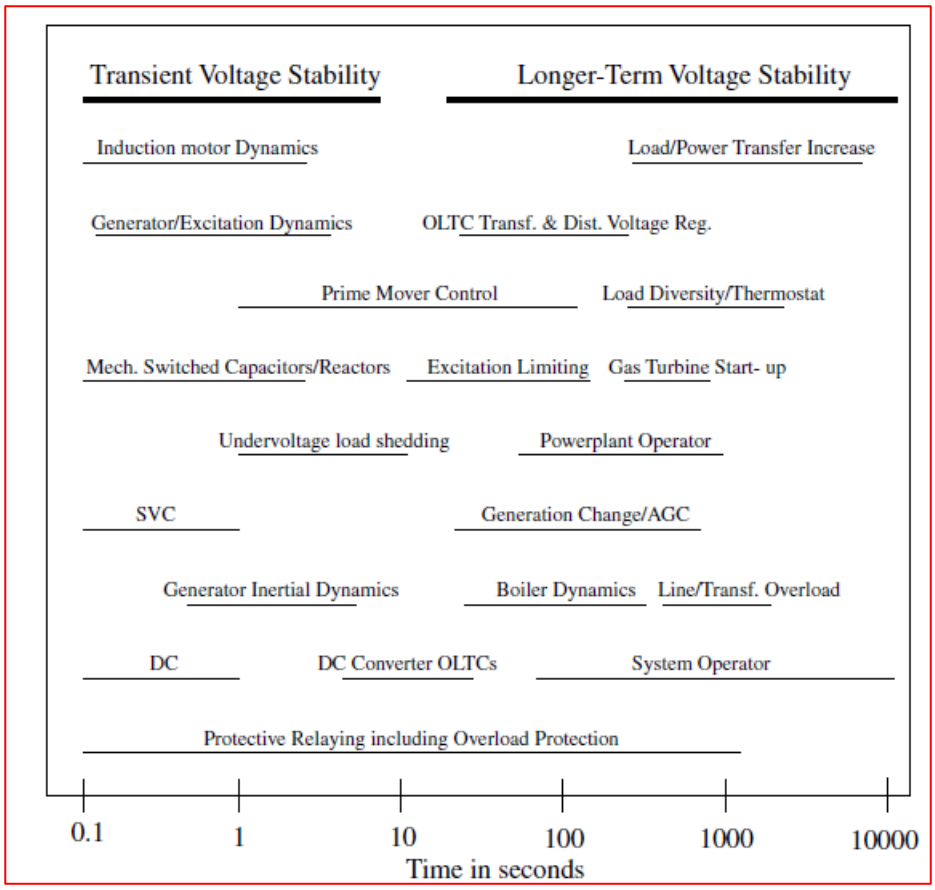

Figure 2.9: Responses to voltage stability phenomena [36]

- Protective relaying of equipment, which includes overload and under frequency protection (this applies over the time spectrum from 0.1s<t<1000s);

- under voltage load shedding protection, which applies for periods of over 1s<t<10s;

- line or transformer overload protection, which serve as a form backup protection in the event that the main protection measures fail to operate for time scale 500s<t<200s

In the Western Cape power grid, the main protection against voltage instability disturbance is the under frequency protection that is placed at strategic load centres. When an under frequency event occurs, in most cases this is initiated by an imbalance between the generation and the demand, load is shed in stepwise manner in accordance to predefined frequency setpoints.

In the following sections is a discussion of the components that need to be modelled to predict critical points on the power system in order to allow the prevention of voltage instability. The components include the generator field, amateur current limiters, under load tap changers, and load types

Chapter 3. Component Model Development for Simulation and Analysis

3.1 Modelling components for voltage stability analysis

In order to measure the contribution of the dynamic characteristics of the components of a power system, dynamic models need to be included in the power system simulation tool. For instance, to simulate synchronous and asynchronous machines, the control systems of the voltage regulator and the speed governor need to be included. For other studies, such as the small signal stability, the power system stabiliser needs to be included in the synchronous generator model.

3.1.1 *Excitation system and automatic voltage regulator*

The main function of the excitation system is to provide a direct current to the field winding of the synchronous generator. How this fits into the complete system model of the synchronous machine is shown in figure 3.1.

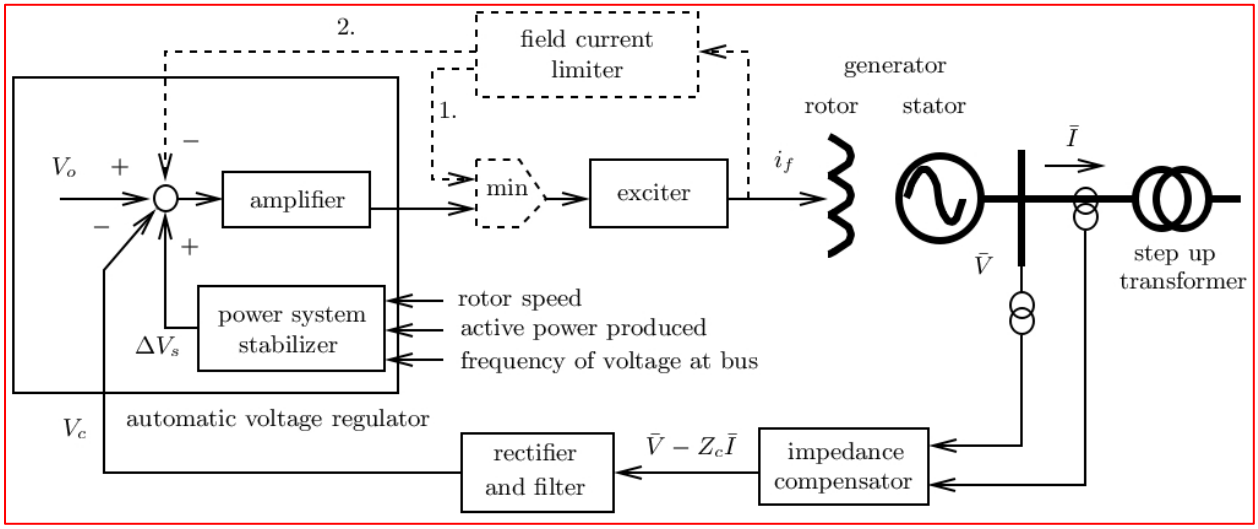

Figure 3.1: Model of the excitation system that will be used in the explanation of the synchronous machine model [33]

The excitation system should change of the excitation field automatically with the goal of maintaining the terminal voltage under normal and abnormal network disturbance conditions [19]. While excitation systems may take different forms, the typical ones are listed below:

- DC excitation system as shown in figure 3.2: In this system, the field current is produced by the DC generator and fed to the stator through slip rings and brushes. For this system, the DC generator and the synchronous generator are on the same shaft. This type of system has a slow response, and given

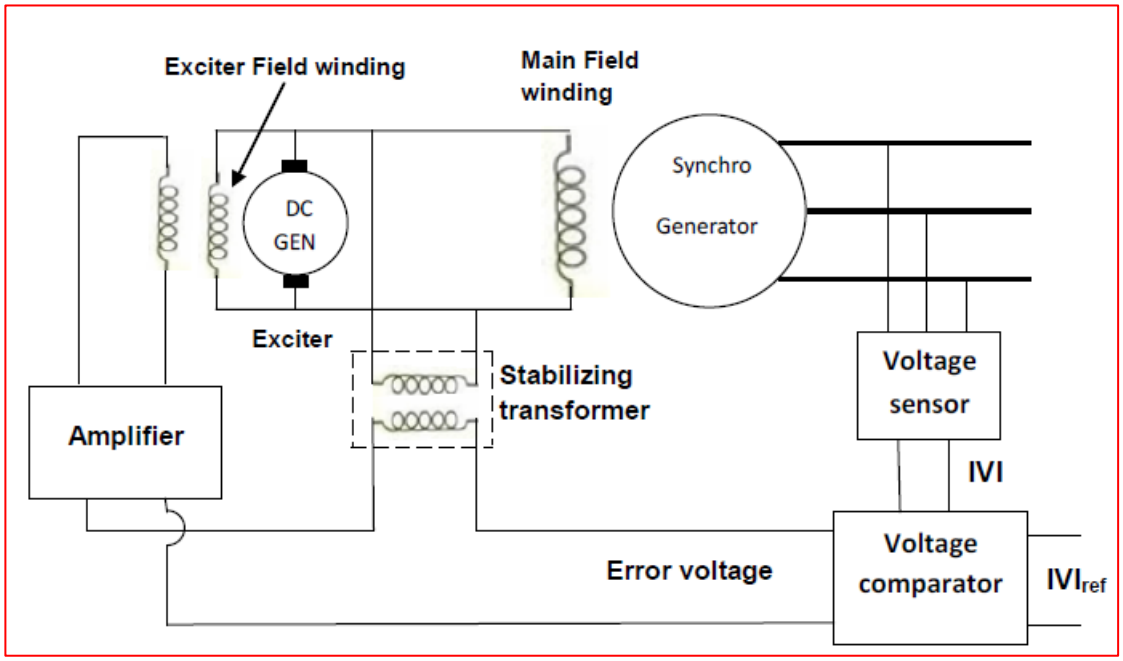

the power requirement (20 – 35kW), a large DC generator is required.

Figure 3.2: Typical DC excitation system [18]

- AC excitation system as shown in figure 3.3: In this system, the DC generator is replaced by an AC machine or alternator that supplies the necessary DC field current. To achieve this, three-phase AC machine voltage is rectified to a suitable DC supply. The rectifiers used can either be of static or rotating type. In modern day, alternators use electronic amplifier regulators.

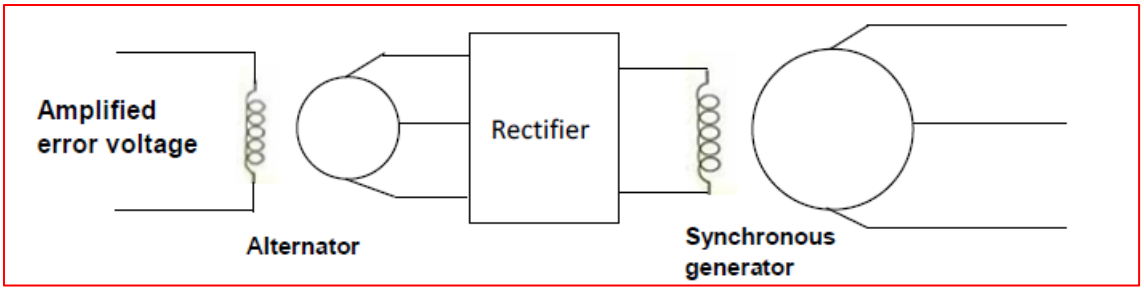

Figure 3.3 : Typical AC excitation system [18]

- Brushless AC excitation system as shown in figure 3.4: In this system design, the need for slip rings and brushes is eliminated. The system eliminates the perceived problem that exists when supplying high field currents to large generators.

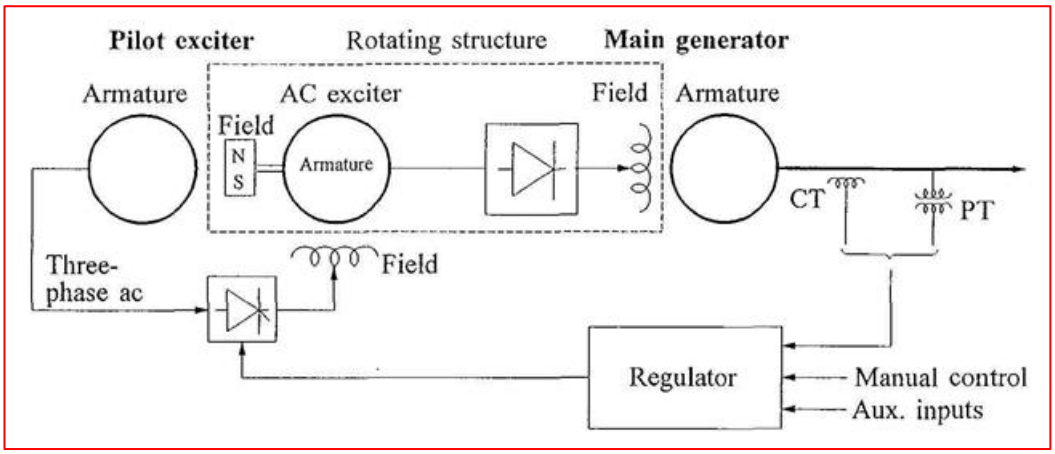

Figure 3.4 : Brushless AC excitation system [20]

- Static excitation system as shown in figure 3.5: A portion of the AC from each phase of the synchronous generator is fed back to the field windings. This is done through a system of transformers, rectifiers, and reactors. For initial excitation of the field windings, this system requires an external source of DC.

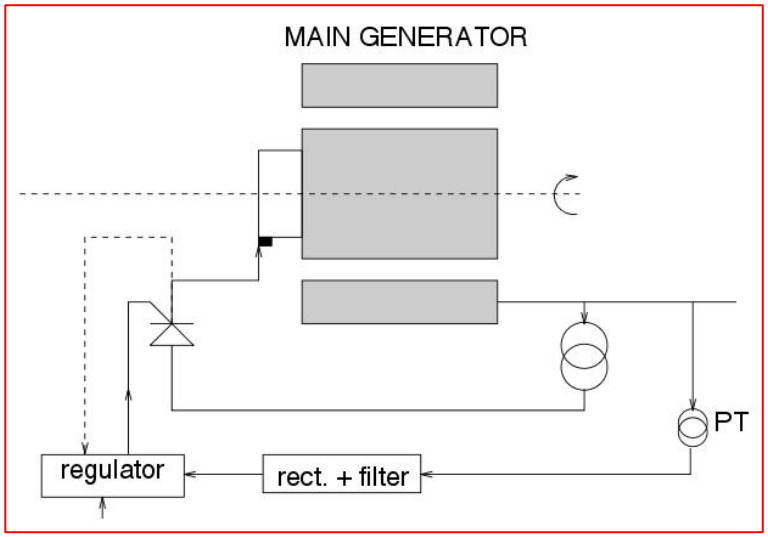

Figure 3.5: Static excitation system [21]

The model of the excitation system is based on the Institute of Electrical and Electronics Engineer's Std 421.5 5th edition of 2005. This will be the basis for the

explanation of the parameters to consider when configuring the model for simulation that follows.

When modelling the excitation system, the following per unit system base needs to be considered [33].

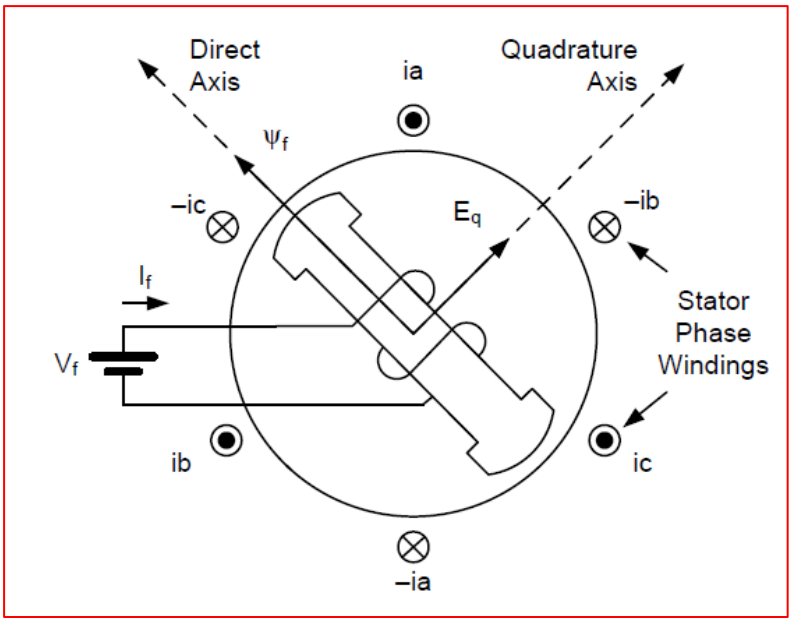

Figure 3.6: Mechanical and electrical structure of synchronous generator

- $V_{fB,}$ as shown in figure 3.6, which refers to the field voltage that produces the nominal voltage V_B at the open circuit terminals of the generator; and
- $I_{fB,}$ as shown in figure 3.6, which refers to the field current that, produces the nominal V_B at the open circuit terminals of the generator.

When the steady state is considered,

$$\mathbf{v_f = R_f i_f} \qquad \textbf{(2.3)}$$

and in the per unit the field voltage:

$$\boldsymbol{v_{fpu}} = \frac{\boldsymbol{v_f}}{\boldsymbol{v_{fB}}} = \frac{\boldsymbol{R_f i_f}}{\boldsymbol{R_f I_{fb}}} \qquad \textbf{(2.4)}$$

Given the generic model below as shown in figure 3.7, the following parameter definitions apply:

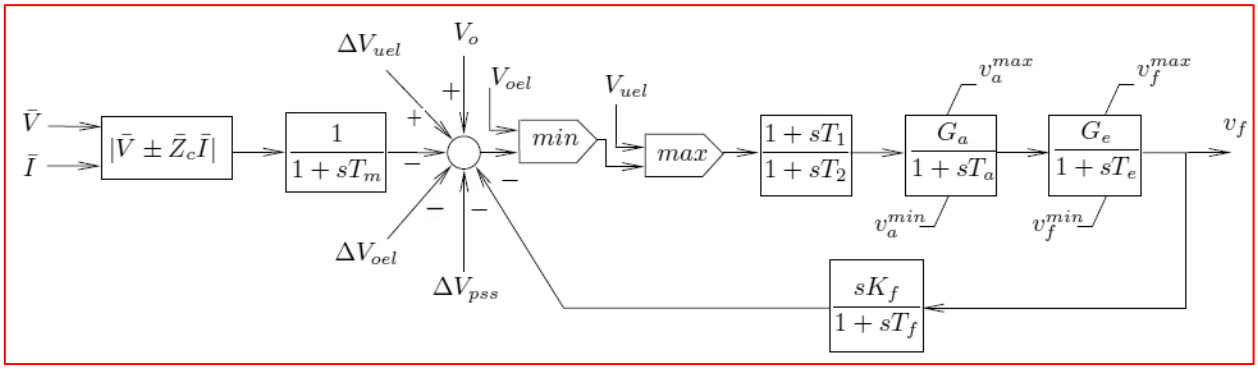

Figure 3.7: Simple generic model of the excitation system and the AVR [33]

In Figure 3.7,

$$\boldsymbol{V_0} \text{ : Voltage set} - \text{point}$$

$$\boldsymbol{Z_c} \text{ : Compensation impedance}$$

$\Delta\mathbf{V_{pss}}$: Output of the power system stabilizer

$\frac{\mathbf{1}}{\mathbf{1+sT_m}}$: **relates to the rectification and filtering of the AC voltagel** $\mathbf{T_m} \cong \mathbf{0.05s}$

$\frac{\boldsymbol{G_a}}{\mathbf{1+sT_a}}$: **relates to an amplifier;** $\boldsymbol{T_a} \cong \mathbf{0.05s}$

$\frac{\boldsymbol{G_e}}{\mathbf{1+sT_e}}$: **relates to the excitation system** $\mathbf{T_e}$ **can vary from 0.01 to 0.1s**

Internally, the AVR is compensated for the dynamic response through either a lead lag filter as shown in figure 3.7 in the direct path $\frac{1+sT_1}{1+sT_2}$ or through a derivative in the feedback path $\frac{sT_f}{1+sT_f}$.

For the sake of completeness, the over and under excitation limits will now be discussed. The function of the OEL limiter is to ensure that that the excitation system does not supply excess field current. The field current can go above the full load level when the system voltage is suddenly reduced and when there is a fault on the

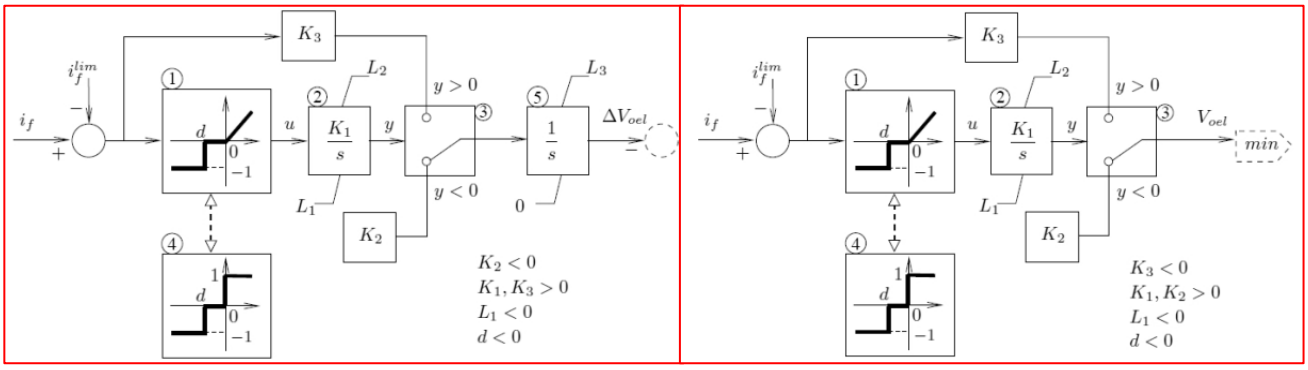

Figure 3.8 : OEL acting through the summation point of AVR or min gate AVR [34]

machine itself. To avoid a possible voltage collapse will require the field current to be increased for long duration to sustain the grid voltage until the fault is cleared. In the model above shown in figure 3.7 and figure 3.8, the OEL acts either through the minimum (min) gate or the correction signal ΔV_{oel}

On the other hand the function of the under excitation limiter (UEL) is to ensure that that the field current does not go lower that a minimum value, or that the reactive power will go lower than a minimum. If the UEL limits are not maintained this can lead to excitation loss and asynchronous operation. In contrast to OEL, the under excitation limiter (UEL) acts either through the maximum (max) gate of the correction signal ΔV_{uel} as shown in figure 3.7.

The AVR and excitation for the Koeberg nuclear power plant are shown below in figure 3.9:

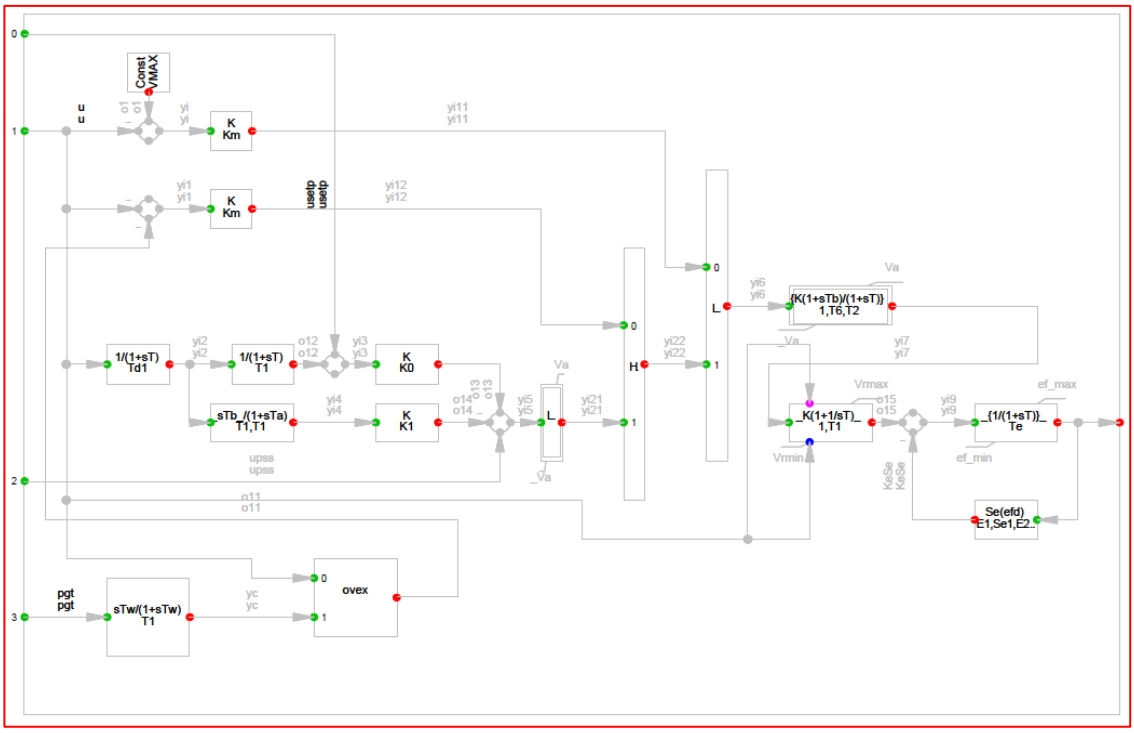

Figure 3.9 : AVR Koeberg implemented in DigSilent PowerFactory®

Discussed below in section 2.5.2 is the power system stabiliser model required to stabilise the dynamic response caused by the high loop gain $\frac{G_a}{1+sT_a}$ as, shown in figure 3.7 that is required for static accuracy.

3.1.2 Power system stabiliser

As mentioned previously, a high loop gain is required for static accuracy; this unfortunately "*cause[s] an undesirable dynamic response and possibly instability*" [21]. To solve this problem, the power system stabiliser (PSS) is added in series with AVR (see figure 3.10). The introduction of the small signal stability problem is mainly caused by the introduction of time (T_e , T_a, T_2) as shown in figure 3.7, which causes a phase advance. The introduction of the PSS will have the net effect of moving the complex eigenvalues that are associated with the unstable mode to the desired region of the complex plane [33].

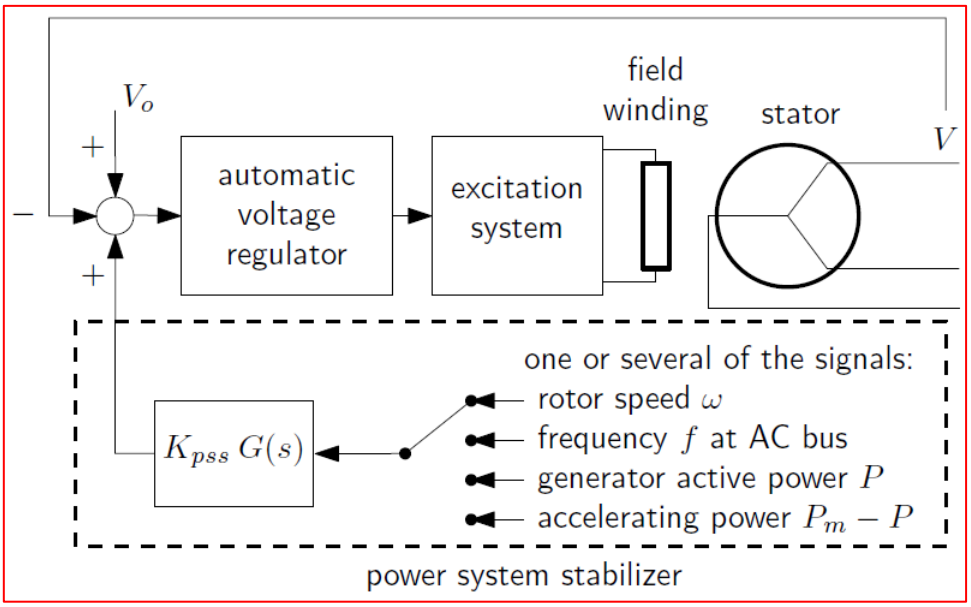

Figure 3.10: PSS added to reduce the phase advancement caused by series time constraints [34]

The PSS model implemented at the Koeberg power station is shown in figure 3.11.

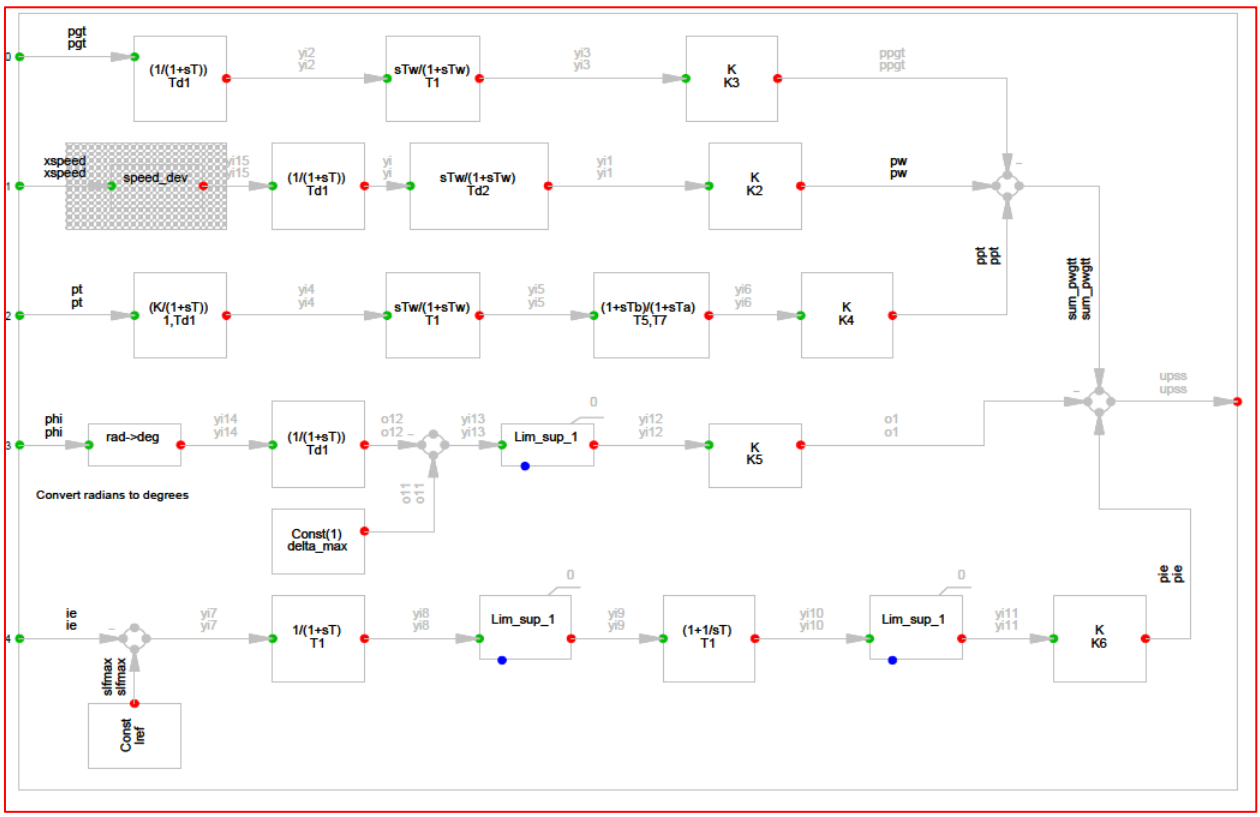

Figure 3.11: PSS for Koeberg power station

3.1.3 Speed/ turbine governors

Governors are not considered during the first swing transient stability studies mainly due to the fact that the responses of the governor during these events are neglected. For all the dynamic case studies simulated the governor slots have been made inactive taking into consideration the beforementioned fact and the duration of the studies, i.e less than 10seconds. For illustrative purposes the implemented governor slot is shown below in figure 2.12.

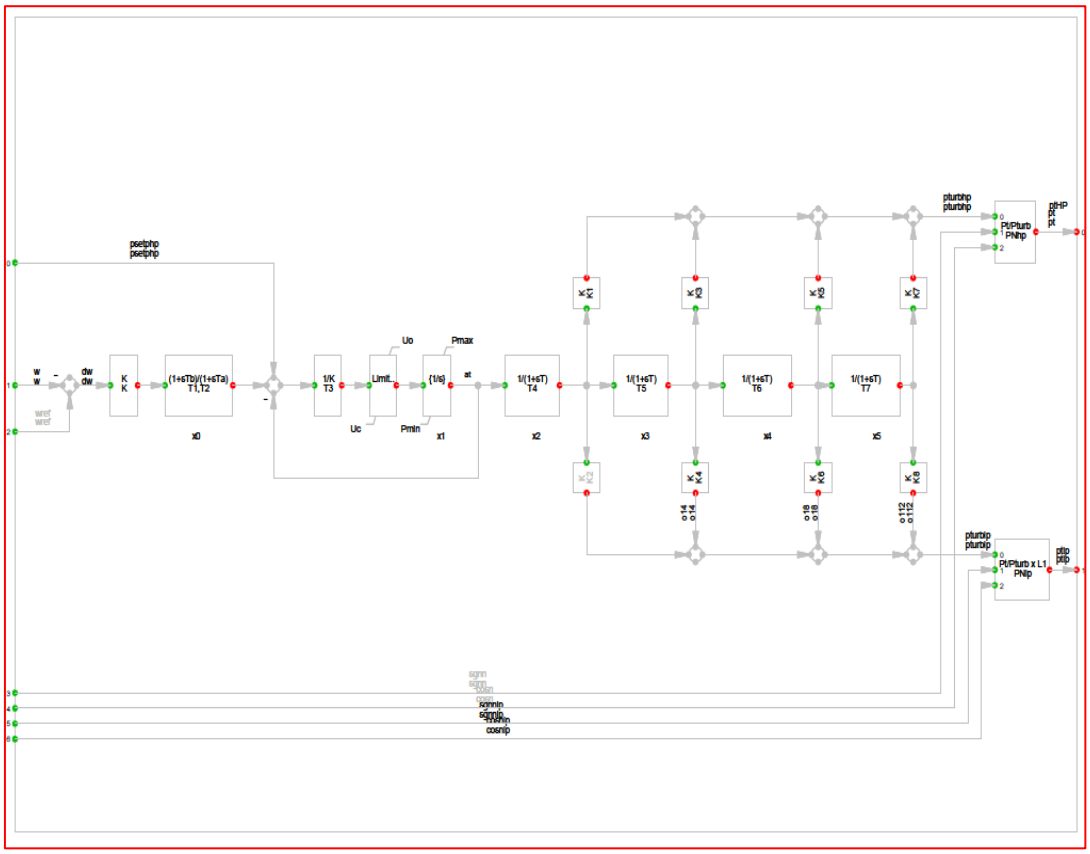

Figure 3.12: Speed governor slot implementation for the Koeberg unit

The basic function of a turbine governor is to control speed and/or load [6]. In the figure 3.13 the complete thermal cycle for a speed governor is shown. In the figure 3.13, SG refers to speed governor, CV refers to control valves (note that these are adjusted by the SG under normal operation), IV refers to intercepted valve (which is closed in the event of over speeding), MSV refers to main stop valve, and RSV refers to reheated stop valve (which is activated during an emergency).

In the figure 3.13 it's illustrated how the speed of the shaft is monitored and the valves are appropriately actuated to control the steam flow. This is the primary way in which the speed/load control function operates through the feedback of the speed error to control the gate position.

.

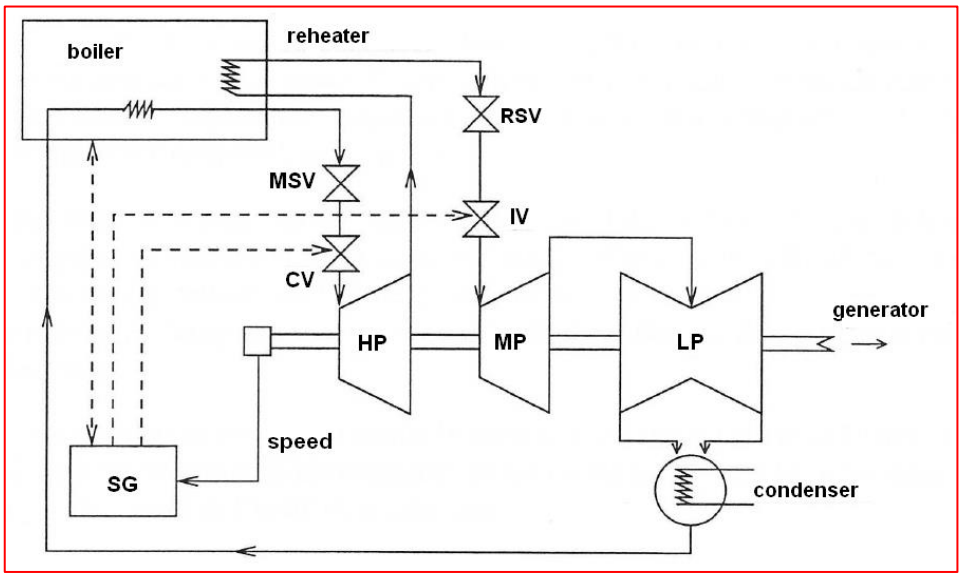

Figure 3.13: Speed governor position in thermal cycle [34]

3.1.4 Dynamic load characteristics

Major voltage collapse incidents have shown that the load type can have a significant effect on the voltage stability of a power system [14]. The modelling of loads can be difficult given the diversity of load types existing on a single network. As such, it is often better to approximate the loads into the following categories:

- Industrial;
- Commercial; and
- Residential.

The complex nature of loads is caused by the fact that loads do not behave as constant admittances; rather, most loads tend to recover their pre-disturbance power level after a system incident. The recovery times for dynamic loads are shown in the table below:

Table 3.1 : Dynamic load response after system disturbance (adapted from [33])

Component	Time Scale	Internal Variable	Equilibrium Condition
Induction motor	~ 1 second	Motor speed	Mechanical torque = electromagnetic torque
Load tap changer	~ few minutes	Transformer ratio	Control the voltage within a death band

Thermostatically controlled load	~ few minutes to tens of minutes	Amount of connected load	Temperature within dead band

In a simulation environment, loads should be defined as being a certain type to be able to observe the behaviour under network disturbances. For balanced load flow studies, as is performed in this dissertation, only P_0 and Q_0 need to be specified. To express the voltage dependency of the loads, DigSilent PowerFactory® uses the three-polynomial terms equation (2.5) shown below [37]:

$$\boldsymbol{P = P_0(\, aP.\left(\frac{v}{v_0}\right)^{e-aP} + bP.\left(\frac{v}{v_0}\right)^{e-bP} + (1 - aP - bP).\left(\frac{v}{v_0}\right)^{e-cP})} \qquad \textbf{(2.5)}$$

where P_0 *is the initial active power flow,* $1 - aP - bP = cP$ *and* v *is the busbar voltage in per unit*" [37]. Table 3.1 provides information on the selection for the different load types.

Table 3.2 : Exponent selection for different load types

Exponent Constant	Constant
0	Power
1	Current
2	Impedance

Summary of different types of loads:

- C*onstant impedance*: This load model, which is also called a constant admittance, is a static load model wherein the power varies directly with the square of the voltage magnitude [4];

- *Constant current*: This load model is a static load model wherein the power varies directly with the voltage magnitude [4];

- *Constant power*: This load model, which can also be called a constant MVA model, is a static load model wherein the power does not vary with changes in voltage magnitude. This model is sometimes considered a conservative representation for induction motor loads but should be used with caution [11]. The constant MVA characteristic is only true for the active part of the load and only above a certain voltage (80-90%). The reactive part of an induction motor load can be expected to increase as the voltage decreases beyond a certain value.

In an attempt to overcome shortcomings, many load models in power system simulation packages provide the option to change from constant MVA to constant impedance without tripping the load below a specified voltage [3].

The two types of loads that were modelled in this study are the linear load (constant power) and the non–linear load (constant impedance). To demonstrate the difference in response to a trip at the HV busbar, RMS/EMT was simulated using Digsilent PowerFactory® software. The model, together with the resultant real and reactive power curves are shown in Appendix G – Figure G.1 – G.3. The results of the simulations to illustrate the response of the two load types are discussed in the Appendix G – Table G.1.

3.1.5 Under Load Voltage Tap Changer

In order to improve voltage quality and reduce losses, it is advisable to install reactive power and voltage elements in the power system. The elements can take the form of on load tap changers fitted to power transformers, capacitor banks, or static VAR compensators.

In transmission and distribution networks, transformers with variable tap ratios are frequently used. To adjust the tap ratio, a tap changer is used. These devices can either be fixed tap (which require energisation to change the tap) or be under load type voltage tap changers. The latter type gives greater flexibility since the voltage can be controlled manually or automatically without disturbing the power flow of the power system.

On load tap changers (OLTC) comprise different parts that can be summarised as follows [22]:

- Selector Switch: Allows for the selection of the active tap;

- Change Over Switch: Inverts the polarity of the tapped winding, thus allowing more tapping positions to be available;

- Transition Mechanism: This includes an arcing or diverter switch that allows for a smooth transition from one tap to another; and

- Driving Mechanism: This includes a motor, gearbox, and control system to drive the system.

To maintain an acceptable voltage profile in accordance with standard licencing requirements, distribution and transmission operators should make use of OLTCs that fall within the category of AVRs. In this scheme, an acceptable voltage profile is maintained without the intervention of network operators.

A typical under load tap changer logic is shown in figure 3.14.

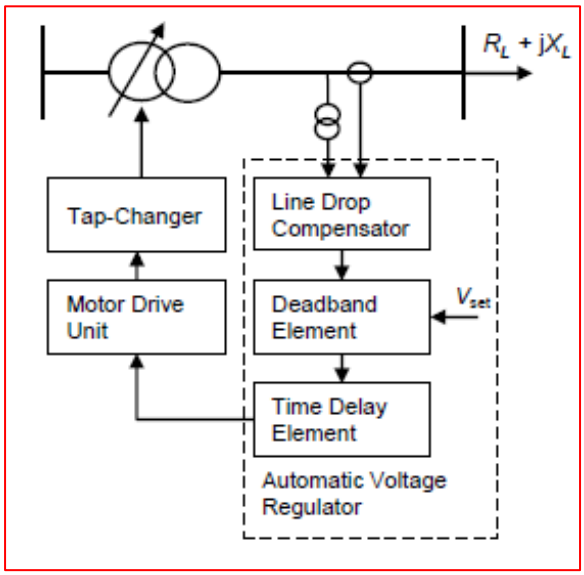

Figure3.14 : OLTC control scheme with load drop compensator [23]

From figure 3.14, it is seen that the AVR needs to maintain voltage around a predetermined value (Vset) within a certain tolerance as the load fluctuates during high and low demand cycles. As such, the scheme needs to measure voltage continuously at the regulation point. With the new schemes that use the circulating current limit to ensure that iron losses are kept to a minimum for the transformers, current measurement might also be required.

The different elements of the control scheme will be presented by using an actual implementation as shown below.

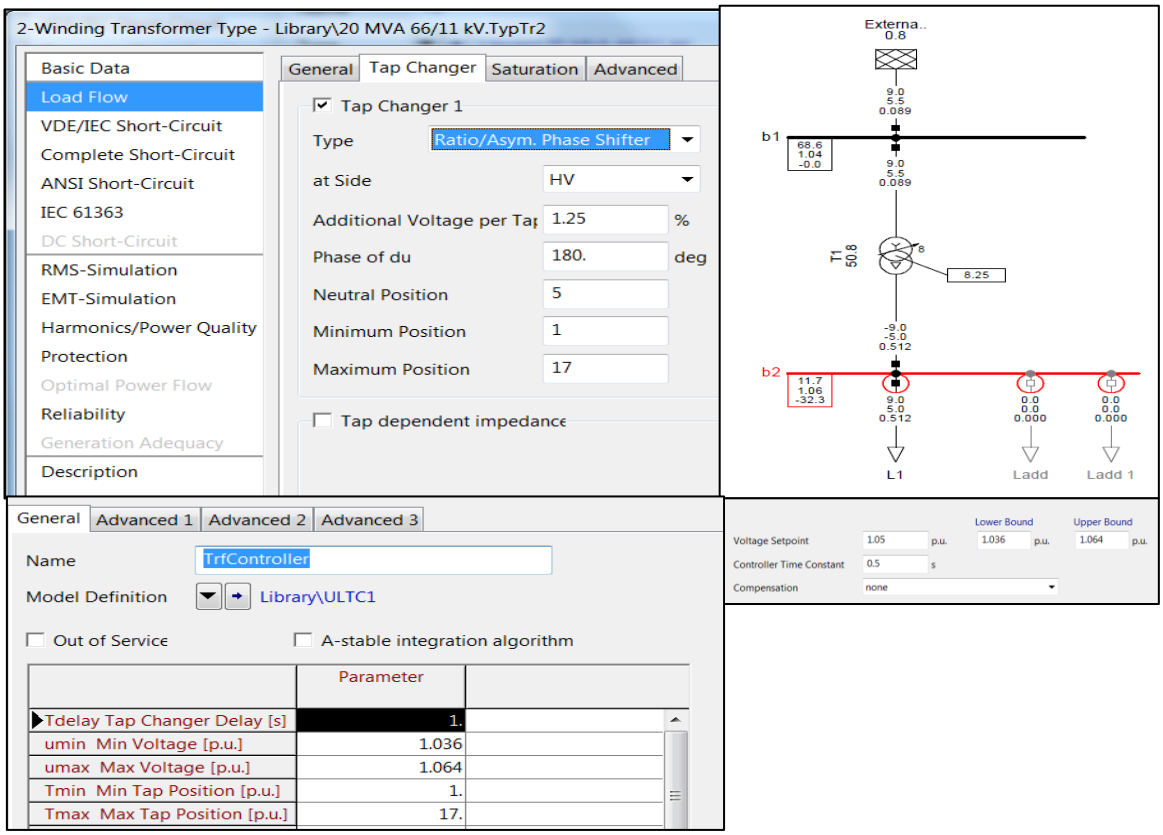

Figure 3.15 : OLTC control scheme set up for 66 / 11kV transformer

In this example, the transformer tapping arrangement is configured in the simulation programming Digsilent PowerFactory. To test the system, a sequence of load additions, as shown in table 3.3, is configured to test the correct operation of the OLTC control scheme.

Table 3.3 : Test sequence for OLTC operation

Sequence	Time (s)	Connect Load (MVA/pf)	Disconnect Load
1	-1	10/0.875	
2	0	7.5/0.9	
3	10	11/0.9	
4	30		11/0.9
5	40		7.5/0.9

The resultant voltage profile illustrating the actions of the voltage regulation scheme is shown below in figure 3.16 and 3.17, and a discussion of the major observations is provided in table 3.4.

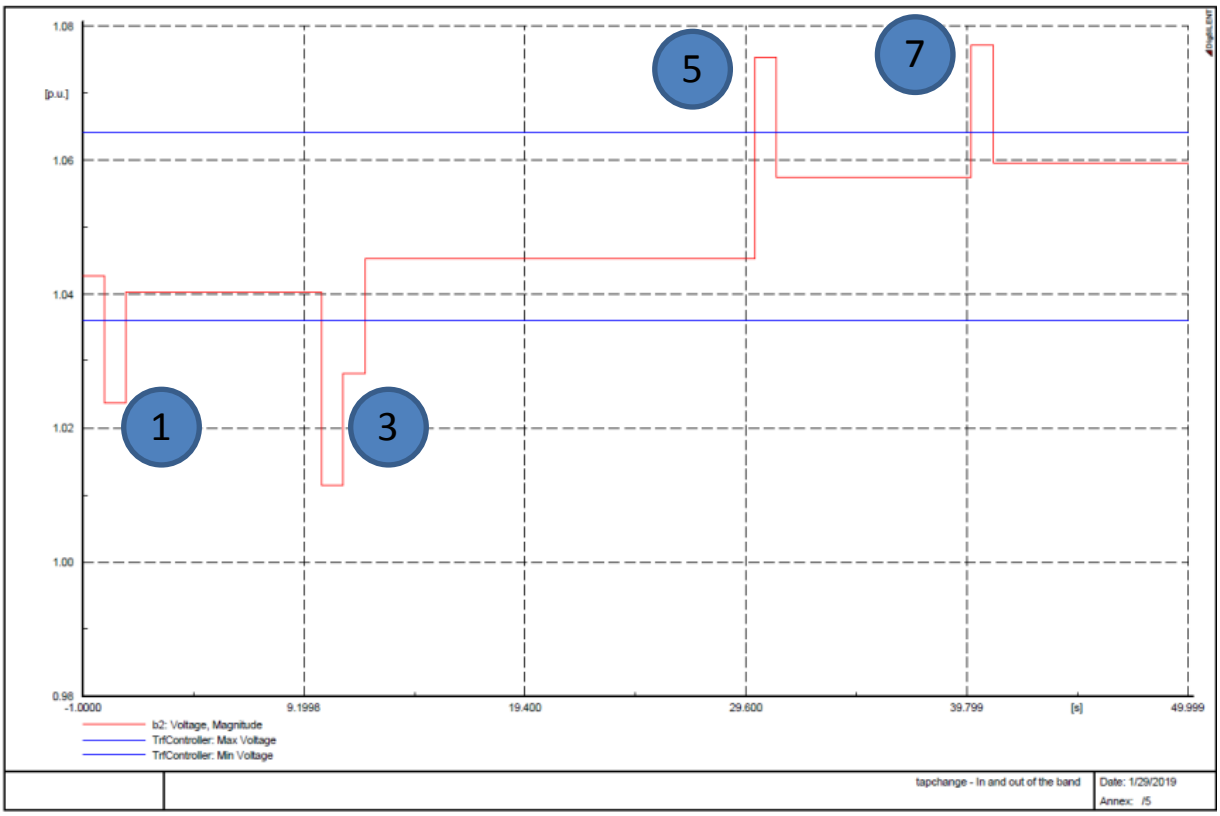

Figure 3.16 : OLTC control scheme set up for 66 / 11kV transformer OLTC control scheme operation showing how the tapping change the busbar voltage within the programmed bandwidth - 1.036pu and 1.064 pu voltage

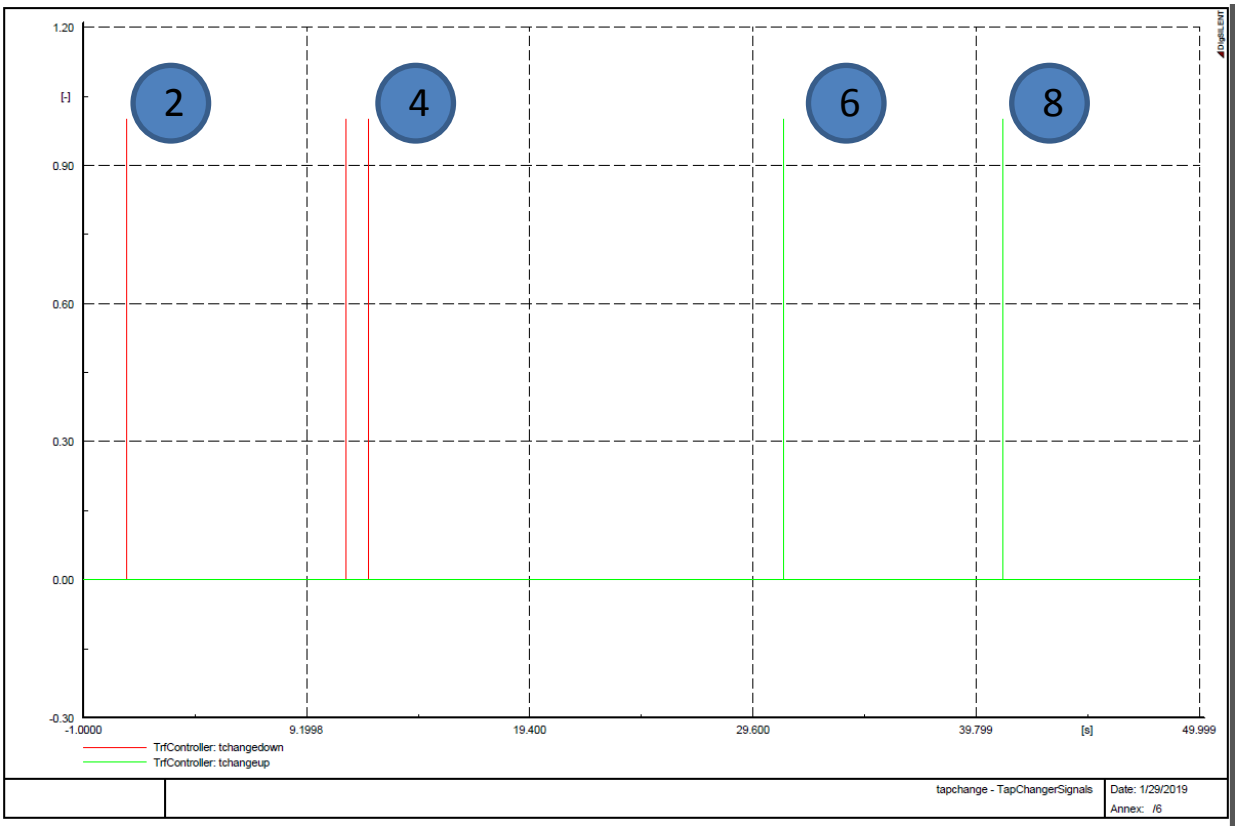

Figure 3.17 : OLTC control scheme set up for 66 / 11kV transformer OLTC control scheme operation showing how the tapchanging signals from the OLTC control scheme initiates tapping to keep the busbar voltage within the programmed bandwidth - 1.036pu and 1.064 pu voltage

Table 3.4 Sequence event during tap changing event with critical values highlighted

Legend	Time(s)
1	A load of 7.5MVA is switched in, thus the total load on the 20MVA transformer will be 17.5MVA. The voltage on the 11kV busbar drops to 1.024pu from 1.042pu.
2	To bring voltages into the required limits the OLTC taps one tap position down.
3	A load of 11MVA is switched in, thus the total load on the 20MVA transformer will increase to 28.5MVA. The voltage on the 11kV busbar drop to 1.011pu from 1.042pu.
4	To bring the voltage into limits, the OLTC need to tap 2 positions down.
5	A load of 11MVA is disconnected, thus the total load on the 20MVA transformer – 17.5MVA. The voltage on the 11kV busbar will rise to 1.075pu from 1.05pu.
6	To bring the voltage into limits, the OLTC need to tap up one position.
7	A load of 7.5MVA is disconnected, thus total load on the 20MVA transformer decrease to 10MVA. The voltage on the 11kV busbar will rise to 1.077pu from 1.06pu.
8	To bring voltage into limits, the OLTC need to tap up one position.

The under voltage regulator dynamic model has been successfully implemented in the 2003 DigSilent Powerfactory case file and the 2017 DigSilent Powerfactory case file. Further information on the on load tap changer frame, the tap changer controller script, as well as the set points for a particular example i.e. the Koeberg 400/132kV transformer, is shown in Appendix B section B2.

Chapter 4. Simulation and Results for Voltage Stability Analysis of Nuclear Power Plant

Network section 7.6.5 of the South African grid code refers to the integration of new power stations and states that transient stability shall be retained for the following conditions:

- "*A three-phase line or busbar fault, cleared in normal protection times, with the system healthy and the most onerous power station loading condition*"; or

- "*A single-phase fault,cleared in 'bus strip' times, with the system healthy and the most onerous power station loading condition*"; or

- "*A single-phase fault, cleared in normal protection times, with any one line out of service and the power station loaded to average availability*".

Taking into consideration the grid code requirement, as mentioned above and the events that occurred on 15 October 2003, a set of case studies concerning voltage stability is established.

Case: Incident on 15 October 2003

The base case for this voltage stability study is centred on the incident that occurred at 04h23 on 15 October 2003 involving Koeberg unit A. The particulars form part of a confidential report, thus the information that will be highlighted here will only be based on the sequence of events and the state of the network equipment at the time of fault. This information will assist with the assessment of the voltage stability analysis around Koeberg and surrounding networks. A description of the events follows.

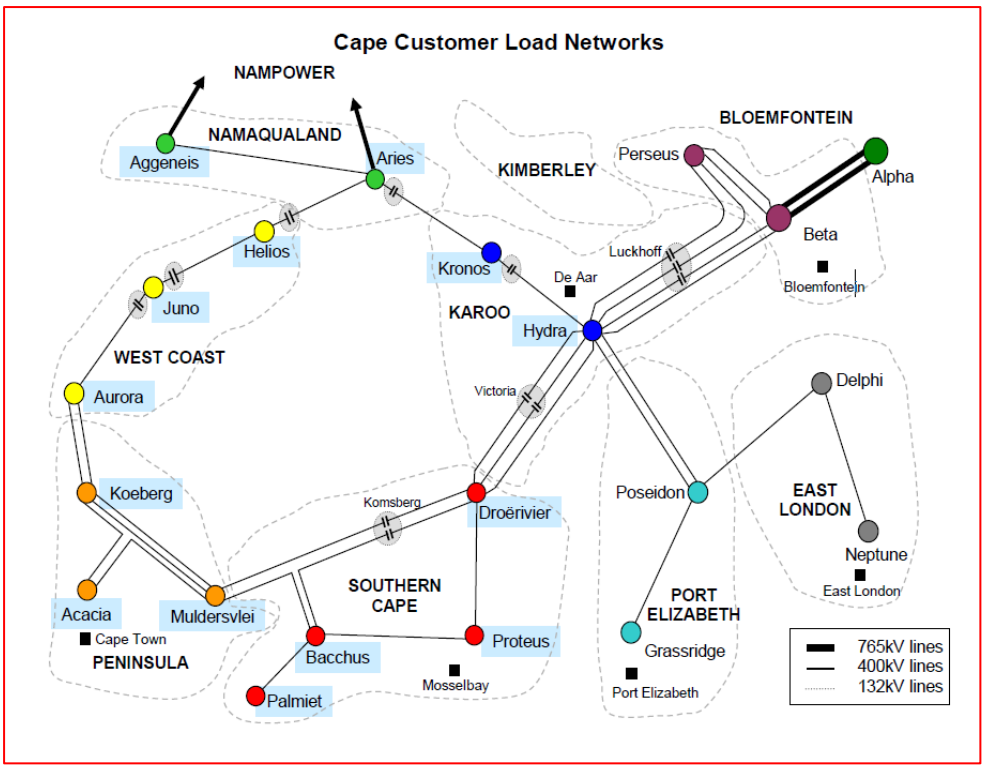

Figure 4.1: Network as on 15 October 2003 when 2 x Koeberg Units were out of service

In unit A, one of two units experienced a stator earth fault on the 24kV busbar, in particular in the blue phase. Figure 4.1 shows that the units are located within the Peninsula area of the Western Cape grid. The protection operated within 180ms. At the particular time, 04h23, unit B was on outage and the pump storage plants were in pumping mode [a total of 490MW]. At the time of the incident, the total Western grid load was 2516MW.

As a consequence of the incident, there was a drop on the power system to 49.95Hz and an oscillation of between 49.64 Hz and 49.95 Hz. Under-frequency and under voltage protection scheme [Namaqua Sands, Saldanha Steel, PetroSA] then initiated dropping of load and disconnection of the pump's storage schemes at 49.39Hz and 49.42Hz respectively. The total load shed was ~160MW. The particulars of the load shed and the triggers are summarised in Table 4.1

Table 4.1 : Load shed on 15 October 2003

Load name	Load lost as per customer report (MW)	Shedding load type
Pumping load		
Steenbras	96 MW	49.39 Hz (Under-frequency)
Palmiet	386 MW	49.42 Hz(Under-frequency)

Other loads		
Namaqua Sands	60 MW	Under-voltage trip
Saldanha Steel	70 MW	Under-voltage trip
Petro SA (Mossgas)	15 MW	Under-voltage trip
PPC Riebeek West	7 MVA	Under-voltage trip
PPC De Hoek	8 MVA	Under-voltage trip
Total	642	

For the following days, part of the network experienced high voltages due to the 100MVar shunt reactor being out of service. The situation was rectified when a series reactor was by-passed, thus increasing the admittance of the overall Western Grid and reducing the busbar voltages.

For a more complete view of the power system equipment involved in the incident, table 4.2 reflects the time line of the events to link up with the load that was affected as shown in table 4.1.

Table 4.2 : Sequence of events on 15 October 2003

TIME	EVENT
04H21	Koeberg unit 1 tripped on earth fault on 24 kV busbar.
04H23	Palmiet units tripped on under-frequency from pumping to SCO pumping mode
	Steenbras units 3 & 4 tripped on under frequency
	Drakensberg units 1 & 2 tripped on under frequency
04H50	City Council of Cape Town (CCC) offered a 45 MW mutual assistance
06H01 – 20H08	Van Der Kloof unit 2 generated out of merit to reduce transfer to the Cape
06H24 – 07H25	Palmiet unit 1 operated in Generation Mode
06H44 – 21H45	Gariep unit 4 generated out of merit to reduce transfer to the Cape
06H50 – 21H23	Gariep unit 3 generated out of merit to reduce transfer to the Cape
07H00 – 10H57	Palmiet unit 2 operated in Generation Mode
07H00 – 24H00	Nampower reduced load by 132 MW
07H25 – 07H36	Palmiet unit 1 operated in Pumping Mode
08H05 – 21H19	Gariep unit 2 generated out of merit to reduce transfer to the Cape
10H24 – 12H03	Palmiet unit 1 operated in Generation Mode
11H25 – 23H03	Palmiet unit 2 operated in Generation Mode
18H07 – 22H05	Palmiet unit 1 operated in Generation Mode
19H00 – 20H31	Gariep unit 1 generated out of merit to reduce transfer to the

	Cape
19H05 – 20H03	Van Der Kloof unit 1 generated out of merit to reduce transfer to the Cape
19H29 – 19H52	Acacia unit 1 generated out of merit to reduce transfer to the Cape
19H41 – 20H30	CCC assisted with 45 MW (Mutual Assistance)
20H50 – 22H40	EB Steam reduced load by 44 MW:
	Tygerberg - 15 MW
	Paarl - 10 MW
	CCC - 19 MW
23H01 – 00H00	Gariep unit 4 generated
23H07 – 00H00	Palmiet unit 1 operated in Pumping Mode
23H30 – 00H00	Palmiet unit 2 operated in Pumping Mode

At the time of the incident, the Koeberg unit B was out for scheduled refuelling, leaving the grid vulnerable with regard to the reactive and generation resources available to the grid. The peaking generation station that provides reactive support to the system was in pumping mode at the time of the incident, as per table 4.2. All other lines in the Western Cape were in service, with a peak of 2516MW recorded.

As a result of the incident a 19.5% Z-class dip was experienced which lasted for 600ms. The system frequency went as low as 49.4Hz at certain substations, prompting to the operation of the UFLS schemes. The frequency profile confirming this is shown in figure 4.2 below. The recordings of the measured profiles are for Tutuka power station, Muldersvlei substation and Palmiet power station.

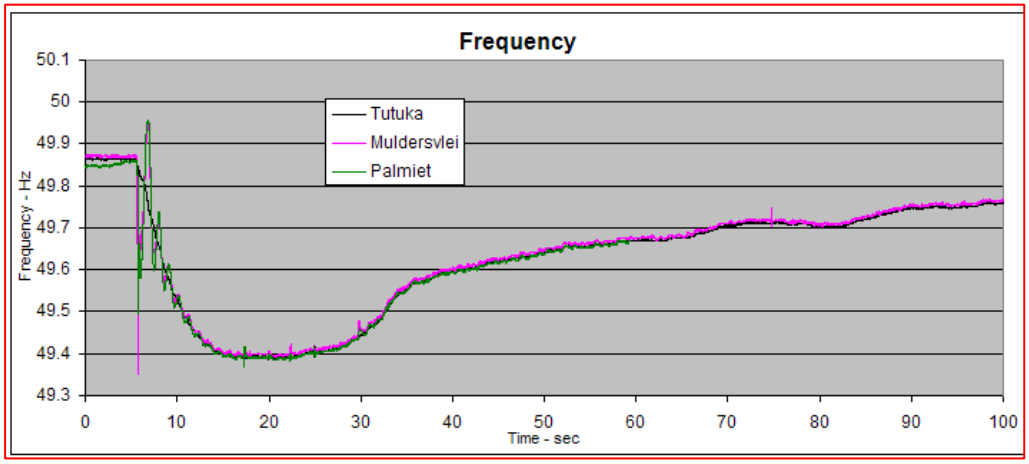

Figure 4.2 : Frequency profile for the earth fault at Koeberg earth fault (Source: ESKOM incident report)[35]

Due to the shedding of the load, several substations experienced high voltage. The problem was further exaggerated by the unavailability of 2 x 100MVar reactors that play a critical role in the voltage regulation in areas of high voltages, in particular in

the Northern Cape. The 100MVar reactor was out –of –service due to a component failure.

The net effect on the customer side can be summarised as follow:

- A customer that uses a DC arc-furnace, as shown in figure 4.3 that adds a load of approximately 60MW was disconnected from the system – "*the plant Tronox Namakwa Sands produces high-titania slag for the TiO2 pigment industry and low-manganese pig iron for foundries producing castings for the automotive and engineering components industry*" [27]. The plant consists of two DC current electric arc furnaces that require power of 25MW and 35MW respectively.

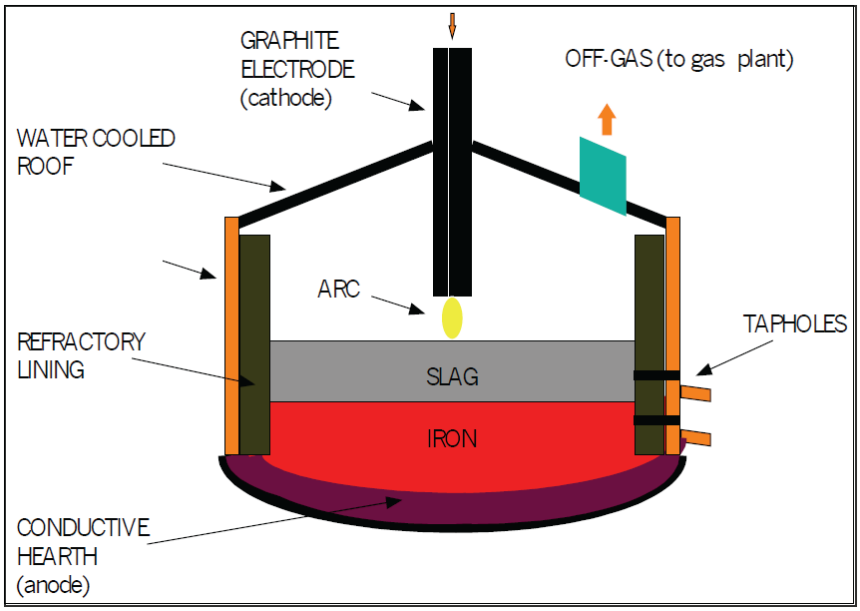

Figure 4.3 : Schematic of a DC arc furnace used at Namakwa Sands [27]

- At Saldanha Steel, a voltage dip caused the variable speed drives (VSD) used for the roller mills to operate. Operation of the VSDs caused the plant to be offline for 45 minutes;

- PetroSA's gas-to-fuel operation was affected as the equipment has sensitivity to a 20% voltage dip that last longer than 40 minutes;

- A shut down of cement manufacturing company PPC's crusher mills, resulting in a loss of 15MW.

The net effect on the grid equipment can be summarised as follow:

- When the incident occurred, Palmiet and Steenbras pumping power stations were in motor mode. Both tripped on UFLS at 49.42 Hz and 49.39Hz respectively.

The under frequency phases that operated and the duration of the under frequency events are in table 4.3 below:

Table 4.3 : Different phases of the UFLS operation and duration for condition

Tripping phase	Frequency setting (Hz)	Required duration at specified frequency for load shedding command to be issued (seconds)
Phase 1	49.6	32.3
Phase 2	49.5	3.2
Phase 3	49.4	2.3

- In total, the event resulted in 642MW being shed, causing the total demand to reduce to 1874MW.

Contingency action following the event included notifying customers of the situation, requesting City of Cape Town authorities to be ready in the event that emergency supplies would be required, the availing of a peaking power station (a total of 540MW) by Eskom generation, and the placing on standby of gas fired and pump storage (865 MW). Other than this, interruptible customers (i.e., those customers that have agreements with ESKOM to reduce their load on request by the utility) were requested to shed load, availing a total of 85MW.

4.1 Simulation software: DigSilent PowerFactory® software

The effect of the loss of a generator in the Western Cape grid has not been analysed using a simulation package before. In this dissertation, the abnormal network will be reconstructed to analyse the effect that the reduction of generation within the isolated Western Cape power grid, which is situated far from the main generation centre, will have on the loading of the lines and reactive compensation devices. This is to determine the critical busbars on the Western Cape's power grid to avoid a voltage collapse or a total power system blackout.

To model the transient and steady state phenomenon on the power system, DigSilent PowerFactory® software (which has three levels of simulation functionality) will be used. Some of the functions of the simulation software are [10]:

- "*A basic function which uses a symmetrical steady-state (RMS) network model for mid-term and long-term transients under balanced network conditions*";

- "*A three-phase function which uses a steady-state (RMS) network model for mid-term and long-term transients under balanced and unbalanced network conditions, i.e. for analysing dynamic behaviour after unsymmetrical faults*"; and

- *"An electromagnetic transient (EMT) simulation function using a dynamic network model for electromagnetic and electromechanical transients under balanced and unbalanced network conditions. This function is particularly suited to the analysis of short-term transients"*.

"*In addition to the balanced RMS simulation events, unbalanced fault events can be simulated, such as: single-phase and two-phase (to ground) short-circuits, phase to phase short-circuits, inter-circuit faults between different lines, and single- and double-phase line interruptions. All of these events can be modelled to occur simultaneously or separately, hence any combination of symmetrical and asymmetrical faults can be modelled.*

Time-domain simulations in DigSilent PowerFactory® are initialised by a valid load flow, and DigSilent PowerFactory® functions determine the initial conditions for all power system elements (including all controller units and mechanical components). These initial conditions represent the steady-state operating point at the beginning of the simulation, fulfilling the requirements that the derivatives of all state variables of loads, machines, controllers, etc., are zero".

4.2 Analysis of PV curve: case 2003 vs 2017 fault

The single line diagrams used in the assessment of the 2003 and 2017 case studies are shown in figures 4.5 and 4.6.

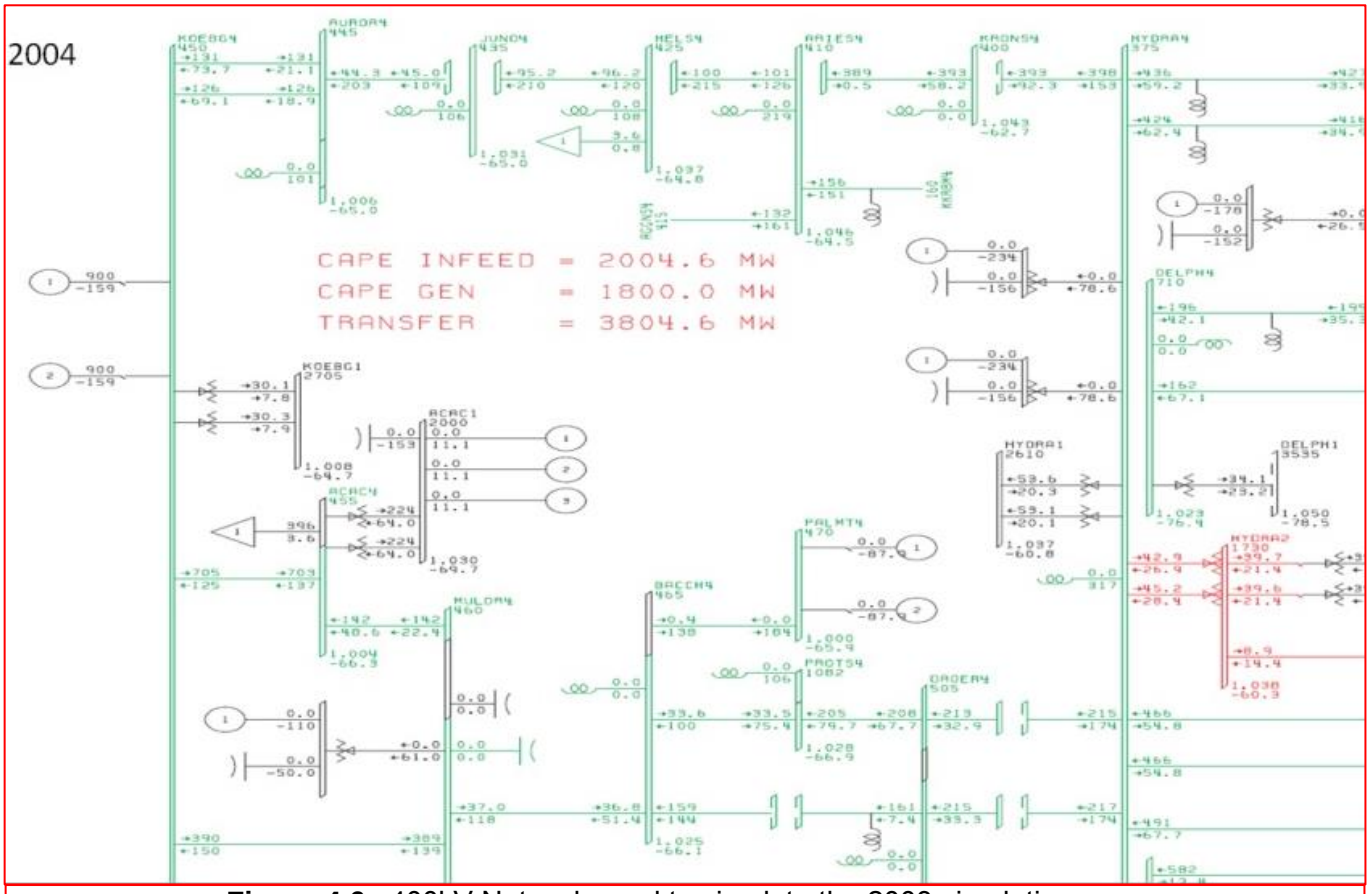

Figure 4.6 : 400kV Network used to simulate the 2003 simulation case

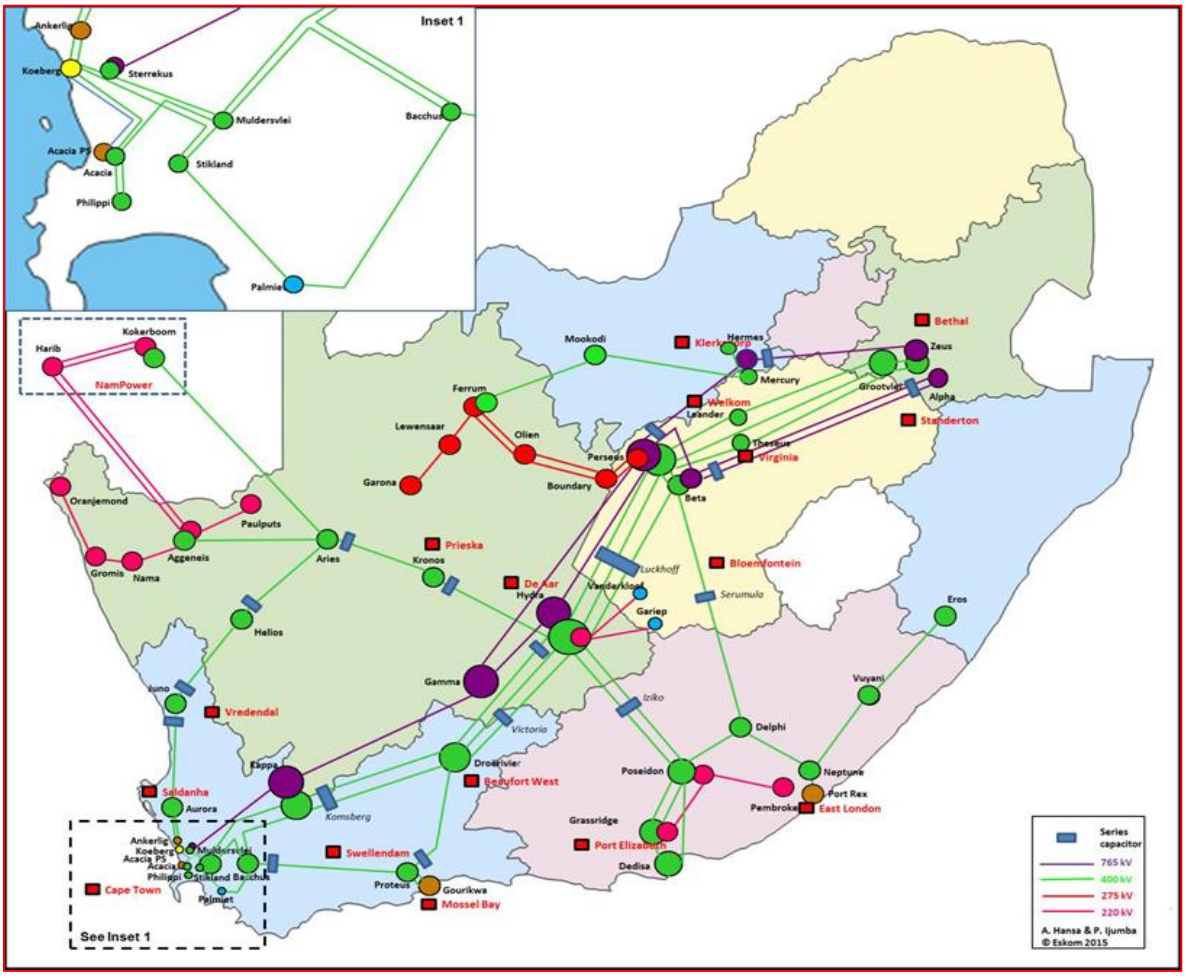

Figure 4.5: 400kV network used to simulate the 2017 simulation case

For the evaluation, the load was scaled to present the loading on the morning of the fault on 15 October 2003. The loading of the critical substations is tabulated in Appendix A and shown in Table 4.4 for the 2003 and 2017 cases simulated.

Table 4.4 : 2003 and 2017 400kV Loads evaluated to in the PV and QV curves analysis

No	Connection	Year: 2003	P(MW)	Q(MVar)	Year: 2017	P(M)	Q(MVa)
1	A	Koeberg - 132kV	122	32		122	32
2	AB				Ankerlig		
3	B	Aurora - 132kV	114	3.5		114	3.5
4	C	Juno - 132kV	14.25	4.684		14.25	4.684
		Juno - 66kV	16	13		16	13
5	D	Helios -22kV	6	-1		6	-1
6	E	Aries	53.8	-83.4		53.8	-83.4
7	F	Kronos					
8	G	Hydra					
9	G1				Gamma		
10	G2				Kappa		
11	H	Droerivier-132kV	19	-14		19	-14
12	I	Proteus-132kV	341	75		341	75
13	I1				Gourikwa		
14	J	Bacchus	341	8		341	8
15	K	Palmiet					
16	L	Muldersvlei-132kV	557	138		557	138
17	KL				Stikland	342	56
18	M	Acacia - 132kV	249	-7		249	-7
		Phillipi - 132kV	485	37		485	37

What was considered when compiling Table 3.4 was that since the 2003 fault, various network reconfigurations have taken place, in particular, the introduction of a new transmission substation to cope with increases in load demand in the Western Cape power grid. The additional power stations include the introduction of 2100MW of peaking generation in the form of Open Cycle Gas Turbine (OCGT's) generation to cope with peak-time demands and the strengthening of the transmission network through the introduction of the 765kV line in addition to the 4 x 400kV transmission lines from Hydra substation in De Aar. The Ankerlig OCGT power station close to Atlantis is shown in figure 4.7.

Figure 4.7 : Ankerlig Power Station in the Atlantis area, which is not far from the Koeberg NPP, has 9 x 150MW OCGT units)

For the studies performed, the peak loading for the period to be studied, i.e., 2017, loading was kept the same as the 2003 fault except for the addition of a new network and a new load added to the 400kV (known as Stikland substation)network. Shown in Appendix A is the status of the reactive devices; this information is critical in the study of any voltage phenomenon. The peak loading was recorded at the Muldersvlei South loading; this equated to 557MW and reactive power of 138MVar.

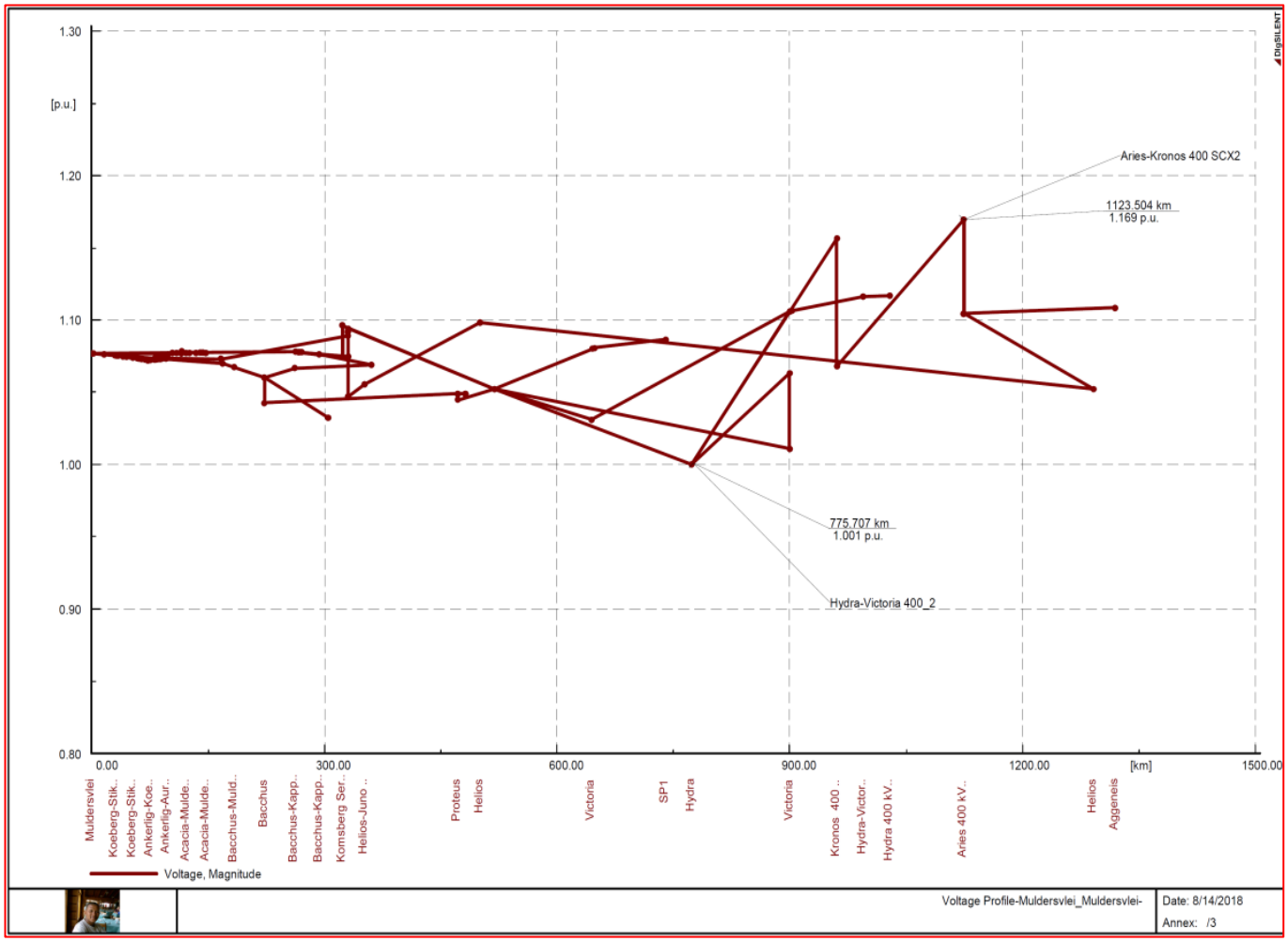

Figure 4.8 : 400kV Load Profile networks in the Western grid where NPP is present - 2003 Configuration-

The resultant voltage profile for the 2003 network configuration shown in figure 4.8 reveals:

- The highest voltage was 1.169pu at the Aries 400kV busbar; and

- The lowest recorded voltage was 1.001pu at the Victoria-Hydra series capacitor bank.

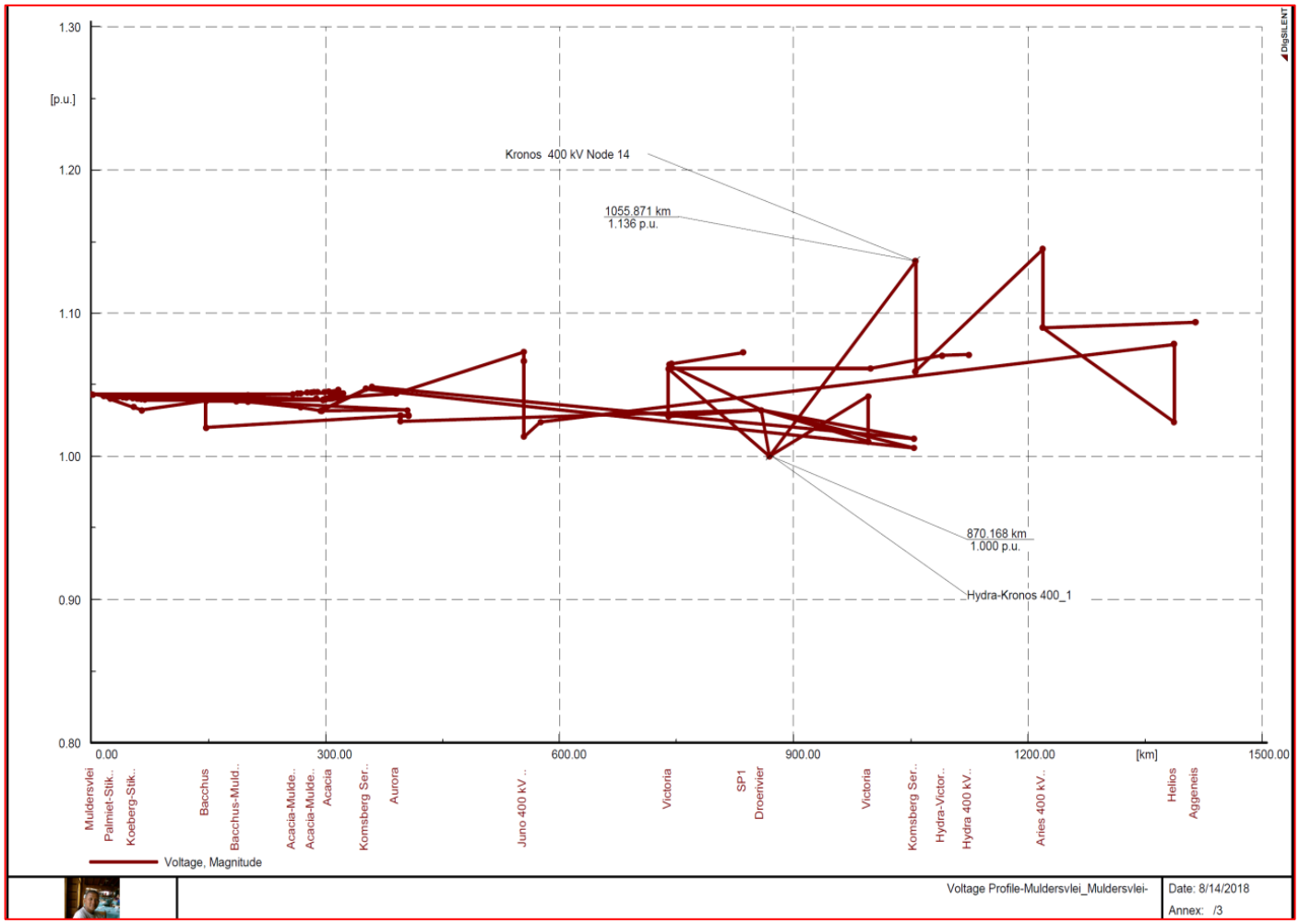

Figure 4.9: 400kV Load Profile networks in the Western grid where NPP is present - 2017 Configuration

The resultant voltage profile for the 2017 network configuration shown in figure 4.9 reveals:

- The highest voltage was 1.138pu at the Kronos 400kV busbar; and

- The lowest recorded voltage was 1.00pu at the Hydra busbar.

To pin point the critical busbars other than those highlighted by the voltage profiles heat maps were generated in the DigSilent PowerFactory® simulation software. The results of the evaluations shown in figure 4.10 to 4.13 indicate the critical network equipment on a heating scale based on the loading and the voltage low and high values throughout the network. The result of the critical points is described as part of the description of the figure. The result of this evaluation is also useful to determine the PV and PQ busbars to be evaluated and to recommend the technical solutions to improve the network stability margins of the overall grid.

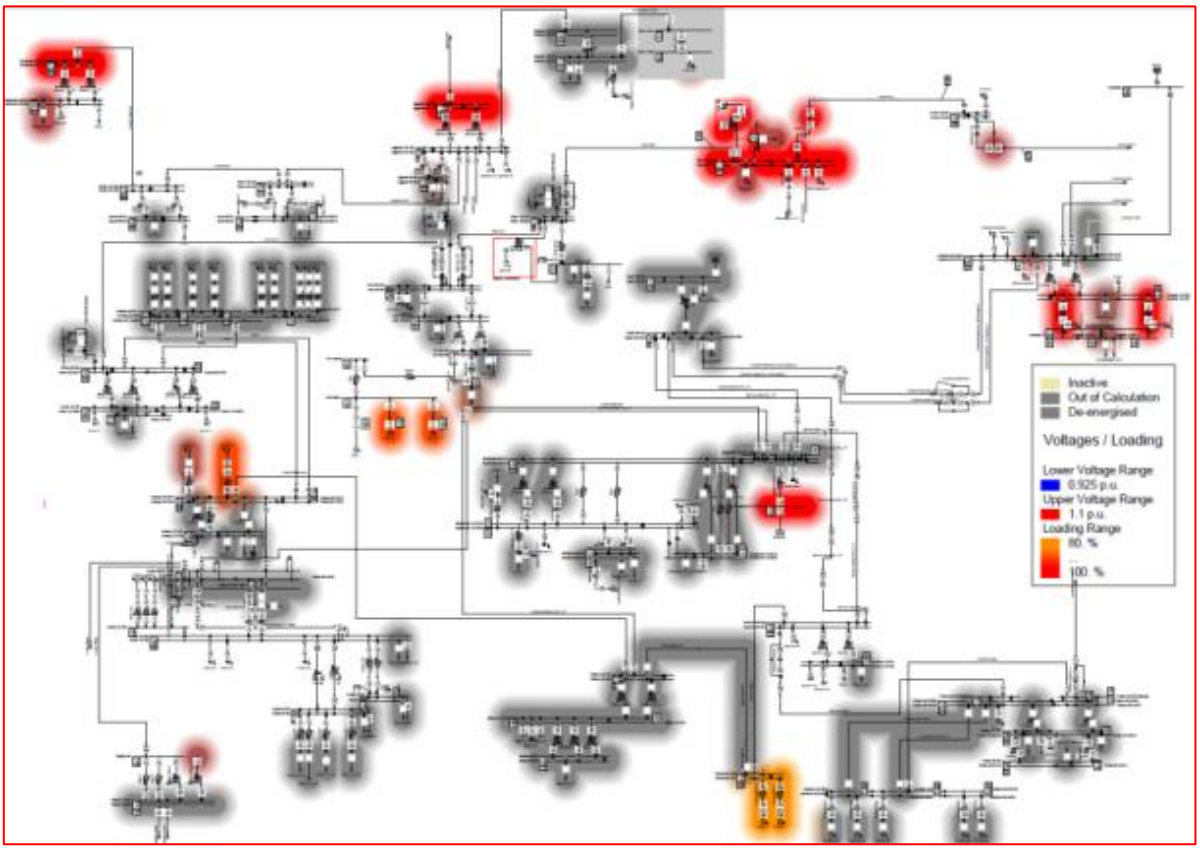

Figure 4.10: Heat Map for Time **04h00 - 2003** on the day of the fault showing the high voltages that were present and the high loading due to pumping at the time of the faults at Palmiet SS

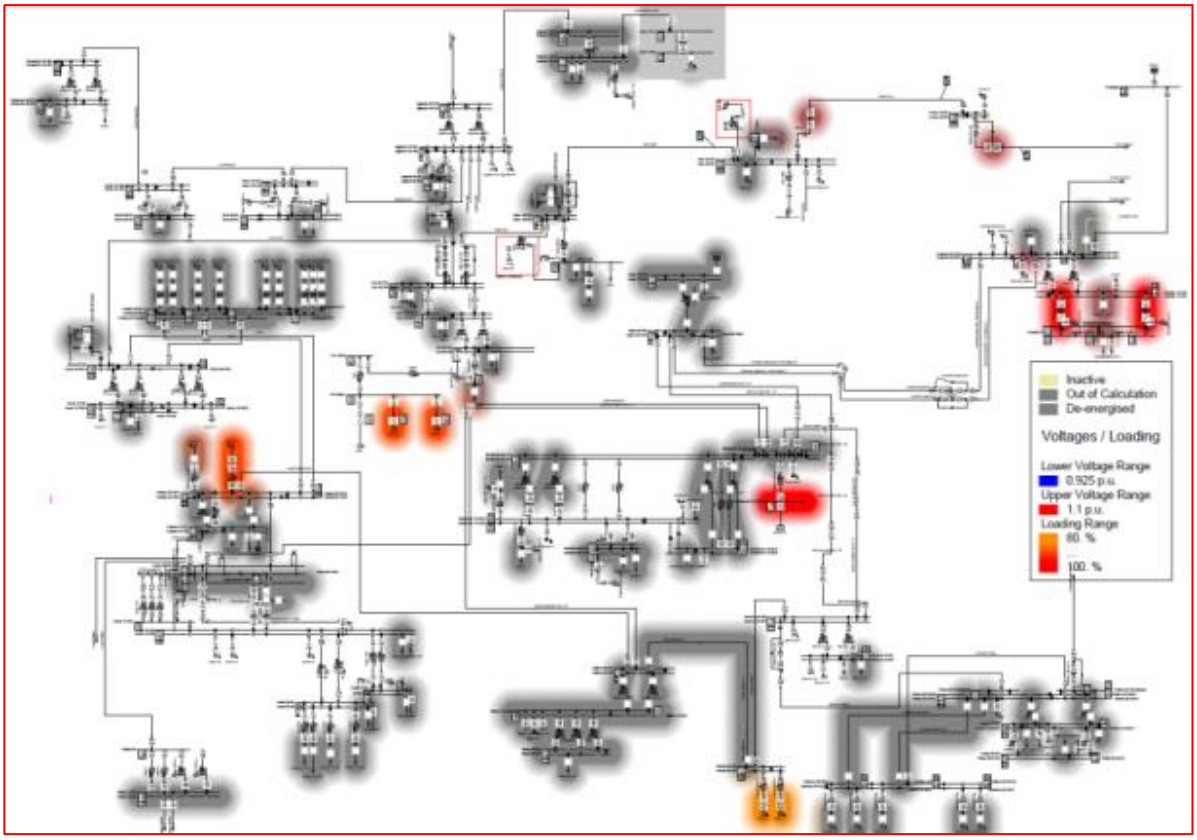

Figure 4.11: Heat Map for Time **12h00pm - 2013** showing less high voltages in the network

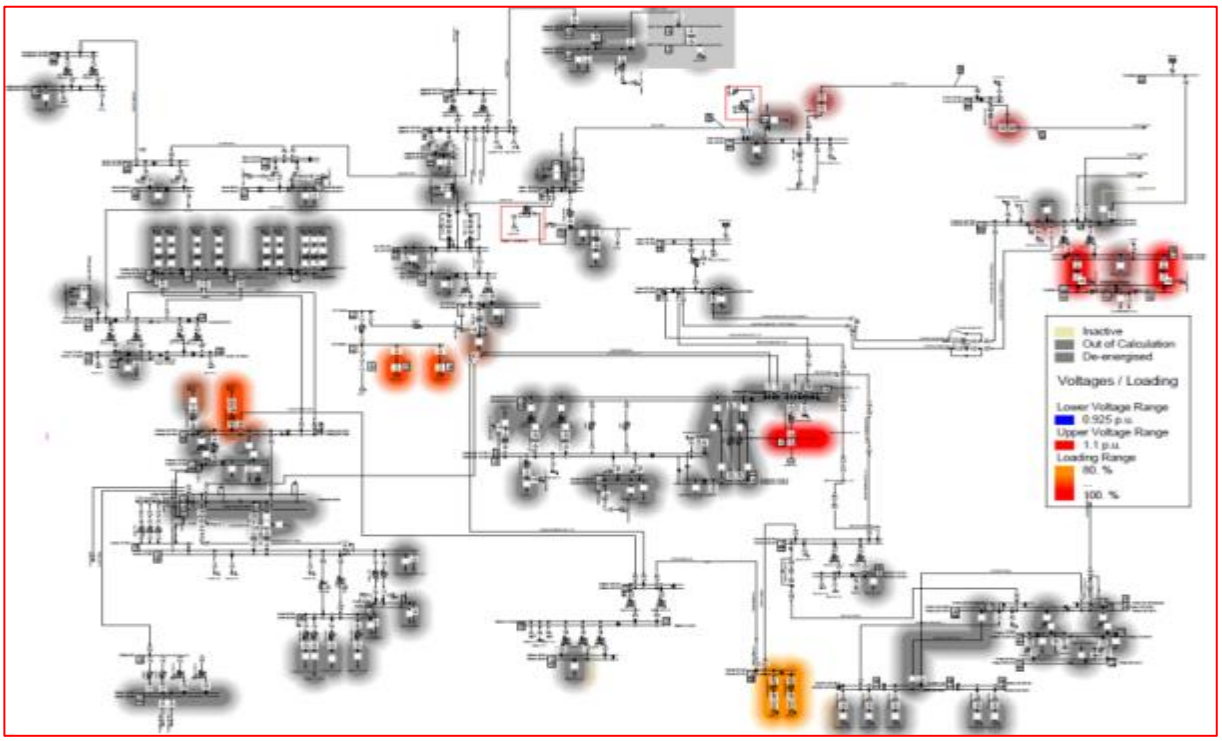

Figure 4.12: Heat Map for Time **04h00 - 2017** showing no high voltages as was the case in 2003 due the network strengthening and the addition reactive devices at Kappa transmission station

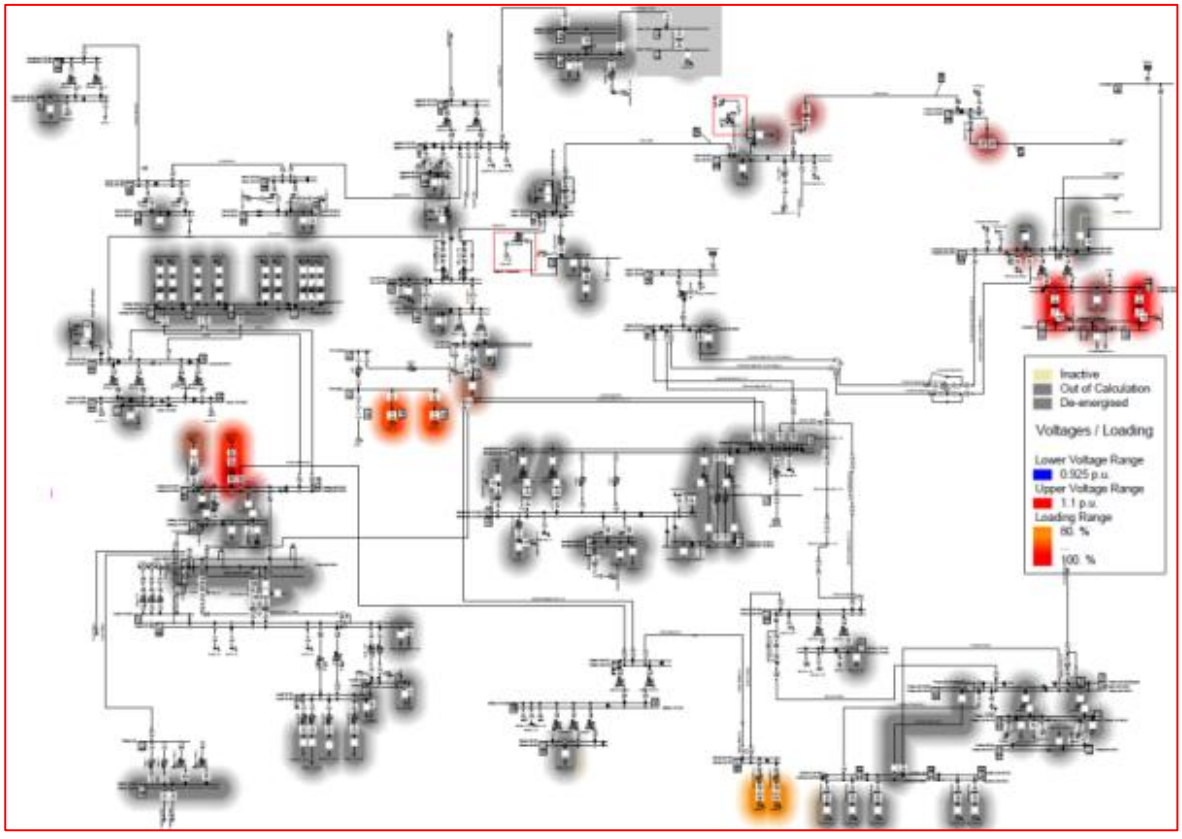

Figure 4.13 : Heat Map for Time **12h00pm - 2017** on the day of the fault showing the high voltages that were present and the high loading due pumping at the time of the faults at Palmiet SS

Given the system loading and in-service reactive devices before the network abnormality, no accurate knowledge exist as to the how close the system was to voltage instability due to this event. A tool that has been proposed to assist to answer this particular question in recent years is the so-called PV and PQ curve analysis methods for voltage stability evaluation. The fundamentals of this method are explained in Appendix B.

The evaluation of the PV curve is carried out in the Digsilent PowerFactory® simulation environment using the PV script V1.0 as described in Appendix A6. The PV curve analysis is performed at all load busbars for the sake of being thorough to determine the margin of MW before the onset of a voltage collapse. This critical point, also known as nose point, is located in the system where the equilibrium is lost, due to the change in the system loading [30]. This is considered in the analysis to determine the loadability margin or the amount of MW required in load shedding schedules in order to avoid a potential system blackout due to voltage collapse around the NPP.

Two cases are simulated:

- Case 1: Network results for the case before the n-2 contingency took place, i.e., 1 x Koeberg out of service for maintenance; and

- Case 2: Network results after fault has taken place, i.e., 2 x Koeberg power stations out-of-service.

The resultant PV curves are shown in Appendix C section C3. Observations made from the generated PV curves are based on:

- available MW (maximum loadability); and

- a ranking of the highest margin to the lowest margin of real power availability.

A summary of the results of the simulations for the 2003 and 2017 network cases is presented below.

Table 4.5: MW margin before voltage collapse for 400kV busbar and the rate of change of the voltage for four different scenarios of the PV curve analysis

Substation	Working point (MW)	MW margin 2003 Scenario-1 x Koeberg in service (MW)	Rate of change dy (volts)	MW margin 2017 – 1 x Koeberg in service (MW)	Rate of change dy (volts)	MW margin 2003 – 0 x Koeberg in service	Rate of change dy (Volts)	MW margin 2017 – 0 x Koeberg in service	Rate of change dy (Volts)
Bacchus	341.00	1261.70	-0.20	1636.80	-0.20	920.70	-0.15	1364.00	-0.18
Muldersvlei	557.00	1169.70	-0.16	1448.20	-0.13	557.00	-0.16	1002.60	-0.21
Phillipi	485.00	1164.00	-0.14	1406.50	-0.14	630.50	-0.21	921.50	-0.17
Acacia	250.00	921.30	-0.16	946.54	-0.14	622.50	-0.20	796.80	-0.17
Proteus	341.00	818.40	-0.21	1091.20	-0.23	647.90	-0.19	988.90	-0.20
Droerivier	19.00	596.60	-0.08	602.30	-0.06	585.20	-0.08	604.20	-0.06
Juno	14.25	497.33	-0.16	498.75	-0.14	456.00	-0.18	480.23	-0.15
Aries	53.80	247.48	-0.11	247.48	-0.11	242.10	-0.11	247.48	-0.11
Aurora	114.00	247.48	-0.11	991.80	-0.19	570.00	-0.26	752.40	-0.23
Koeberg	122.00	195.20	-0.06	195.20	-0.03	183.00	-0.06	195.20	-0.05
Helios	6.00	156.60	-0.04	155.40	-0.04	159.60	-0.05	157.80	-0.04

The data was plotted to indicate which busses had the highest and lowest MW margin; this is shown below in figure 4.14.

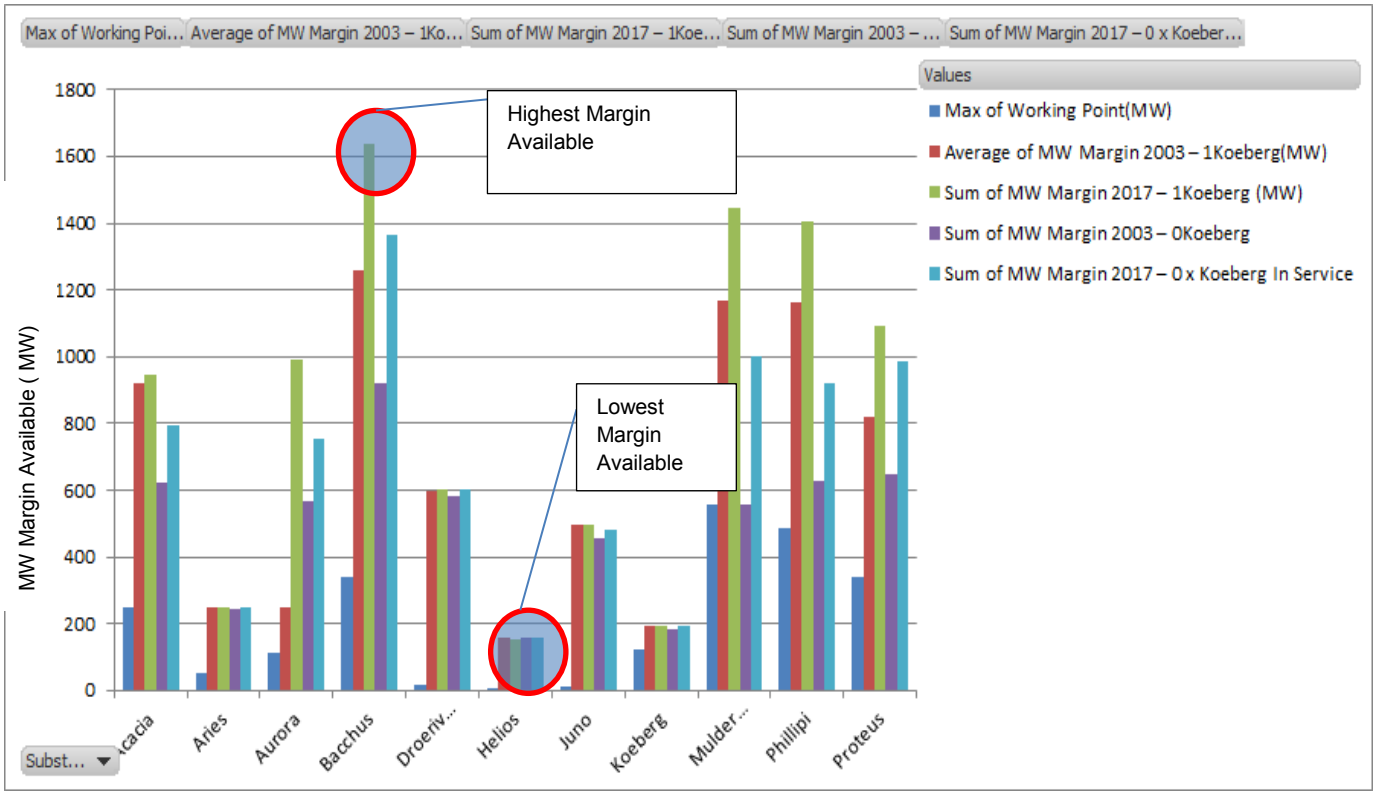

Figure 4.14: Tabulated results visualising MW reserves for the different 400kV busbars

- Bacchus substation has the highest MW reserve available before a potential collapse takes place;

- Helios, which recorded some of the highest voltages, has low fault levels. In addition, the lowest loading has the least MW margin before a voltage collapse can occur;

- At Koeberg, the MW margin is ~200MW; thus, given the current loading of 122MW, the load at the substation can grow to 322MW at 132kV level before a voltage collapse scenario is possible; and

Further to the above, the graph gives a clear indication as to the amount of load that needs to be shed if a voltage collapse is to occur.

The rate of change of a voltage can also give an indication as to how rapid an event can take the power system in to a critical contingency. In figure 4.15 the rate of change for the400kV busbars are plotted.

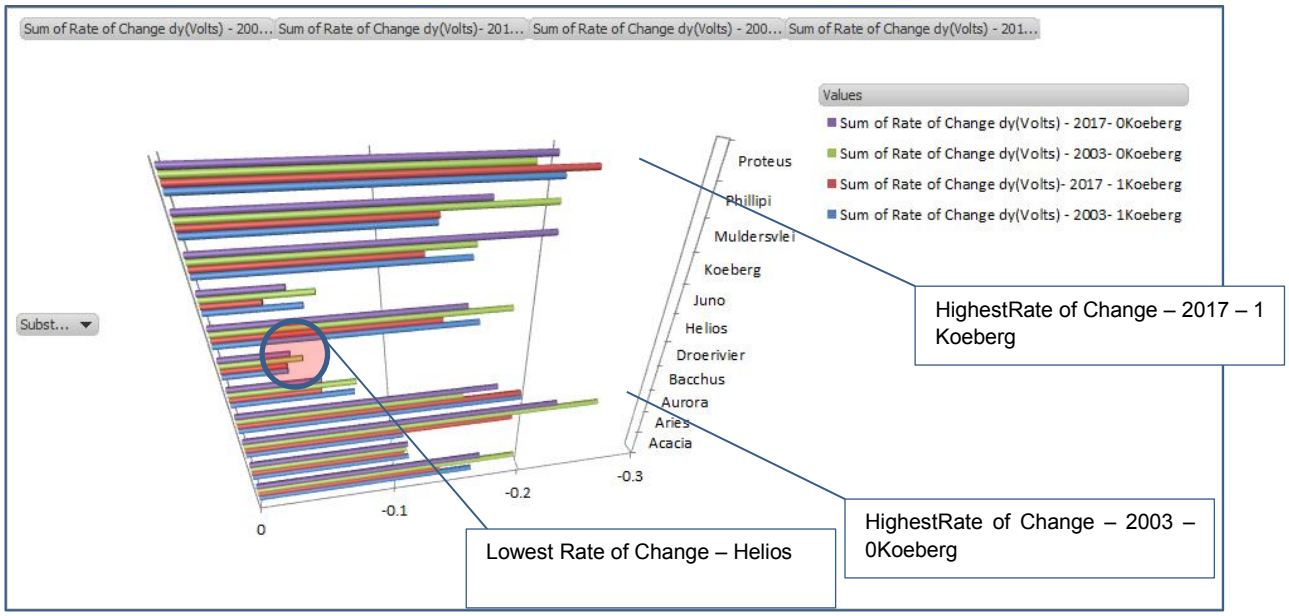

Figure 4.15: Rate of change of voltage (dV) for the different 400kV busbars

The following observations are made:

- The highest rate of voltage change (dV) for the 2017 case with 1 Koeberg in service, i.e,. a rate of 0.227 was recorded at Proteus substation;

- The highest rate of voltage change (dV) for the 2003 case with zero Koeberg in service, i.e., a rate of 0.26 was recorded at Aurora substation; and

- The lowest rate of change was recorded for the substation that showed the lowest MW margin available, i.e., Helios. Although the MW margin is low, the rate of voltage instability will be slow at this busbar.

4.3 Analysis of QV curve case 2003 vs 2017 fault

The evaluation of the QV curves is carried out in the Digsilent PowerFactory® simulation environment using the QV script V1.0 (as described in the Appendix A6). The QV curve analysis is performed at critical load busbars as identified during the PV analysis. At these load busbars, a temporary static generator is applied, which consumed zero real power while, the reactive power is varied to observe the MVar requirement. In the script described in Appendix D section D2, the reactive power is incremented and voltage and reactive power recorded in a matrix. During this test, the load needs to put out of service and transformer tapping needs to be deactivated. The resultant QV curves are shown in Appendix D section D3.

The summary of the results of the simulations for the 2003 and 2017 network cases is presented below.

Table 4.6: MVar reserve for five critical transmission station busbars

Substation	MVar margin 2003 – 1 x Koeberg in service (MW)	MW margin 2017 – 1 x Koeberg in service(MW)	MW margin 2003 – 0 x Koeberg in service	MW margin 2017 – 0 x Koeberg in service
Koeberg	224.80	223.00	230.86	225.98
Muldersvlei	1649.52	1749.52	1212.59	1427.76
Proteus	918.57	918.57	885.72	885.72
Phillipi	1252.17	1064.76	971.34	865.42
Juno	357.99	388.84	349.19	329.68

In figure 4.16, the data is plotted to show which busses had the highest and lowest MVar margins:

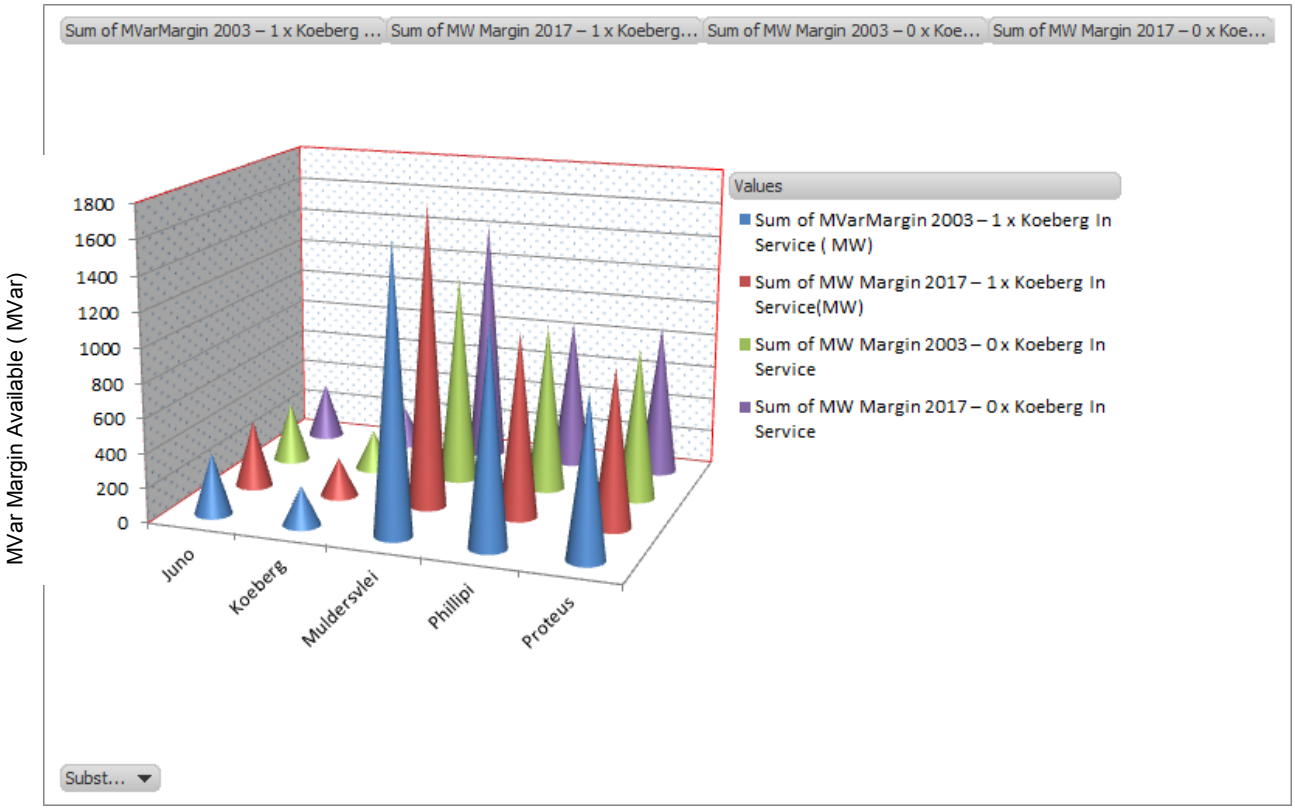

Figure 4.16: Resultant graphic representation showing MVar margins of critical busbars in the different QV simulation cases

The following observations are made:

- All substations at the critical busbars have a MVar reserve margin both for the 2003 and the 2017 case ;

- The highest available MVar margin before a voltage instability could potentially occur is at Muldersvlei, and the value observed was 1749.52MVar for the 2017 with 1 Koeberg in service case; In 2003 the MVar reserve was 100MVar less than in the 2017 case;

- The Koeberg margin of 200MVar corresponds with the machine MVar limitation; and

- The lightly loaded, low fault level busbar of Juno shows the second lowest MVar available It has a value of 357.99MVar for the 2017 case with one Koeberg and a higher margin of 388.84MVar for the 2003 case

4.4 Dynamic voltage stability analysis case 2003 vs 2017

For configuring the dynamic model to simulate the events of 2003 and evaluate the network response, the approach that was taken was:

- To only configure daily profiles for critical load busses. These were identified as Koeberg 132kV load, Muldersvlei 132kV load, Proteus 132kV load, Philippi 132kV load, and Juno 132kV load. The different profiles configured are shown in Appendix E and are based on the load profile of 11 July 2017, a peak day for the Western Cape Grid. The morning (a.m.) section of the profile has similar characteristics in loading as that of the morning of 15 October 2003; and

- To test if the model is in a working state, the Koeberg dynamic model was calibrated, as this would test the critical clearing times (by applying a three-phase fault at the generator's 24kV terminals for different clearing times and obsesrving the machine transient response). The results of the calibration are shown below in Figures 4.17 and 4.18.

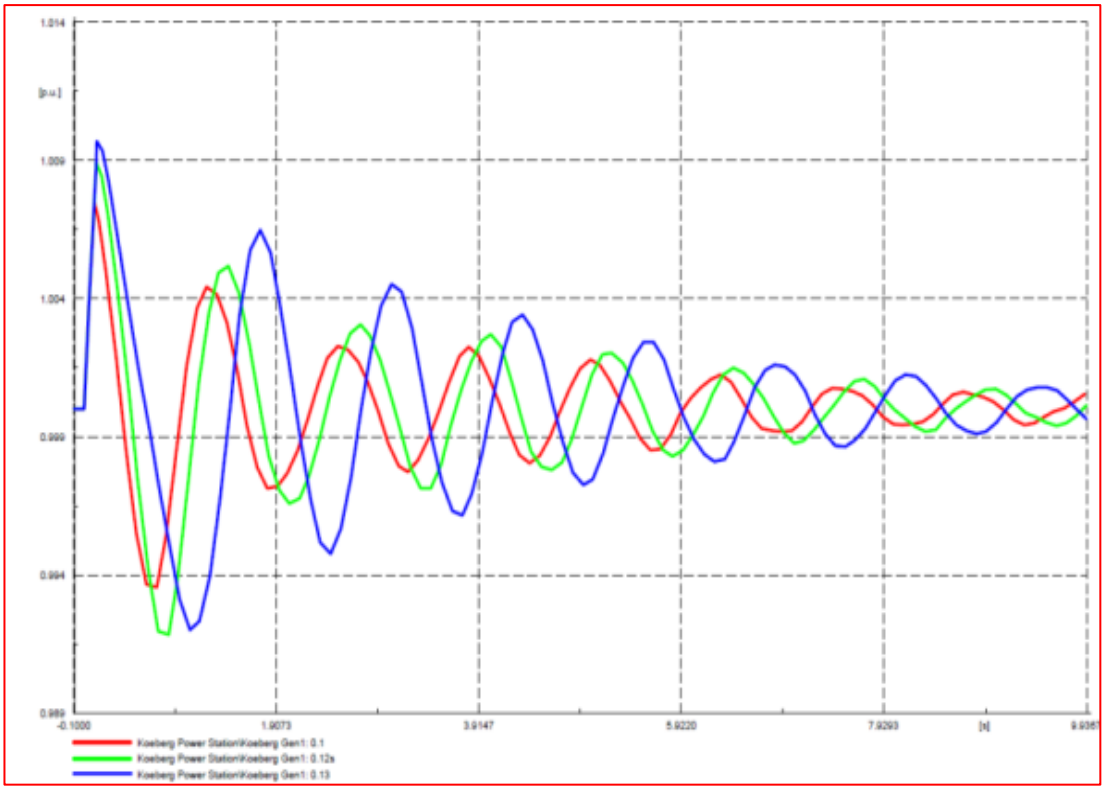

Figure 4.17: Koeberg in-service unit reaction to solid busbar fault for clearing times of 0.1, 0.12 and 0.13 seconds. i.e the machine stable for the worst case fault applied)

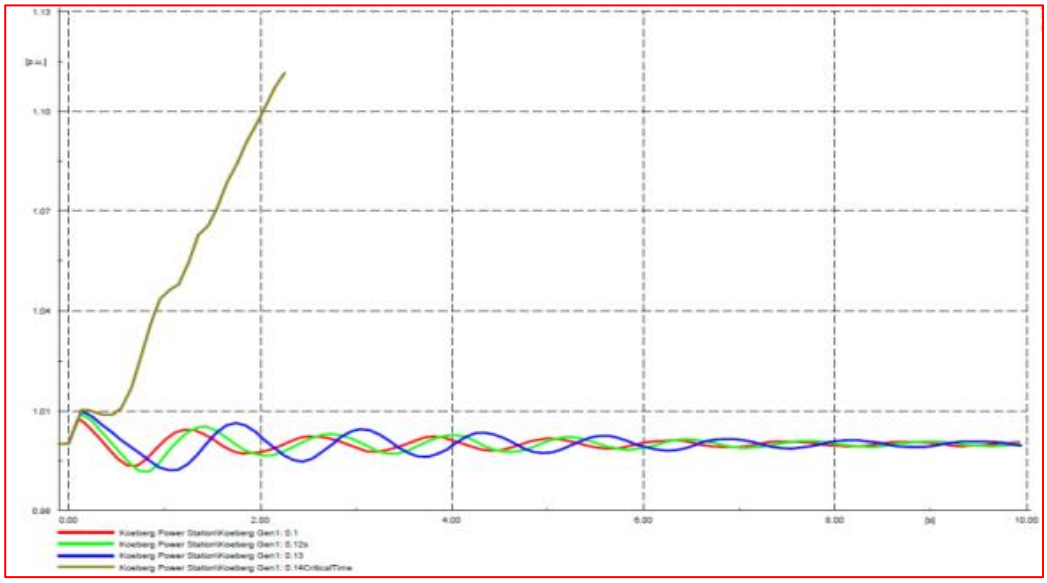

Figure 4.18: Koeberg in-service unit reaction to solid busbar fault. The graph illustrates an unstable situation if the clearing time is >0.14seconds after fault

The cases that are studied when evaluating the dynamics of the event in 2003 and the response after the network strengthening that occurred are listed below:

Case 1

Perform RMS/ EMT simulation (runtime 1 minute). Network configuration with 1 x Koeberg unit out of service as per the before-network fault — 2003 vs 2017 — and a trip event on 1 x Koeberg unit . The sequence configured for the dynamic studies is shown in Appendix F.

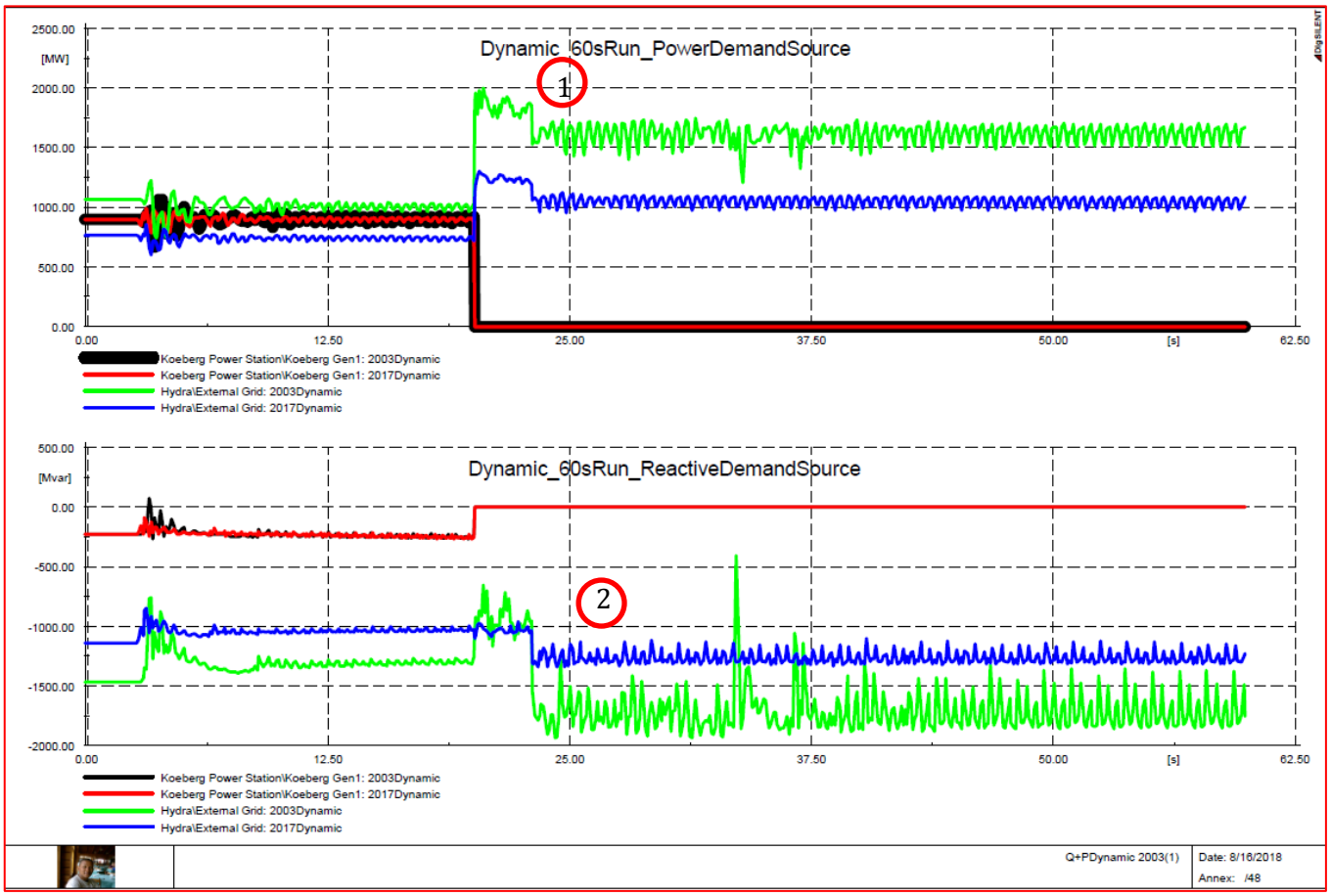

Figure 4.19: Case 1 simulation results: P and Q Dynamics of Western Cape grid sources — before and after the Network Event

The following observations are made for figure 4.19:

- The overall oscillation in the grid has significantly dampened down since the network changes that took place after 2003 – r*eference label nr2 on figure 4.19.* These changes included the strengthening of the 400kV network, the introduction of the 765kV lines into the Western Cape grid and the addition of reactive support equipment in the form of shunt reactors and shunt capacitors. The improved system damping is observed on both the MVar and MW demand plots;

- The MVar demand signal has less of an oscillation at the time of the unit tripping for the 2017 case compared to the 2003 case – *reference label nr2 on figure 4.19*.

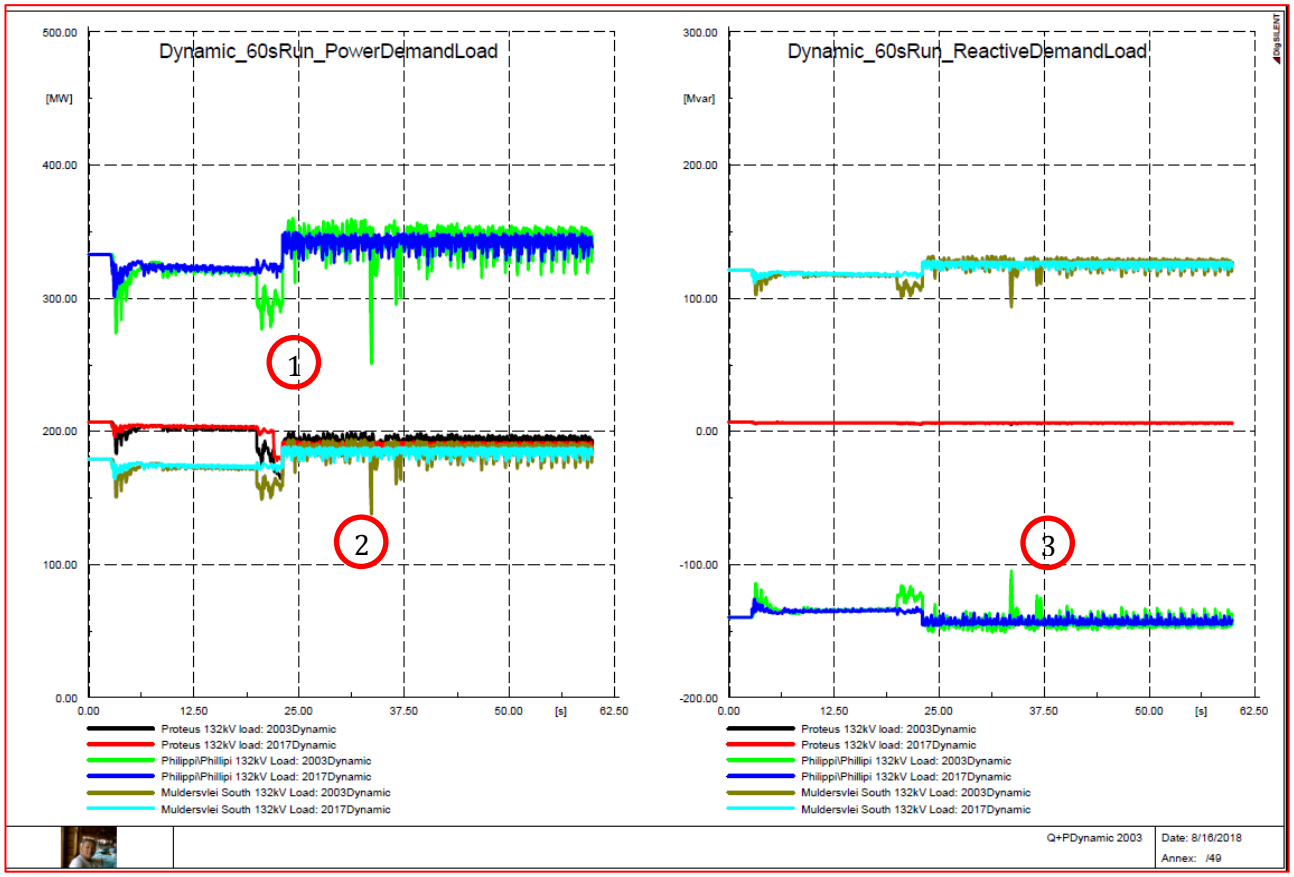

Figure 4.20: Dynamic load Q demand and critical loads power demand behaviour for dynamic simulation

The following observations are made with regard to figure 4.20:

- Immediately following the unit trip and the load shedding event at time 20 and 23 seconds respectively, the power demand on the Phillipi load dips for the 2003 case; however, for the 2017 case, load demand is stable and no power dip is observed – *reference label nr 1 on figure 4.20*

- After the load shedding event at time 22 seconds, a power dip is observed at both the Muldersvlei and Phillipi loads for the 2003 case; no initiating event is programmed at time ~31.25 seconds. This is confirmation of the fact that the 2003 case was more transient and instable for large events such as the unit trip – *reference label nr 2 on figure 4.20*; and

- After the unit trip, reactive demand at the Phillipi substation increased (this is a typical characteristic of a constant power load) – *reference label nr 3 on figure 4.20.*

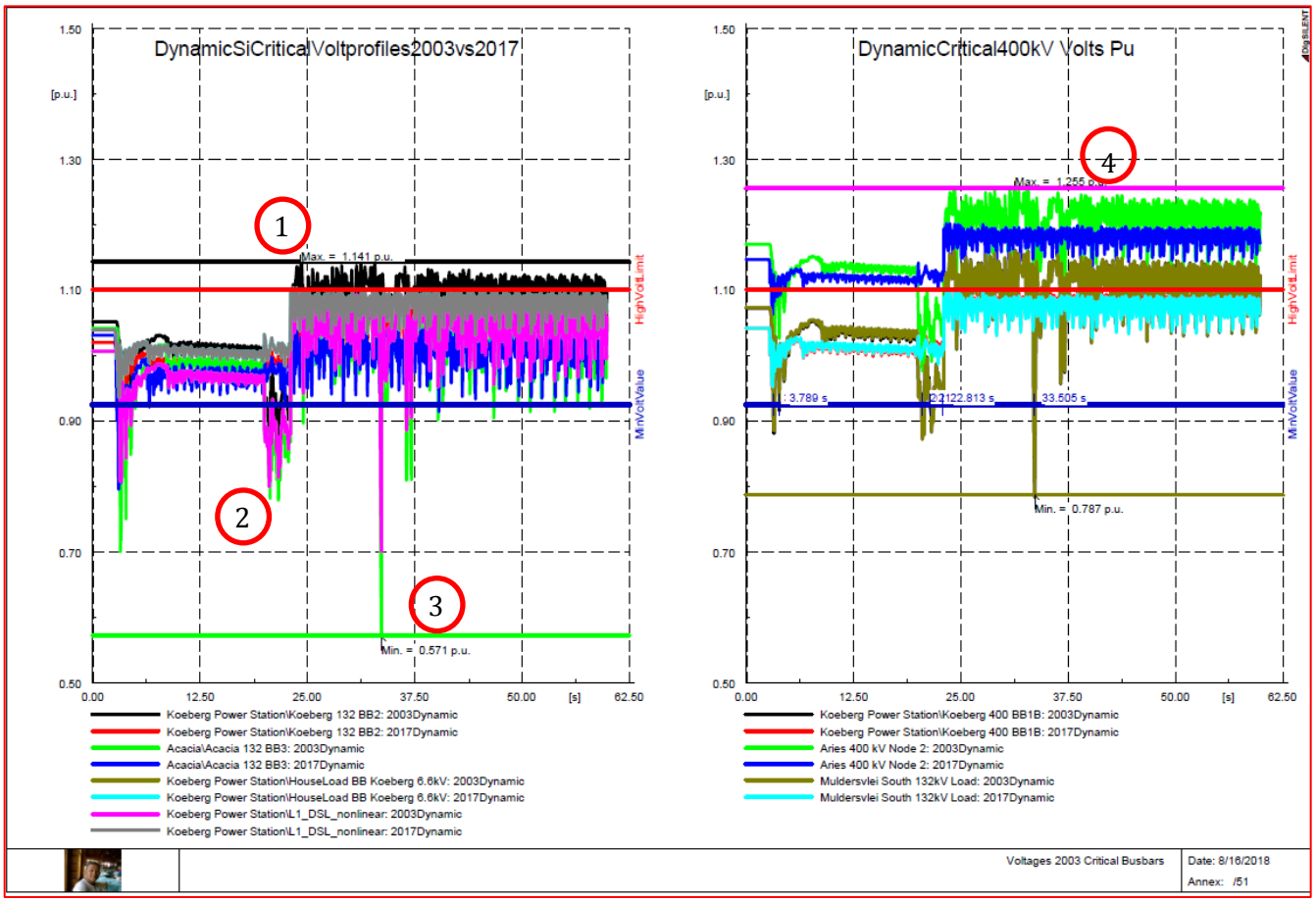

Figure 4.21 : Dynamic load and critical busbar voltage measurements for the 2003 and 2017 fault cases

The following observations are made with regard to figure 4.21:

- The maximum busbar voltage observed during the RMS/ EMT simulation was at Koeberg's 132kV busbar following the load-shedding event. The voltage rose to 1.141pu – *reference label nr 1 on figure 4.21*. The voltage rise in the network observed through simulation is confirmation of what was recorded on the day of the NPP unit trip event ,

- After the unit trip in the 2003 case, the dynamic load connected to the 6.6kV busbar dropped from 1.0pu to ~0.85pu – *reference label nr 2 on figure 4.21*-, which is an unhealthy voltage for the critical cooling system of an NPP. For the 2017 case the voltage observed for the dynamic load connected to the 6.6kV busbar was 1.05pu Thus no low voltage was not observed in the 2017 case, again showing the impact of the network improvements had on the overall network transient stability;

- As with the Phillipi event at time ~31.25 seconds, the 132kV busbar at Acacia, which serves as the off-site supply for Koeberg, dropped from 1.05pu to ~0.571pu – *reference label nr 3 on figure 4.21*. This is not an acceptable voltage for a NPP and can lead to a unit tripping onto the back-up generator

supply as a means of ensuring a more stable supply for the core cooling system and other essential house loads. At the same time for the 2017 case no voltage drop is experienced and the voltage stays stable around 1.0pu ;

- Sustained high voltages of 1.255pu for a period more than 27 seconds, - *reference label nr 4 on figure 4.21* were observed on the Aries 400kV BB after the unit operation and implementing of load shedding. This served as confirmation of the actual events as described in the recordings of the day. The reason for this was due to the unavailability of a reactor at Juno substation.

Case 2

Perform quasi-dynamic simulation (run time 1 day) with events as per event on 15 October 2003 and as if the same events would have occurred on 15 October 2017 with the improvements and expansion of the 400kV network.

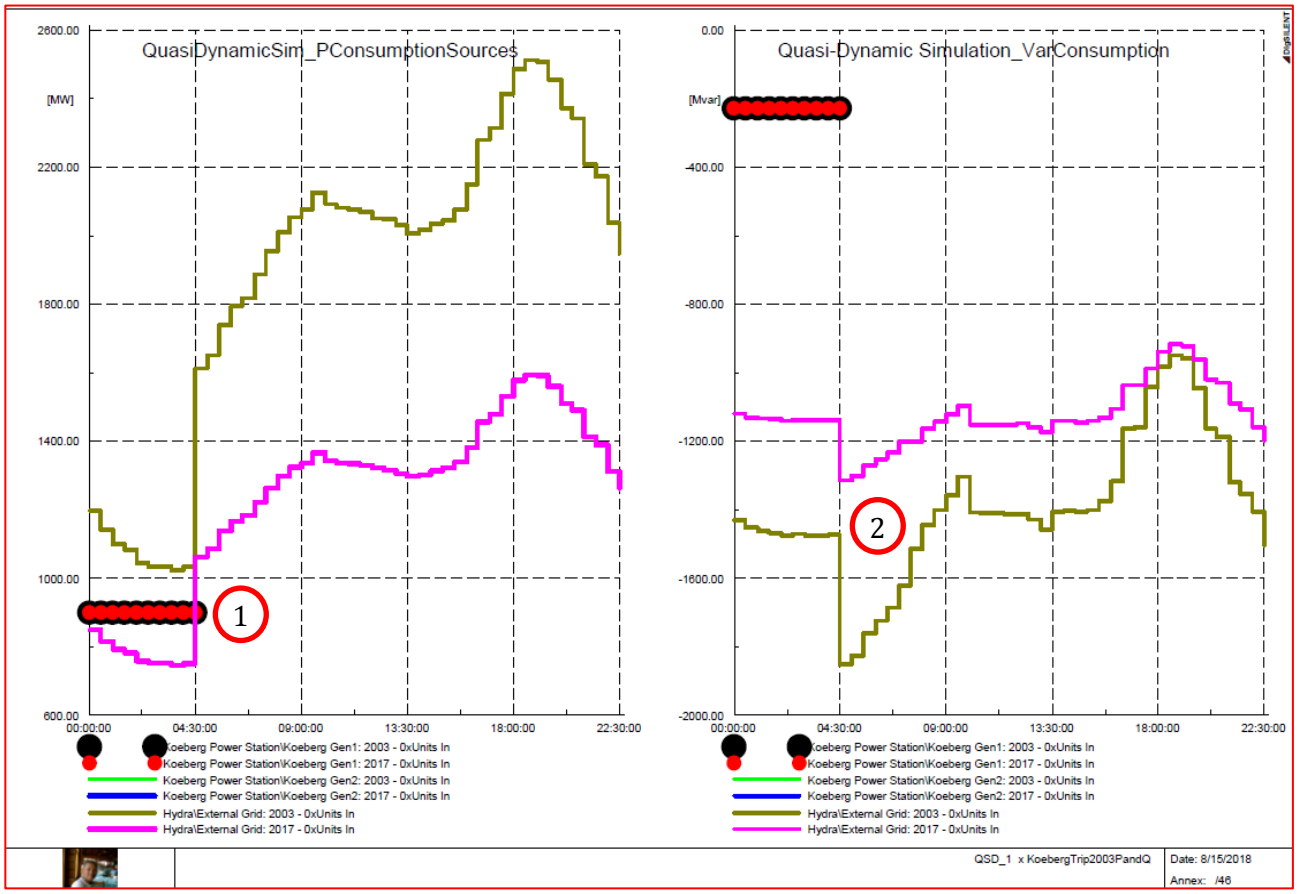

Figure 4.22: Quasi-dynamic simulation — sources response for case 2

The following observations are made with regard to figure 4.22:

- The overall demand on the external grid decreased for the 2017 case. It decreased to ~1000MW from 1600MW post the unit trip. This have been mainly due to the fact that the 765kV network have been commissioned in the year 2017, thus reducing the demand on the 4 x 400kV lines coming into the Western Cape grid- *reference label nr 1 on figure 4.22*; and

- As expected, MVar demand of the overall system decreased from 1400MVar in 2003 to 1100MVar in 2017. Thus a reduction of 20% overall over the 14 year period due to network strengthening and the introduction of reactive compensation devices - *reference label nr 2 on figure 4.22* .

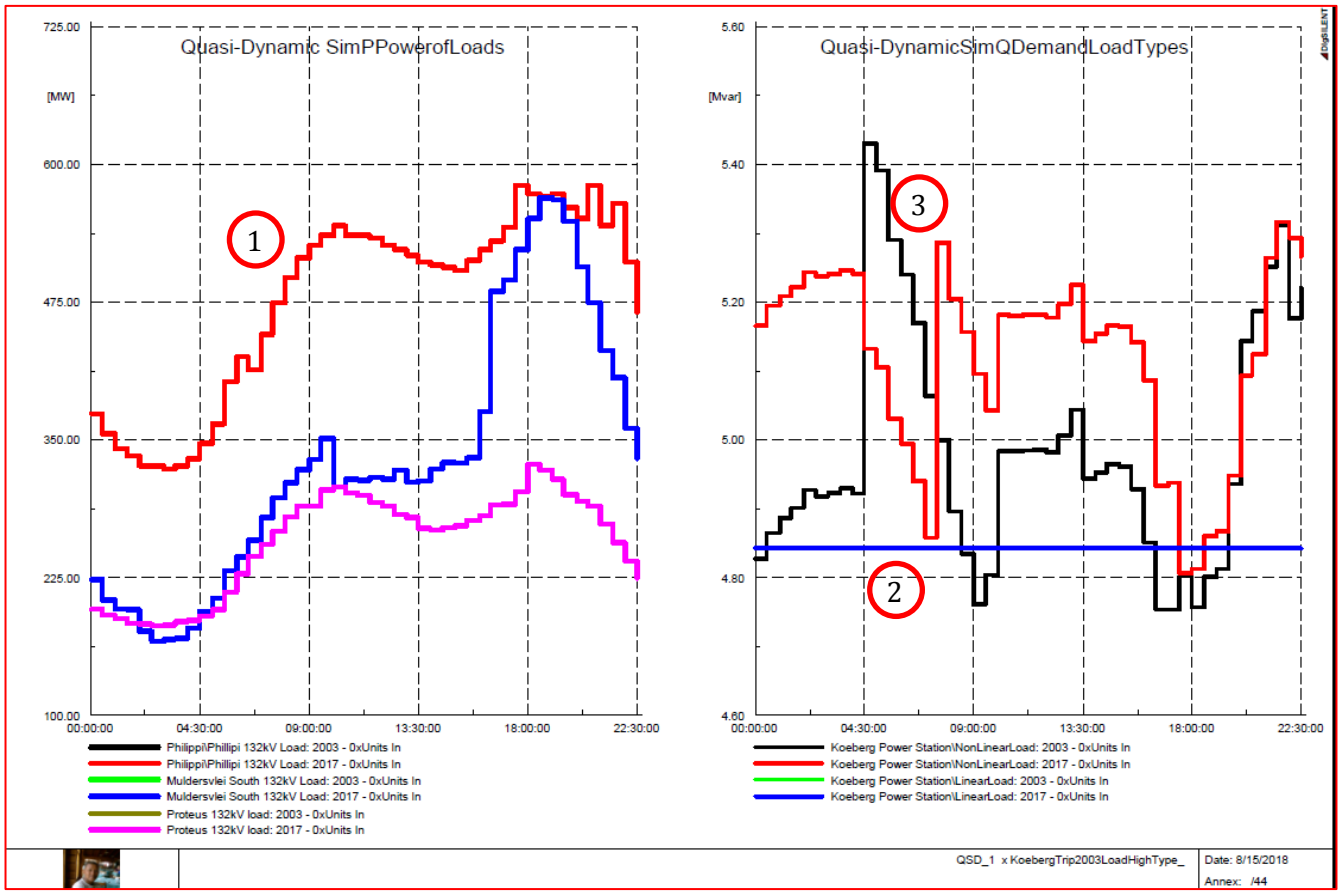

Figure 4.23: Critical substation loads and dynamic and linear load responses — quasi-dynamic simulation

The following observations are made with regard to figure 4.23:

- The load profiles for the critical substation are a reflection of the characteristics that have been programmed into the constant power loads- *reference label nr 1 on figure 4.23*;

- The linear load connected to the 6.6kV busbar feeding the essential loads show that the reactive power demand remains constant throughout the trip of the NPP unit. This is not a true reflection of how loads behave in the real power system. Rather, this is a demonstration as to why loads should be modelled as constant power loads, as this allows a closer reflection of what effect loads have on the system's overall transient performance - *reference label nr 2 on figure 4.23* ; and

- The dynamic load behaves differently for the 2003 case, where after the trip operation the Var demand increased, compared to the 2017 case, where the Var demand effectively decreased compared to the pre-fault condition. The reason for this is the fact that network strengthening leads to increased overall system voltage support. Thus decreasing the Var demand compared to a weaker network as was the case in 2003- *reference label nr 3 on figure 4.23*

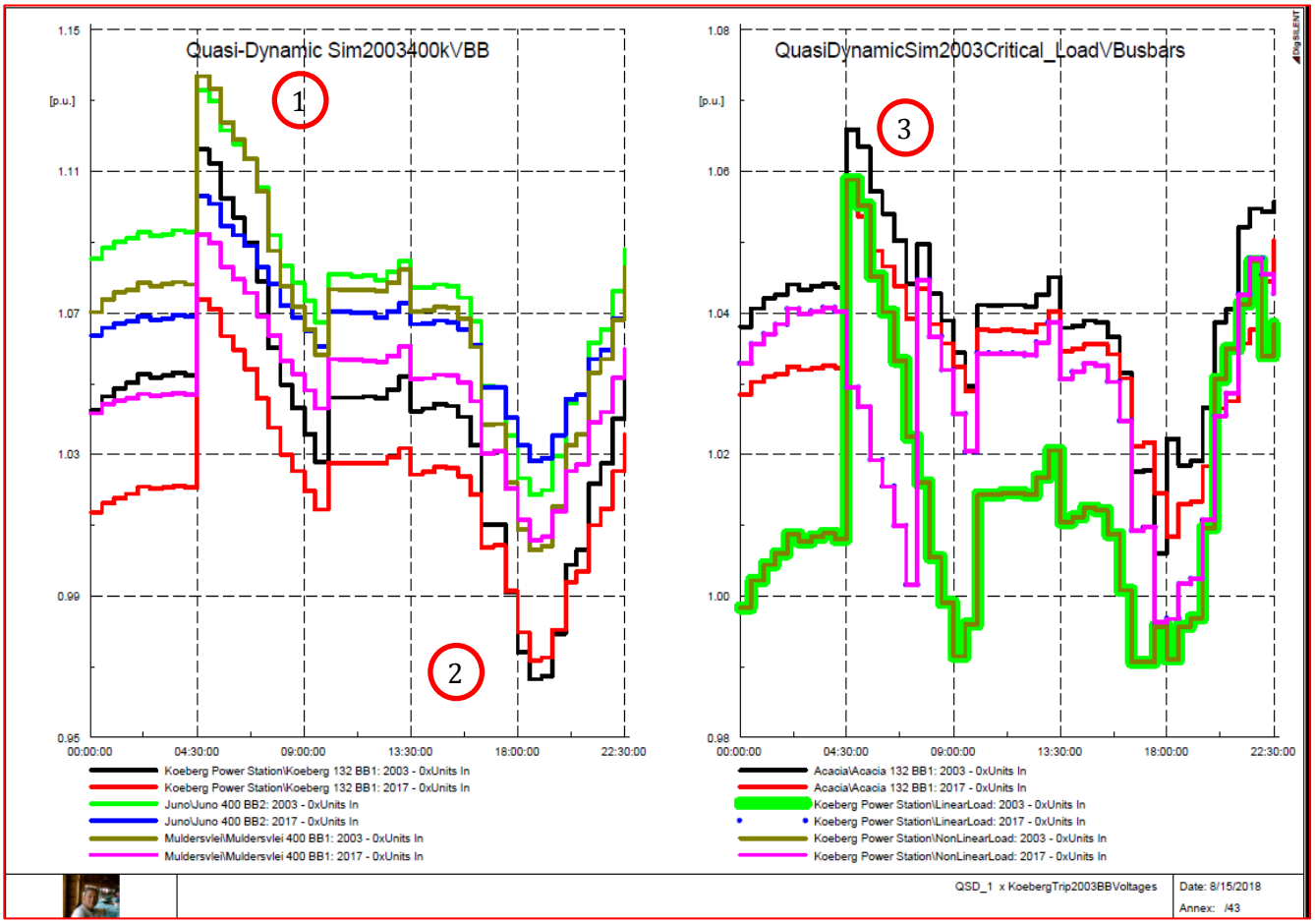

Figure 4.24: Critical substation busbar,linear and non-linear voltage response for quasi dynamic studies — case 2

The following observations are made with regard to figure 4.24:

- Immediately after the unit trip, the voltage rises at all critical busbars, with the highest being at Juno (1.13pu) and Muldersvlei's 400kV busbars(1.14pu) for the 2003 case. - *reference label nr 1 on figure 4.24* The situation improves for the 2017 case, as the highest voltage on critical busbars is recorded as <1.1 pu at the Juno 400kV busbar;

- A low voltage of 0.97pu is recorded at Koeberg's 132kV busbar at 18h00 post the tripping event - *reference label nr 2 on figure 4.24*. Nevertheless, voltage is within the low volt limit >0.85pu as required power for the cooling system pumps of the NPP – nr 2; and

- The off-site supply at Acacia substation also records a high voltage of 1.065pu post the tripping event - *reference label nr 3 on figure 4.24* . For the 2017 the Acacia 132kV busbar voltage measurement is 1.06pu.

Case 3

Perform quasi-dynamic simulation (run time 1 day) with events as per event on 15 October 2003. With and without load shedding events for both 2013 and 2017 cases

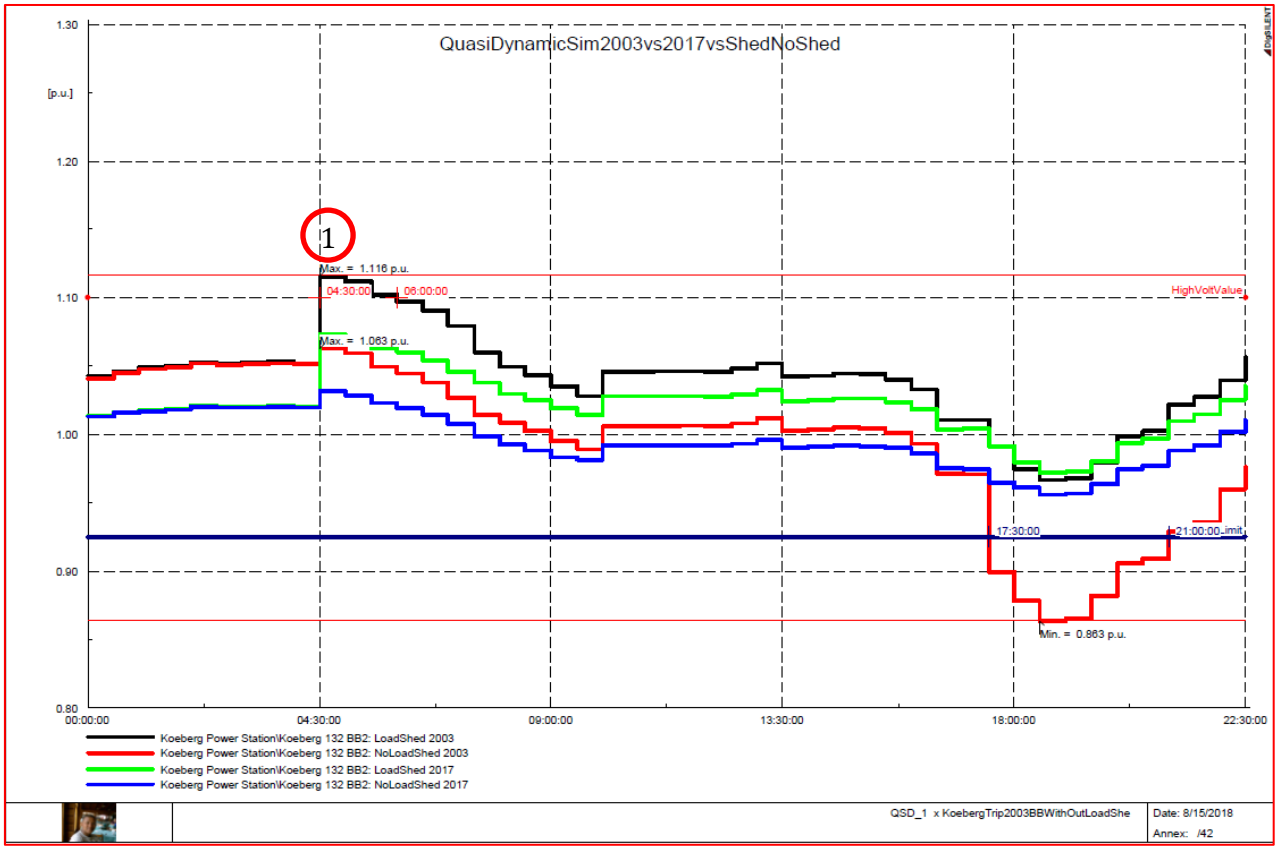

Figure 4.25: 132kV Koeberg busbar voltage with and without load shedding implemented — case 3

To demonstrate the effect of load shedding, a simulation was run for the Koeberg 132kV busbar, an essential bus for the off-site supply requirement as per the nuclear safety regulation act. From the number 1 shown in figure 4.25, it is observed that after the trip, the voltage rises on this busbar above the 1.1pu high volt limit for the 2003 case (this is with load shedding implemented). For the 2017 case, the busbar voltage recorded was 1.063 (this is with load shedding).

This simulation demonstrates the types of improvements that are possible if correct load shedding schemes are implemented. Furthermore, it demonstrates what network stability benefits network strengthening can bring about.

Chapter 5. Conclusions and Recommendations

In this dissertation, a comprehensive study into power system voltage stability with respect to the effect thereof on a NPP plant was undertaken. The author took a systematic approach in this dissertation in order to reach the point of appraising the network voltage stability state.

As a starting point, a thorough literature review was conducted on the different types of network stability modes. This was followed by a specific look at how voltage stability affects NPPs. A list of events effecting NPP plants where voltage stability played a major influence was reviewed, compiled, and tabulated. The information documented reflected on international cases and also at local events affecting the only NPP in Africa (which is in South Africa). Most of this information was gathered from presentations made by Dr. John H. Bickel [34]. The events for the Koeberg NPP were reviewed using public information available in [35], titled "Investigation into the electricity outages in the Western Cape for the period November 2005 to March 2006".

Given the fact that the voltage stability situation is both a short-term and long-term problem, any simulation that has to be performed to evaluate the voltage stability of the system needs to include dynamic as well as steady state simulations. As a starting point a network was build in which power plant equipment is modelled as close as possible to the behaviour it will have in a real-time power system. Two power system models representing the Western Cape grid 400kV network as it was configured in 2003 and 2017 respectively were developed. The loads represented in the model were configured with load charateristics that were available for the date and time under study, which is on 15 October 2017.

The software package that was used was DigSilent PowerFactory®. This software has the ability to perform dynamic studies, quasi-dynamic studies, stead state load flow, and QV and PV curves scripting tools, which have been used extensively in this dissertation. These tools formed part of the simulation tools that assisted to determine the dynamic and steady state voltage stability state of the grid with a NPP embedded.

The network was successfully implemented. All dynamic models were tested and verified, and the results are documented. This work was performed before commencing any network simulation to ensure that the results were predictable and that any anomalies could be explained by the author.

5.1 Conclusions

To conclude, the initial questions that were posed will now be assessed to determine if they have been properly addressed in this dissertation. Further, this section will also detail the final conclusions to the questions that were posed, of which the main ones were:

- What are the voltage stability indices that need to be evaluated to determine the critical busbars that can lead to a voltage collapse in the power system?
    - In this dissertation, the author used PV and QV curve analysis tools to evaluate the voltage stability limits. This analysis method has been performed on all critical busbars on the Western Cape power grid that are connected to the NPP;
    - What has been found for the Western Cape grid is that all busbars have a reserve reactive power margin. No busbar has a reactive power deficit for both the 2003 and 2017 network models. The 400kV busbar within the Northern ring of the Western Cape power grid has the lowest reactive power reserve; and
    - The real power reserves, which can also give an indication as to the loadability of a busbar, for the Western Cape power grid post 2003 have improved significantly, and most of the busbars have sufficient reserve given the loading at the substations. In addition, these busbars are not prone to voltage instability from a PV analyses point of view.

- Which busbars need to be deemed critical for the Western Cape power grid?
    - By performing PQ and PV analyses , which — in essence — is a steady state voltage stability analyses method, the Western Cape grid's busbars have been ranked from those that have the highest to the lowest available reserve MW and MVar margins. None of them can be deemed critical for the 2017 case given the contingency scenarios that were simulated.

- Is the current network future proof with regard to voltage stability given the future expansion plans of the network and the introduction of renewable resources such as wave energy, solar, wind and small modular nuclear reactors:
    - The 2017 network contingency scenarios simulated dynamically and using the steady state voltage stability tools have shown that the Western Cape power grid voltage stability has significantly improved since the contingency scenario of having no nuclear plant in service as it was in the 2003 case.

- Given the sensitivity to voltage deviation, what are the critical contingencies that can affect the NPP house load? In addition, what are the off-site supplies needed to take the decay heat out of the nuclear reactor?
    - The critical busbar to ensure a stable supply to the cooling systems of the NPP is the Acacia 132kV busbar. The busbar should not only be available but the voltage should be stable and be at >0.85pu. The voltage of the busbar was monitored throughout all of the simulations performed. The only scenario that proved to be problematic was the 2003 scenario, with both NPP out of service the per unit voltage at the 132kV busbar went to less than 0.85pu. This was observed during the RMS/ EMT simulation, a state of the power system parameters that can only be observed when performing a dynamic study.

- Are the current network models in the simulation software, i.e. Digsilent PowerFactory® adequate for the evaluation of the voltage stability and dynamic studies to make reasonable engineering decisions?
    - A base case was successfully configured in DigSilent PowerFactory® in order to simulate both dynamic and steady state simulation, as a means of evaluating the voltage stability of a grid that has a NPP connected to it.

5.2 Recommendations

It is recommended that future studies include the assessment of protection devices in order to determine the adequacy of the current schemes to avert a voltage instability scenario that can lead to a voltage collapse.

Other consideration should include the study of the voltage instability if other thermal resources such as coal or open cycle gas resources would have been placed at the same site as the nuclear power plant, i.e. the beforementioned resource have replaced a decommissioned nuclear power plant.

Given the introduction of renewable resources at the transmission level, studies need to be undertaken to assess the impact of the different dynamic plant models as it applies to small signal stability as well as the long-term voltage stability of the Western Cape power grid.

References

[1] R. G. Farmer, “Power System Dynamics and Stability,” *The Electric Power Engineering Handbook*, Boca Raton: CRC Press LLC, 2001, pp. 600-607.

[2] *Prabha Kundur (Canada, Convener), John Paserba (USA, Secretary)*,*Venkat Ajjarapu (USA),Göran Andersson(Switzerland),Anjan Bose (USA), Claudio Canizares (Canada), Nikos Hatziargyriou (Greece),David Hill(Australia),,Alex Stankovic (USA*),*Carson Taylor (USA),,Thierry Van Cutsem (Belgium),* and *Vijay Vittal (USA)*,”Definition and Classification of Power System Stability”, *IEEE Transactions PWRS*, Vol. 19, No. 2, pp. 2-6, May 2004.

[3] A. J. Claassens, “Transient modelling of induction motors in a petrochemical plant using Matlab,” M.Sc. dissertation, Electric and Electronic Engineering, Univ. of Stellenbosch, South Africa, 2008.

[4] IEEE Task Force on Load Representation for Dynamic Performance, “Load Representation for Dynamic Performance Analysis”, *IEEE Trans. on Power Systems*, Vol. 8, No. 2, May 1993.

[5] J. Arrillaga and C.P. Arnold, *Computer Analysis of Power Systems*, West Sussex: John Wiley and Sons Ltd., 1990.

[6] J.R. Smith and M. Chen, *Three Phase Electrical Machine Systems Computer Simulation*, Research Studies Press Ltd. John Wiley and Sons Ltd., 1990.

[7] M. Pavella and P.G. Murthy, *Transient Stability of Power Systems: Theory and Practice,* West Sussex: John Wiley & Sons Ltd., 1994.

[8] Leelaruji, R., and Vanfretti, L. “All-in-one” test system modelling and simulation for multiple instability scenarios. Internal Report. Stockholm: KTH Royal Institute of Technology. April 2011.

[9] W. Nakawiro, “Voltage Stability Assessment and Control of Power Systems using Computational Intelligence” PhD dissertation, Faculty of Engineering, University of Duisburg-Essen, Duisberg, Germany, 2011.

[10] A Zecchino, “Decoupled on Transformer in a Danish Low Voltage Grid with Unbalanced Distributed Generation”, DTU Orbit (30/10/2018) 2014/2015.

[11] J. H. Rust, *Nuclear Power Plant Engineering*, Haralson Publishing Company, 1979.

[12] N, Masoud, "Dynamic Modeling of a Pressurized Water Reactor Plant for Diagnostics and Control," M.S. dissertation, University of Tennessee, USA, 1990.

[13] W. Zhang, “A Comprehensive Simulation Study of The Voltage Stability of a Large Power System”, PhD dissertation, The University of British Columbia, 1993.

[14] M. Gustafsson and N. Krantz, “Voltage Collapse in Power Systems Analysis of Component Related Phenomena Using a Power System Model, M.Sc dissertation, Chalmers University of Technology, Sweden, 1995.

[15] M. Glavic, D. Novosel, E. Heredia, D. Kosterev, A. Salazar, F. Habibi-Ashrafi, and M. Donnelly, “See It Fast to Keep Calm: Real-Time Voltage Control Under Stressed Conditions”, *IEEE Power and Energy* Magazine, Vol. 10, No. 4, pp 43-45, August 2012.

[16] H. Røste, “Dynamic Behaviour of Synchronous Machine During Open Conductor Fault “, M.Sc dissertation, Norwegian University of Science and Technology, 2015.

[17] S Bengtsson, “Modelling of a Power System in a Combined Cycle Power Plant”, M.Sc dissertation, Uppsala Universitet, 2011.

[18] http://www.srmuniv.ac.in/sites/default/files/files/Chapter3Voltagecontrol.pdf, (current as 2018/08/11).

[19] P. Kundur, *Power System Stability and Control*, New York: McGraw-Hill Inc., 1994.

[20] T. Van Cutsem, “Excitation systems and automatic voltage regulators “, November 2017, http://www.montefiore.ulg.ac.be/~vct/elec0014/transp-v.pdf(current as 2018/08/11).

[21] R. D Vecchio, M. Del Vecchio, B Poulin, P. T. Feghali, D. M. Shah, R.Ahuja, Transformer Design Principles: With Applications to Core-Form Transformers. New York: Gordon and Breach, 2001.

[22] L. Mokgonyana, “A Heuristic Optimal Approach for Coordinated Volt/Var Control in Distribution Networks”, M.Eng, University of Pretoria, 2014

[23] J. H. BICKEL, “Grid Stability and Safety Issues Associated with Nuclear Power,” Nautilus Institute for Security and Sustainability; http://nautilus.org/wp-content/uploads/2011/ 12/Bickel.pdf (current as of Nov. 20, 2017).

[24] E.E. Lewis, *Fundamentals of Nuclear Reactor Physics*, Exeter: Academic Press, 2008

[25] C. Concordia, “Considerations in Planning for Reliable Electric Service,” pp. 71-76 in *IEEE Spectrum*, 1968

[26] M Gous, “An overview of the Namakwa Sands Ilmenite Smelting Operations,” *Southern African Pyrometallurgy*, Cradle of Humankind, South Africa, 5-8 March 2006. Jones, R.T. (ed.). Southern African Institute of Mining and Metallurgy, Johannesburg. pp. 189–202

[27] S.G. Mgenge* and J.D. Steenkamp, “Furnace Tapping Practice at Tronox Namakwa Sands”, Furnace Tapping Conference South Africa 2014

[28] S. B. Bhaladhare, A. S. Telang, P. P. Bedekar, “P-V, Q-V Curve – A Novel Approach for Voltage Stability Analysis”, IJCA Proceedings on National Conference on Innovative Paradigms in Engineering and Technology, NCIPET; 2013:5, pp31-35

[29] A. K. Ramasamy, R Verayiah, I.Z. Abidin, S. Gunalan, P. Perumal, “Study on P-V Curve and V-Q Curve of an Unbalanced Three-Phase System with Different Static Loads”, Przeglad Elektrotechniczny, Vol. 92, 2016

[30] K. Mahesh Jung, "Methods for Online Voltage Stability Monitoring," M.Sc dissertation, Iowa State University, 2009

[31] PowerWorld Similation Tools, https://www.powerworld.com/WebHelp/Content/MainDocumentation_HTML/QV_Curves.htm (current as of 2018/08/11)

[32] European Network of Transmission System Operators for Electricity, “Continental Europe Operation Handbook”, 2015.

[33] T. Van Cutsem, “Long-term Voltage Instability: Dynamic Aspects”, December 2017. www.montefiore.ulg.ac.be/~vct (current as of 2018/08/11).

[34] J. H. Bickel, “Brief History of North American Grid – Nuclear Power Plant Disturbances”, http://www.esrt-llc.com/Document%20Library/1.%20Brief%20History%20of%20North%20American%20Grid%20Disturbances.pdf (current as of 2018/08/11).

[35] National Energy Regulator of South Africa, "Investigation into the Electricity Outages in the Western Cape for the Period November 2005 to March 2006," Department of Energy of the Republic of South Africa, 2006.

[36] C. W. Taylor, *Power System Voltage Stability*, New York: McGraw-Hill

[37] DIgSILENT, Technical Reference Documentation General Load, Gomaringen: DIgSILENT, 2013.

[38] The South African Grid Code – Network Code Rev 7.0 – March 2008.

Appendix A. Loading on 15 October 2003

A1. Loads as at 04h23

Load	Name	Act.Pow.	React.Pow.	App.Pow.	I	Pow.Fact.
Nr		MW	Mvar	MVA	kA	
1	Acacia 11kV Trfr 07	0.9499999	0.3122498	0.9999999	0.05248638	0.95
2	Acacia 132kV Load	249	-7.000009	249.0984	1.089523	0.9996051
3	Acacia 33kV Load	16	3.999999	16.49242	0.2885426	0.9701425
4	Acacia 66kV Load	89	24.99999	92.44458	0.8086803	0.962739
5	Aggeneis 220kV Load	14	-0.00000006	14	0.1224682	1
6	Aurora 132kV Load	114	37.46999	120	0.5248639	0.95
7	Aurora 400kV TractionLoad	17	0.9999998	17.02939	0.0245798	0.9982744
8	Bacchus 132kV Load	341	7.999989	341.0938	1.491899	0.9997249
9	Droerivier 22kV Load	34	5	34.36568	0.9018652	0.9893591
10	Droerivier 400kV Load	19	-14	23.60085	0.1032269	0.8050559
11	Gromis 66kV Load	8	-4	8.944271	0.07824209	0.8944272
12	Helios_22kVLoad	6	-1	6.082763	0.1596311	0.9863939
13	Juno 132kV Load	14.25	4.683749	15	0.06560799	0.95
14	Juno 400kV load	22	172	173.4013	0.2502832	0.1268733
15	Juno 66kV Load	16	13	20.61553	0.1803391	0.776114
16	Koeberg 132kV Load	122	32	126.1269	0.5516622	0.9672796
17	Muldersvlei 66kV Load	23	6.999999	24.04163	0.2103097	0.9566739
18	Muldersvlei South 132kV Load	557	138	573.8406	2.509902	0.9706529
19	Nama 66kV Load	17	7	18.38478	0.1608251	0.9246781
20	Onranjemnund 66kV Load	26	-0.0000003	26	0.227441	1
21	Paulputs 132kV Load	11	-8	13.60147	0.059491	0.8087361
22	Phillipi 132kV Load	485	36.99997	486.4093	2.127489	0.9971026
23	Proteus 132kV	340.9999	74.99998	349.1503	1.527137	0.9766565

	load					
24	Proteus 66kV Load	61.99999	17.99999	64.56004	0.5647538	0.9603463

A2. Shunt reactors and Capacitors as at 04h23

	Name	Act.Step	Qmax	Qact	Switchable(On - 1 ; Off - 0)
			Mvar	Mvar	
1	Acacia 132 CX1	0	72	0	0
2	Acacia 132 CX2	0	72	0	0
3	Acacia 132 CX3	0	72	0	0
4	Aggeneis 220 RX11	1	40	40	0
5	Aggeneis 220 RX12	1	40	40	0
6	Aggeneis T1 Shunt RX	1	30	30	0
7	Aggeneis T2 Shunt RX	1	30	30	0
8	Aries 400 RX1	0	100	0	0
9	Aries 400 RX2	1	110.25	110.25	0
10	Aries-Kokerboom 400 RX1	1	100	100	0
11	Aurora 132 CX1	0	72	0	1
12	Aurora 132 CX2	0	72	0	1
13	Aurora 400 RX1	1	100	100	0
14	Bacchus 132 CX1	0	72	0	1
15	Bacchus 132 CX2	0	72	0	1
16	Bacchus 400 RX1	1	100	100	0
17	Bacchus-Droerivier 400 RX1	1	100	100	0
18	Droerivier 400 RX1	0	100	0	0
19	Droerivier 400 RX2	1	100	100	0
20	Droerivier-Muldersvlei 400 RX2	1	100	100	0
21	Helios 400 RX1	1	100	100	0
22	Helios 400 RX2	0	100	0	0
23	Juno 400 RX1	1	100	100	0
24	Juno 420 RX2	0	110.25	0	0
25	Kronos 400 RX	0	100	0	0
26	Muldersvlei 132 CX1	1	72	72	0

27	Muldersvlei 132 CX2	0	72	0	0
28	Muldersvlei 132 CX3	0	72	0	0
29	Muldersvlei 400 CX4	0	100	0	0
30	Oranjemond 66 CX	0	15	0	0
31	Pembroke 132 CX1	1	36	36	0
32	Proteus 132 CX1	0	72	0	1
33	Proteus 132 CX2	0	72	0	1
34	Proteus 400 RX	1	100	100	0
35	Stikland 132 CX1	1	72	72	0
36	Stikland 132 CX2	1	72	72	0
37	Stikland 132 CX3	0	72	0	0

A3. Static VAR compensators as at 04h23

	Name	Q Reactance (>0)	TCR, Max. Limit	Q per Capacitor Unit (<0)
		Mvar	Mvar	Mvar
1	Grassridge SVC1	45	45	0
2	Hydra SVC1	500	500	-250
3	Hydra SVC2	500	500	-250
4	Muldersvlei SVC	350	350	-150
5	Poseidon SVC1	500	500	-250

A4. Static VAR compensators as at 04h23

	Name - Series Reactors	Out of Service (0 - Not ; 1 - Yes)	U Nom.	Rated Power	Rated Current
			kV	MVA	kA
1	Aries-Helios 200 SCX2	0	400	762.1024	1.1
2	Aries-Kronos 400 SCX2	0	400	1108.513	1.6
3	Aurora-Juno 400 SCX1	0	400	762.1024	1.1
4	Bacchus-Droerivier 400 SCX1	0	400	1179.873	1.703
5	Bacchus-Proteus 400 SCX1	0	400	1024.681	1.479
6	Beta-Delphi SCX	0	400	1450.073	2.093
7	Beta-Hydra 400 SCX1	0	400	1385.641	2
8	Droerivier-Hydra 400 SCX1	0	400	976.8766	1.41

9	Droerivier-Hydra 400 SCX2	0	400	976.8766	1.41
10	Droerivier-Muldersvlei 400 SCX2	0	400	1179.873	1.703
11	Droerivier-Proteus 400 SCX1	0	400	1024.681	1.479
12	Helios-Juno 400 SCX4	0	400	762.1024	1.1
13	Hydra-Droerivier 3 SCX	0	400	1894.864	2.735
14	Hydra-Kronos 400 SC	0	400	1150.082	1.66
15	Hydra-Perseus 400 SCX2	0	400	1385.641	2
16	Hydra-Perseus 400 SCX3	0	400	1385.641	2
17	Hydra-Poseidon 1 SCX	0	400	1470.165	2.122
18	Hydra-Poseidon 2 SCX	0	400	1470.165	2.122

	Name - Series Reactors	**Out of Service (0 - Not ; 1 - Yes)**	**U Nom.**	**Rated Power**	**Rated Current**
			kV	**MVA**	**kA**
1	Aries-Helios 200 SCX2	0	400	762.1024	1.1
2	Aries-Kronos 400 SCX2	0	400	1108.513	1.6
3	Aurora-Juno 400 SCX1	0	400	762.1024	1.1
4	Bacchus-Droerivier 400 SCX1	0	400	1179.873	1.703
5	Bacchus-Proteus 400 SCX1	0	400	1024.681	1.479
6	Beta-Delphi SCX	0	400	1450.073	2.093
7	Beta-Hydra 400 SCX1	0	400	1385.641	2
8	Droerivier-Hydra 400 SCX1	0	400	976.8766	1.41
9	Droerivier-Hydra 400 SCX2	0	400	976.8766	1.41
10	Droerivier-Muldersvlei 400 SCX2	0	400	1179.873	1.703
11	Droerivier-Proteus 400 SCX1	0	400	1024.681	1.479
12	Helios-Juno 400 SCX4	0	400	762.1024	1.1
13	Hydra-Droerivier 3 SCX	0	400	1894.864	2.735
14	Hydra-Kronos 400 SC	0	400	1150.082	1.66
15	Hydra-Perseus 400 SCX2	0	400	1385.641	2
16	Hydra-Perseus 400 SCX3	0	400	1385.641	2
17	Hydra-Poseidon 1 SCX	0	400	1470.165	2.122
18	Hydra-Poseidon 2 SCX	0	400	1470.165	2.122

Appendix B. Under Load Tap Changer Modelling

B1. Under Load Tap Changer Frame

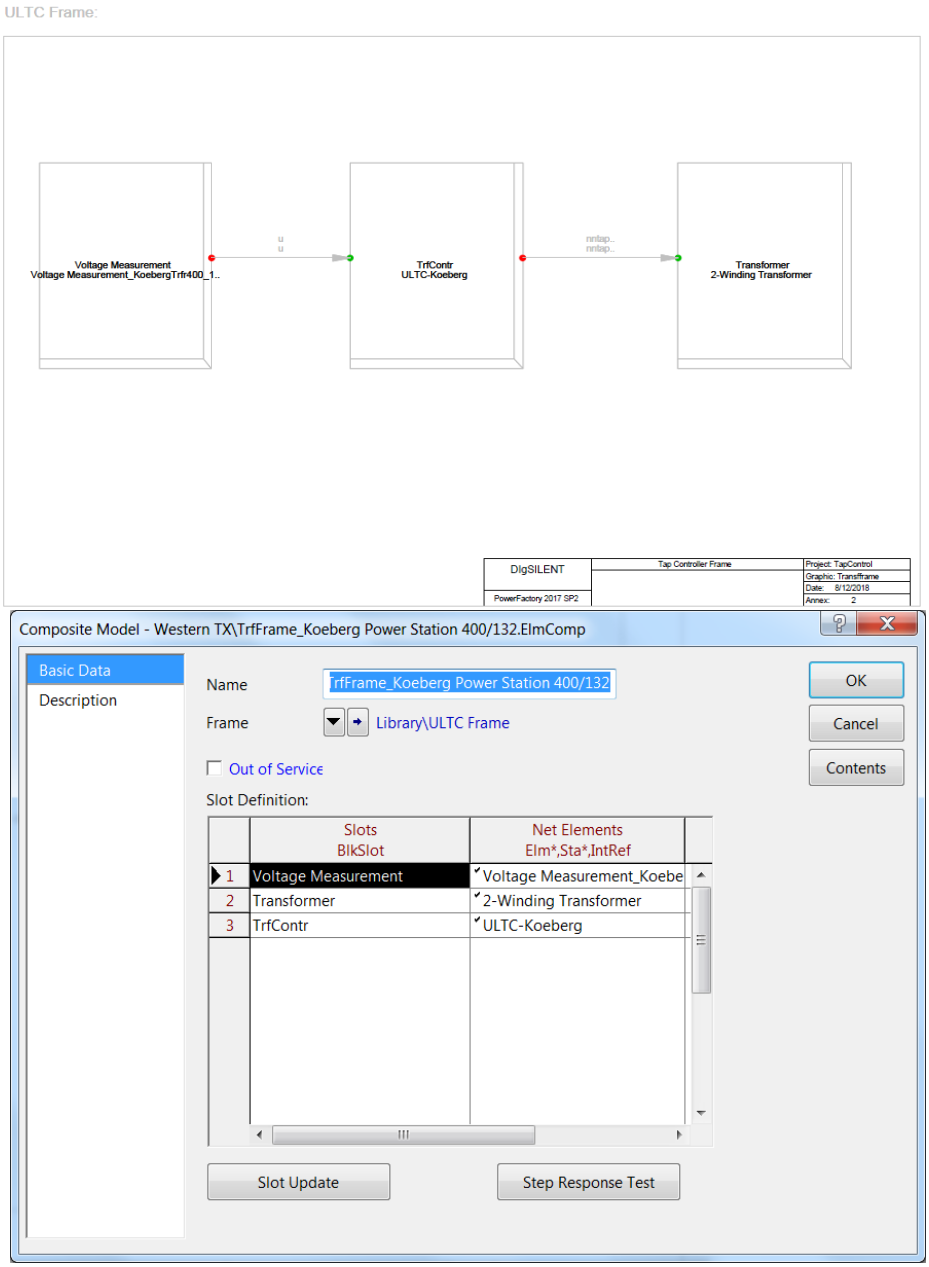

Figure B.1: ULTC Frame Definition with slot definitions for Koeberg 400/ 132kV. Transformer to simulate tap changing

B2. ULTC Transformer Controller Script

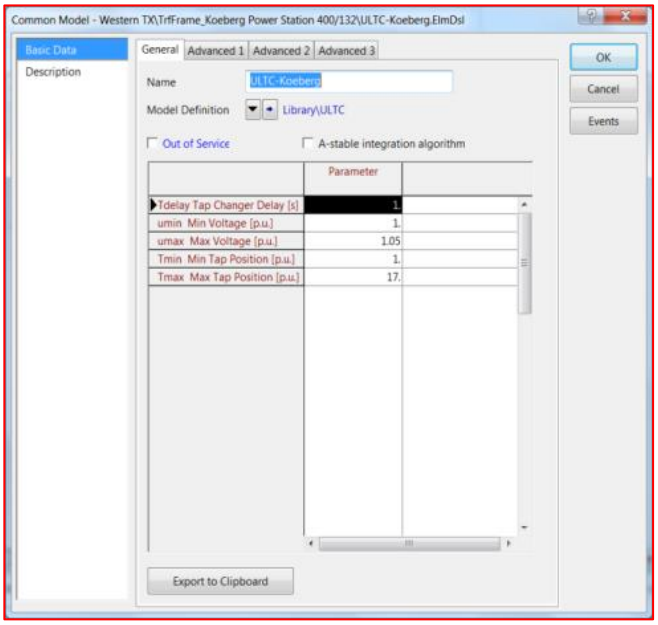

! definition of tap steps

tapdown = nntap0+1.25

tapup = nntap0-1.25

! voltage outside band

changedown = umin - u + 0.5

changeup = u - umax + 0.5

! command to change Tap position = triggering

tchangedown = picdro({nntap0-0.188 >=Tmin.and.changedown.and.
.not.delay(tchangedown,Tdelay/50)},Tdelay,0.0)

tchangeup = picdro({nntap0-0.188 <=Tmax.and.changeup.and. .not.delay(tchangeup,Tdelay/50)
},Tdelay,0.0)

! force event signal zero crossing

evtdown = tchangedown - 0.27

evtup = tchangeup - 0.72

nntapin = nntap0

!lim(select(evtdown,nntap0 - 1,select(evtup,nntap0 + 1,nntap0)),Tmin,Tmax)

! set event

event(0,evtdown,'name=this dtime=0. value=tapdown variable=nntap0')

event(0,evtup ,'name=this dtime=0. value=tapup variable=nntap0')

vardef(Tmin)='p.u.';'Min Tap Position'

vardef(Tmax)='p.u.';'Max Tap Position'

vardef(Tdelay)='s';'Tap Changer Delay'

!vardef(Tap_step)='%';'Variation of tap ratio per position'

vardef(umax)='p.u.';'Max Voltage'

vardef(umin)='p.u.';'Min Voltage'

inc(nntap0)=nntapin

inc(tchangedown)=5

Figure B.2 Transformer controller settings and DSL script

Appendix C. PV Curve Analysis Fundamentals

G1. PV curve analysis theory

In this method of evaluation, power is increased at the area of interest in a certain number of steps. The measured voltage is recorded at the point of interest and the voltage is then plotted against the power. The plotted PV curves will be evaluated to determine the maximum loadability before a voltage collapse is experienced.

For the analysis of the PV curve, [29] suggest evaluating a two bus system with a generator, single generator, single transmission line, and a load. The representation is illustrated in figure C.1

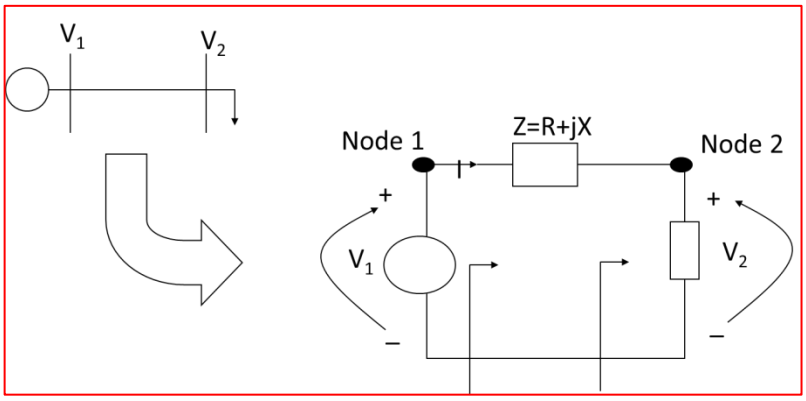

Figure C.1 : Two bus system used in derivation of PV Analysis [29]

The result of the evaluation can be used to determine how much load reduction should take place to ensure low probability of a system voltage collapse.

The load apparent power $S_{12} = P_{12} + jQ_{12}$. And the impedance is expressed as

$$Z = R + jX \Rightarrow Y = G - jB \qquad \text{C1. 1}$$

Using figure C.1, the equations derived for P_{12} and Q_{12} are as follow:

$$P_{12} = |V_1|^2 G - |V_1||V_2| G\cos(\theta_1 - \theta_2) + |V_1||V_2| B\sin(\theta_1 - \theta_2) \qquad \text{C1. 2}$$

$$Q_{12} = |V_1|^2 B - |V_1||V_2| B\cos(\theta_1 - \theta_2) - |V_1||V_2| G\sin(\theta_1 - \theta_2) \qquad \text{C1. 3}$$

By letting G go to zero, the equations become:
S_D can now be determined and exchanging the sub scripts:

$$P_{12} = |V_1||V_2|B\sin(\theta_1-\theta_2) \quad \text{C1. 4}$$

$$Q_{12} = |V_1|^2 B - |V_1||V_2|B\cos(\theta_1-\theta_2) \quad \text{C1. 5}$$

$$P_D = -P_{21} = -|V_1||V_2|B\sin(\theta_2-\theta_1) \quad \text{C1. 6}$$
$$= |V_1||V_2|B\sin(\theta_1-\theta_2) \quad \text{C1. 7}$$

$$Q_D = -Q_{21} = -|V_2|^2 B + |V_1||V_2|B\cos(\theta_2-\theta_1) \quad \text{C1. 8}$$
$$= -|V_2|^2 B + |V_1||V_2|B\cos(\theta_1-\theta_2) \quad \text{C1. 9}$$

Defining the angular difference as $\theta_{12} = \theta_1 - \theta_2$ and with power factor angle of the load being

$$\phi = \angle V_2 - \angle I \quad \text{C1. 10}$$

The equations that are being derived can be simplified to the below:

$$P_D = |V_1||V_2|B\sin\theta_{12} \quad \text{C1. 11}$$
$$Q_D = -|V_2|^2 B + |V_1||V_2|B\cos\theta_{12} \quad \text{C1. 12}$$
$$S_D = P_D + jQ_D = P_D(1+j\beta) \quad \text{C1. 13}$$

Where $\beta = \tan\phi$

P_D and Q_D can be expressed as

$$Q_D = P_D\beta = -|V_2|^2 B + |V_1||V_2|B\cos\theta_{12} \quad \text{C1. 14}$$
$$P_D\beta + |V_2|^2 B = |V_1||V_2|B\cos\theta_{12} \quad \text{C1. 15}$$

If both sides are squared

$$P_D^2 = |V_1|^2|V_2|^2 B^2\sin^2\theta_{12} \quad \text{C1. 16}$$

And

$$\left(P_D\beta + |V_2|^2 B\right)^2 = |V_1|^2|V_2|^2 B^2\cos^2\theta_{12} \quad \text{C1. 17}$$

Squaring both sides of the equation and adding them gives:

$$P_D^2 = |V_1|^2 |V_2|^2 B^2 \sin^2 \theta_{12} \quad \text{C1. 18}$$

$$\left(P_D\beta + |V_2|^2 B\right)^2 = |V_1|^2 |V_2|^2 B^2 \cos^2 \theta_{12} \quad \text{C1. 19}$$

$$P_D{}^2 + (P_D\beta + |V_2|^2 B)^2 = |V_1|^2 |V_2|^2 B^2 (\sin^2 \theta_{12} + \cos^2 \theta_{12}) \quad \text{C1. 20}$$

$$\Rightarrow P_D{}^2 + (P_D\beta + |V_2|^2 B)^2 = |V_1|^2 |V_2|^2 B^2 \quad \text{C1. 21}$$

When all the quadratic terms, i.e.$(|V_2|^2)^2$ and $|V_2|$ are combined, a quadratic equation is formed and has the solution:

$$\left(|V_2|^2\right)^2 + \left[\frac{2P_D\beta}{B} - |V_1|^2\right] |V_2|^2 + \frac{P_D{}^2}{B^2}\left[1 + \beta^2\right] = 0 \quad \text{C1. 22}$$

$$|V_2|^2 = \frac{|V_1|^2}{2} - \frac{\beta P_D}{B} \pm \left[\frac{|V_1|^4}{4} - \frac{P_D}{B}\left(\frac{P_D}{B} + \beta |V_1|^2\right)\right]^{1/2} \quad \text{C1. 23}$$

The equation demonstrates that the voltage at the load point is a function of the power delivered to the load [29]. Given that there are two solutions to the equations, a stable and unstable case exists. The stable case is when the sign is positive and the unstable solution is when one value exists for the solution.

G2. PV curve power factory script

The description for the script for evaluating the PV curves at various busbars and for various loading scenarios is reproduced below. This is taken from Digsilent PowerFactory® licenced software.

PV-Curves v1.0

This script creates PV curves for all the selected busbars, by changing the selected loads. The resulting graphs are automatically displayed.

**Use instructions:*
-Create a DPL selection with the loads that will be swept and the busbars that will be monitored from either the Single Line diagram or the object browser.

-Set the initial scaling factor.
-Execute the script. PV Curves for all selected busbars are now plotted automatically. The plots are also scaled automatically.

**Notes:*
-Initial load scaling factors are restored after DPL execution.
-If no load or no busbar in the general selection, DPL script exits with error message.

**Description:*
PV Diagrams are an essential tool for analyzing the voltage stability of power systems. PV curves are created by increasing the active power of one or a certain number of loads by keeping the power factor constant. The loads are increased until the load flow doesn't converge any more. The efficiency of a PV-curve algorithm is extremely increased if the step size of the power increments is variable. The point of voltage collapse can be found with high precision in that case.

G3. PV curve results for the different relevant substations

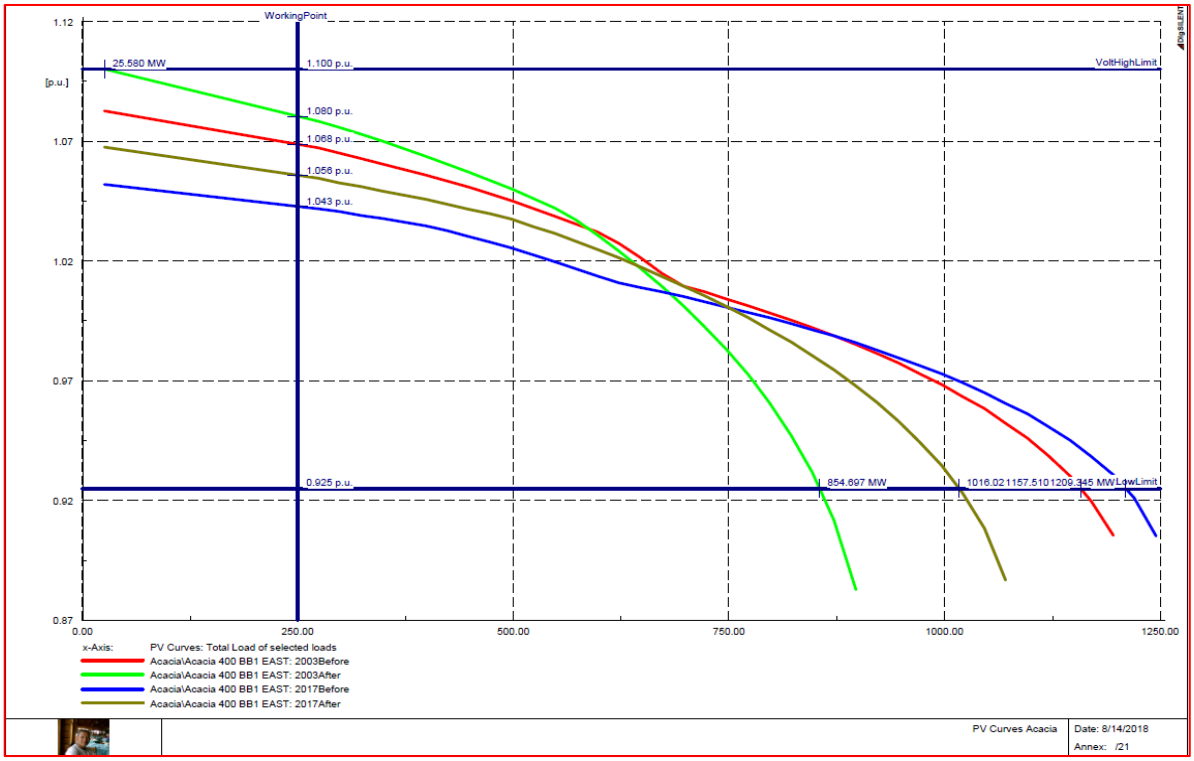

Figure C.2 : Acacia 400kV BB PV Curve 2003 vs 2017 plus OneKoebergOut and TwoKoebergOut

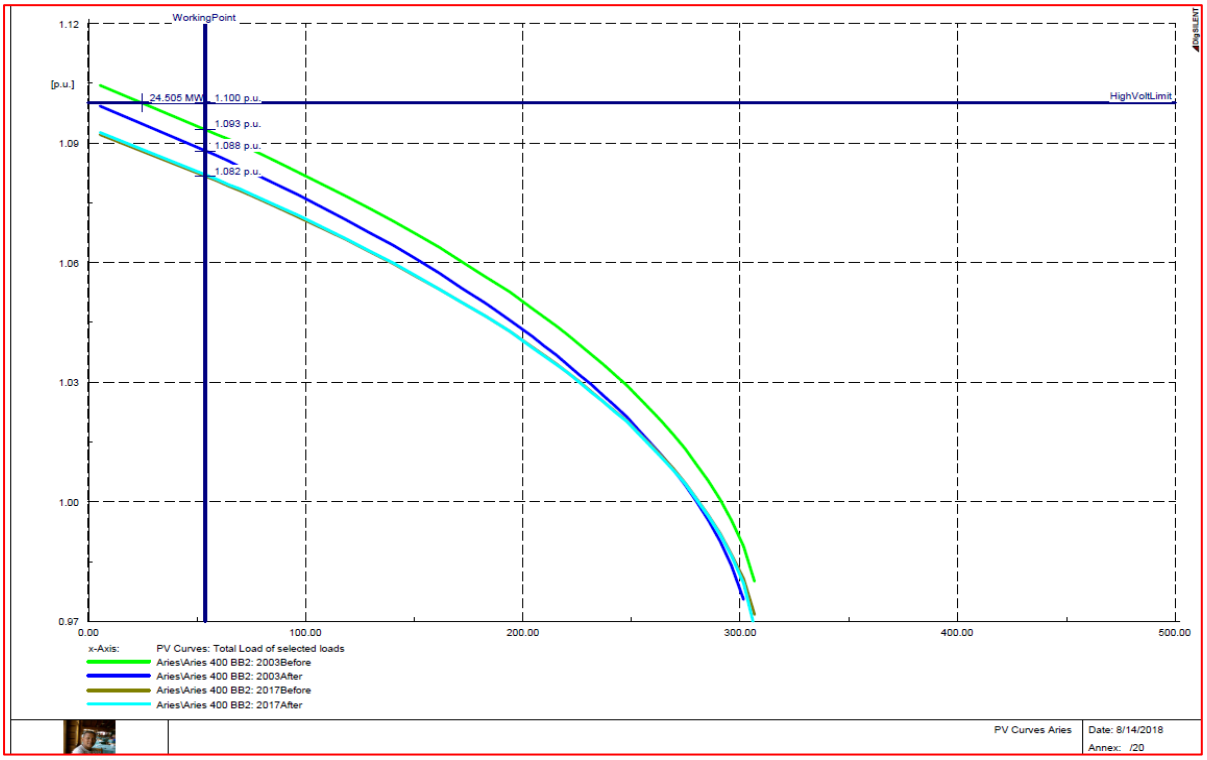

Figure C.3: Aries 400kV BB PV Curve 2003 vs 2017 + OneKoebergOut and TwoKoebergOut

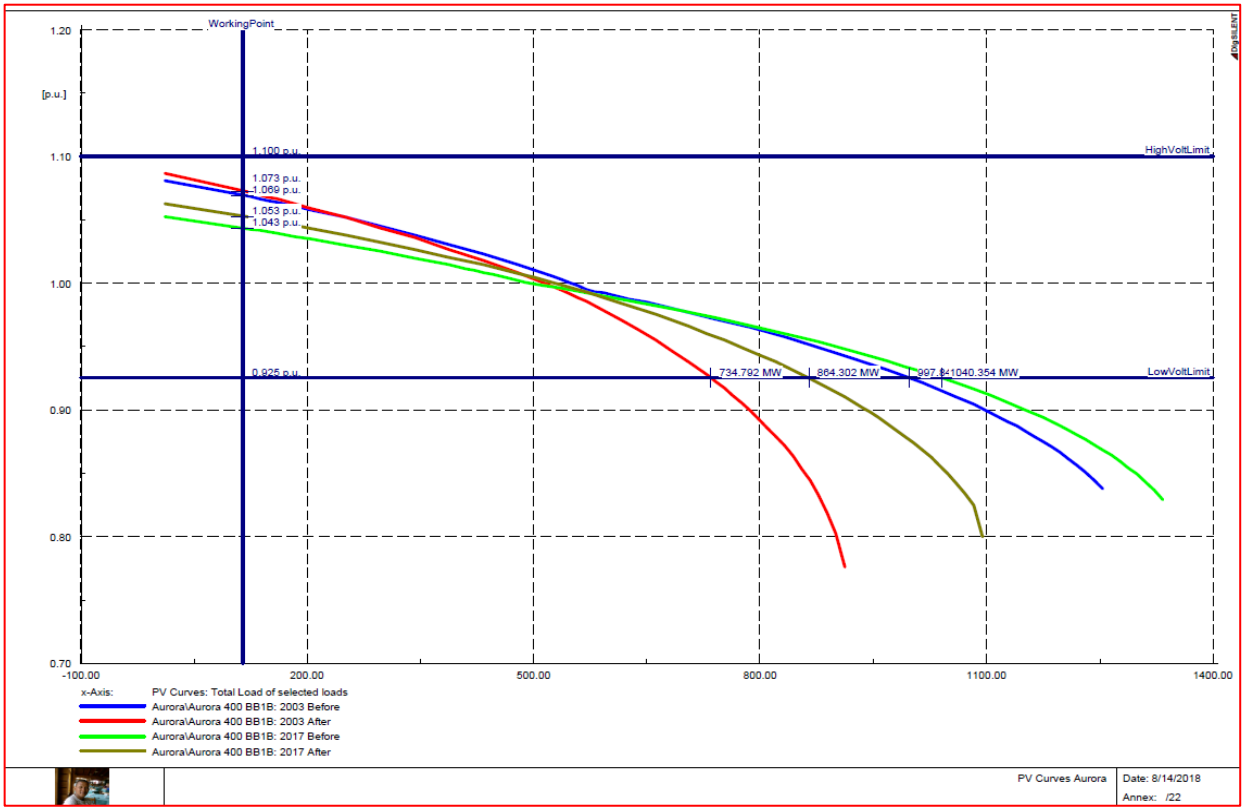

Figure C.4:Aurora 400kV BB PV Curve 2003 vs 2017 plus OneKoebergOut and TwoKoebergOut

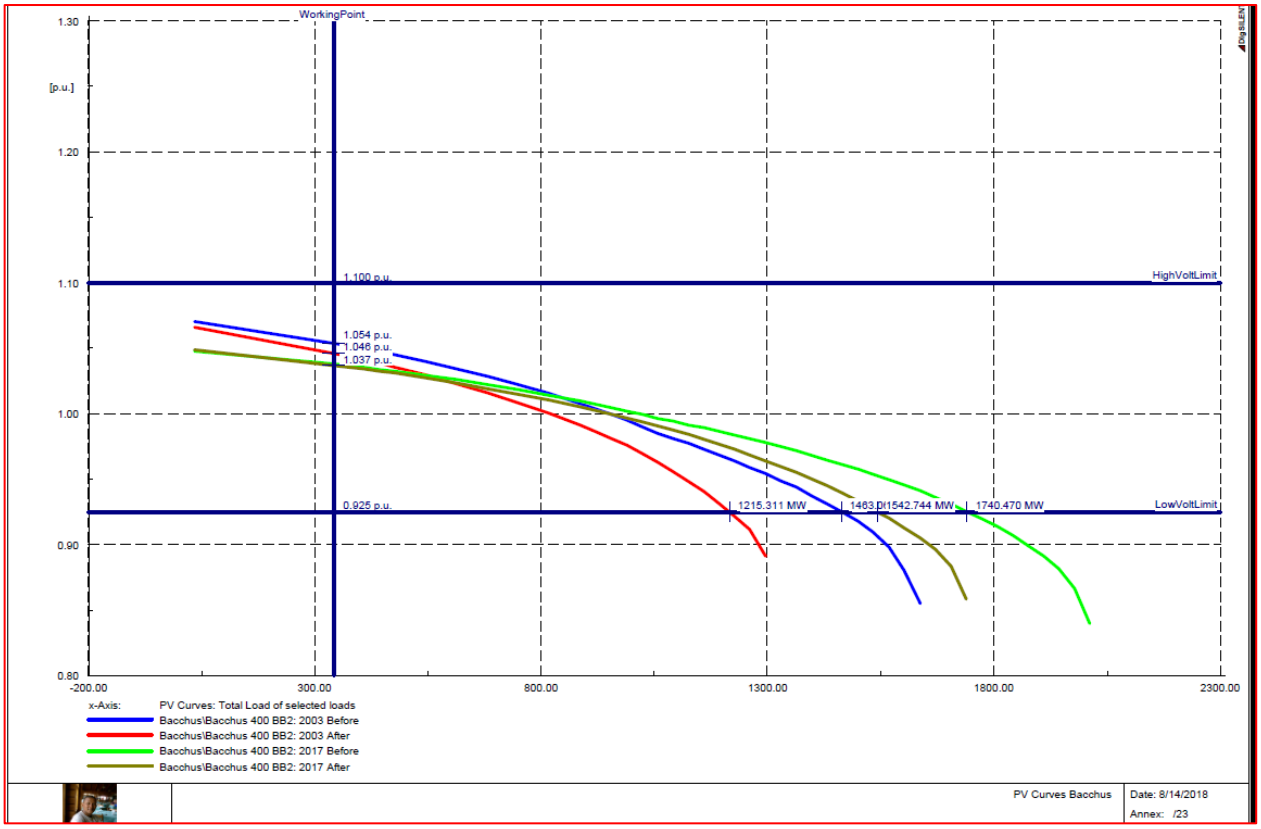

Figure C.5 : Bacchus 400kV BB PV Curve 2003 vs 2017 plus OneKoebergOut and TwoKoebergOut

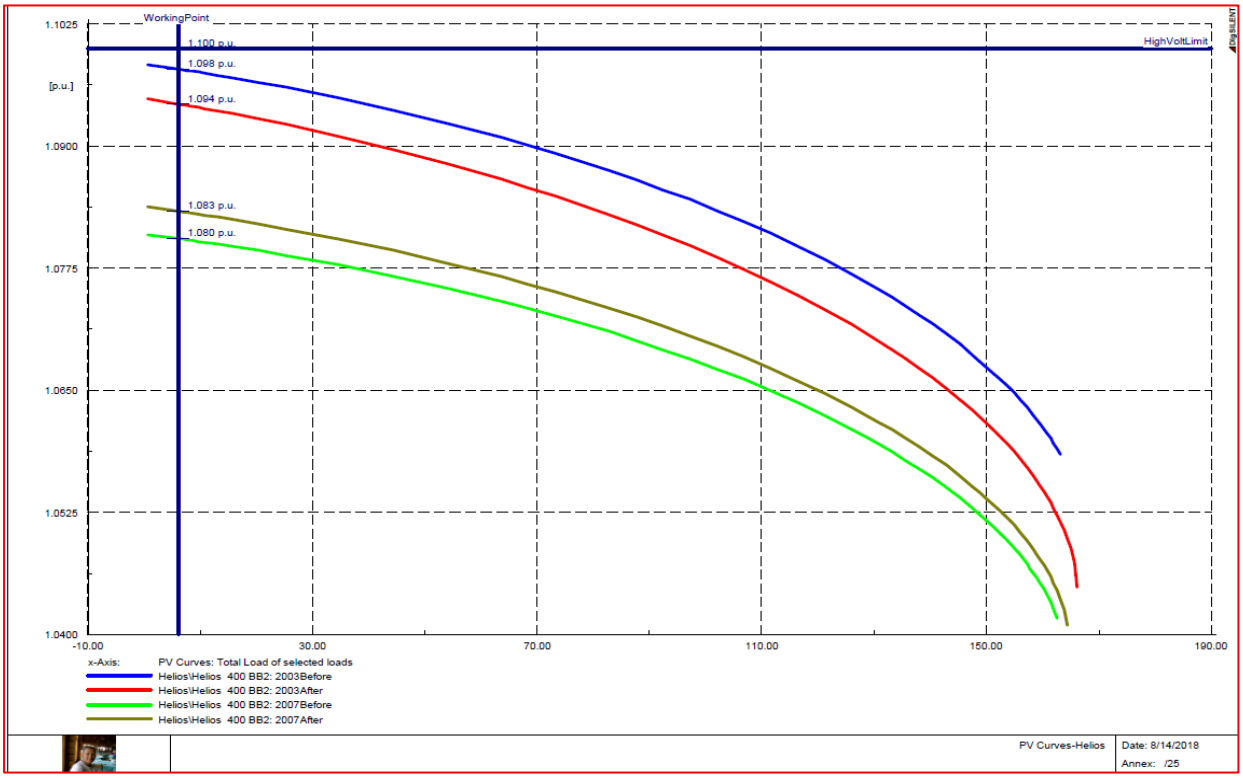

Figure C.6 : Helios 400kV BB PV Curve 2003 vs 2017 plus OneKoebergOut and TwoKoebergOut

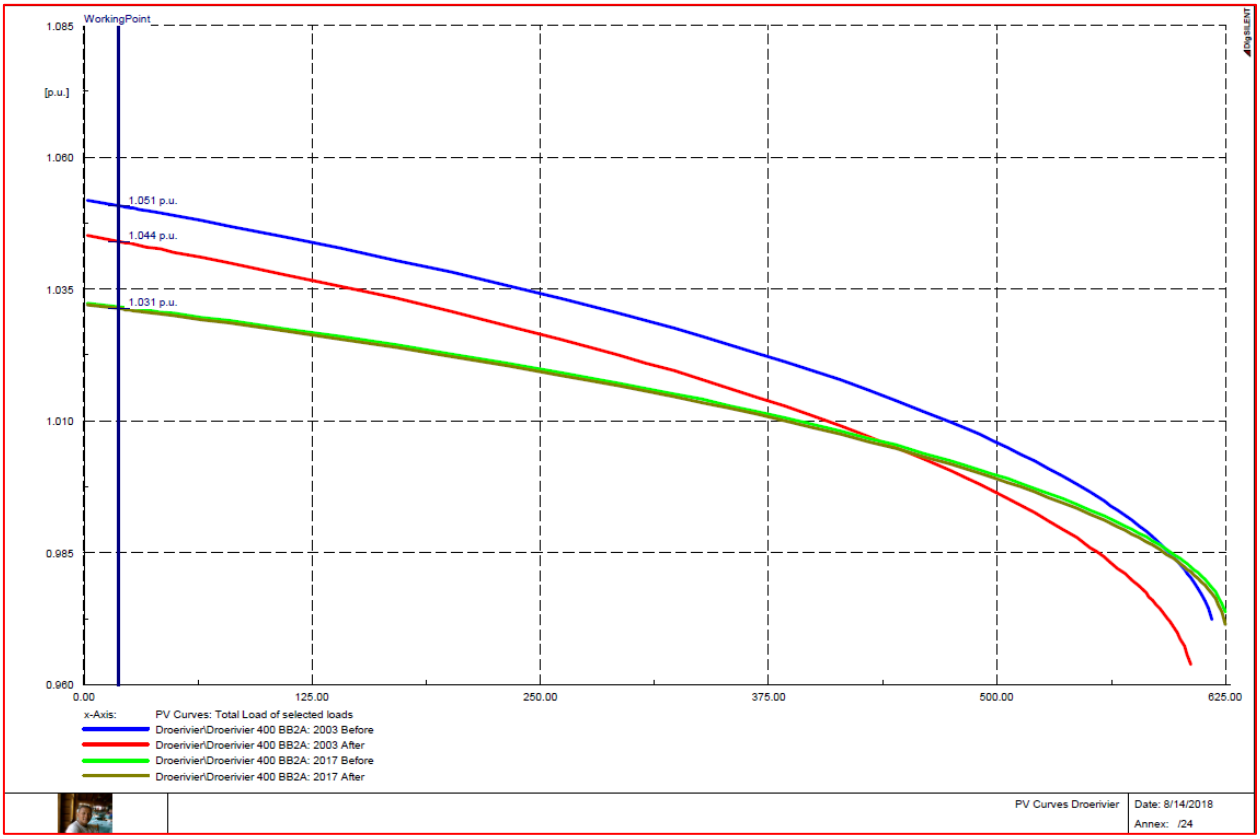

Figure C.8: Droerivier 400kV BB PV Curve 2003 vs 2017 plus OneKoebergOut and TwoKoebergOut

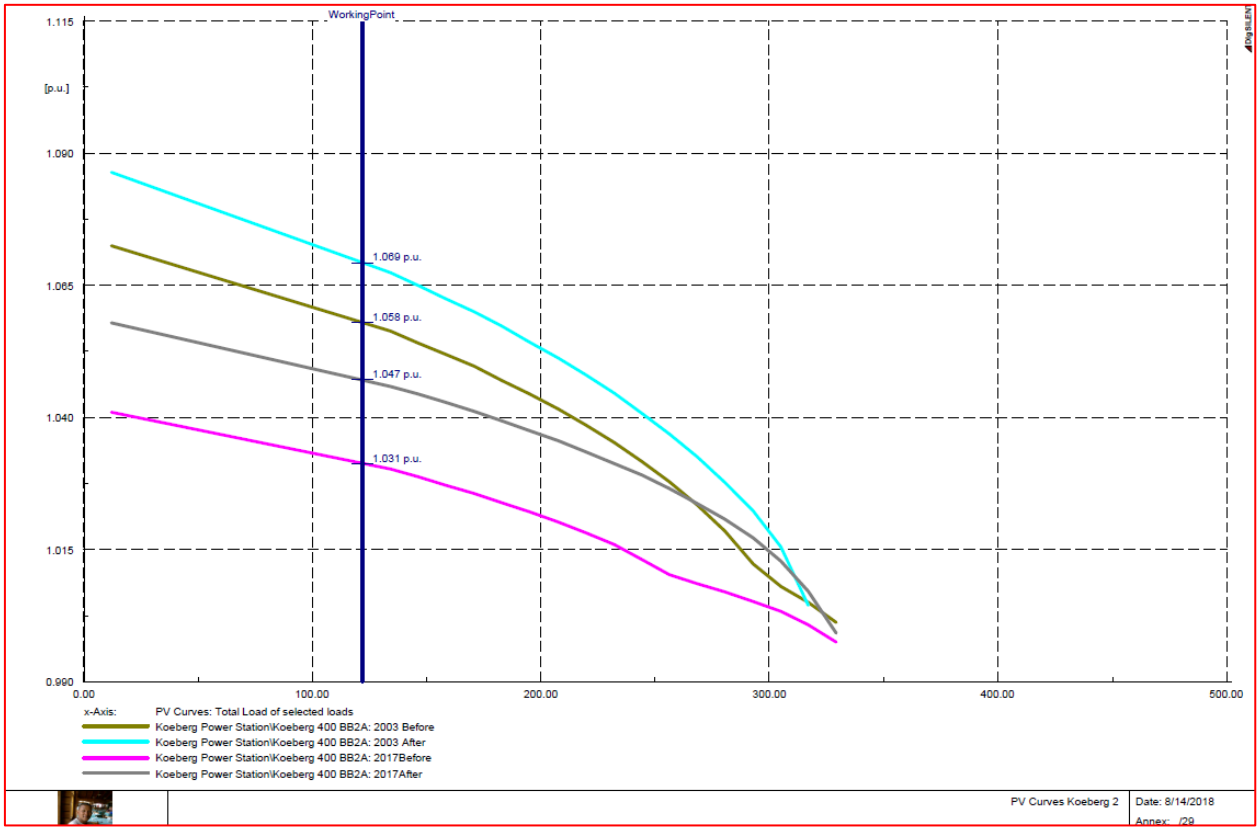

Figure C.7: Koeberg 400kV BB PV Curve 2003 vs 2017 plus OneKoebergOut and TwoKoebergOut

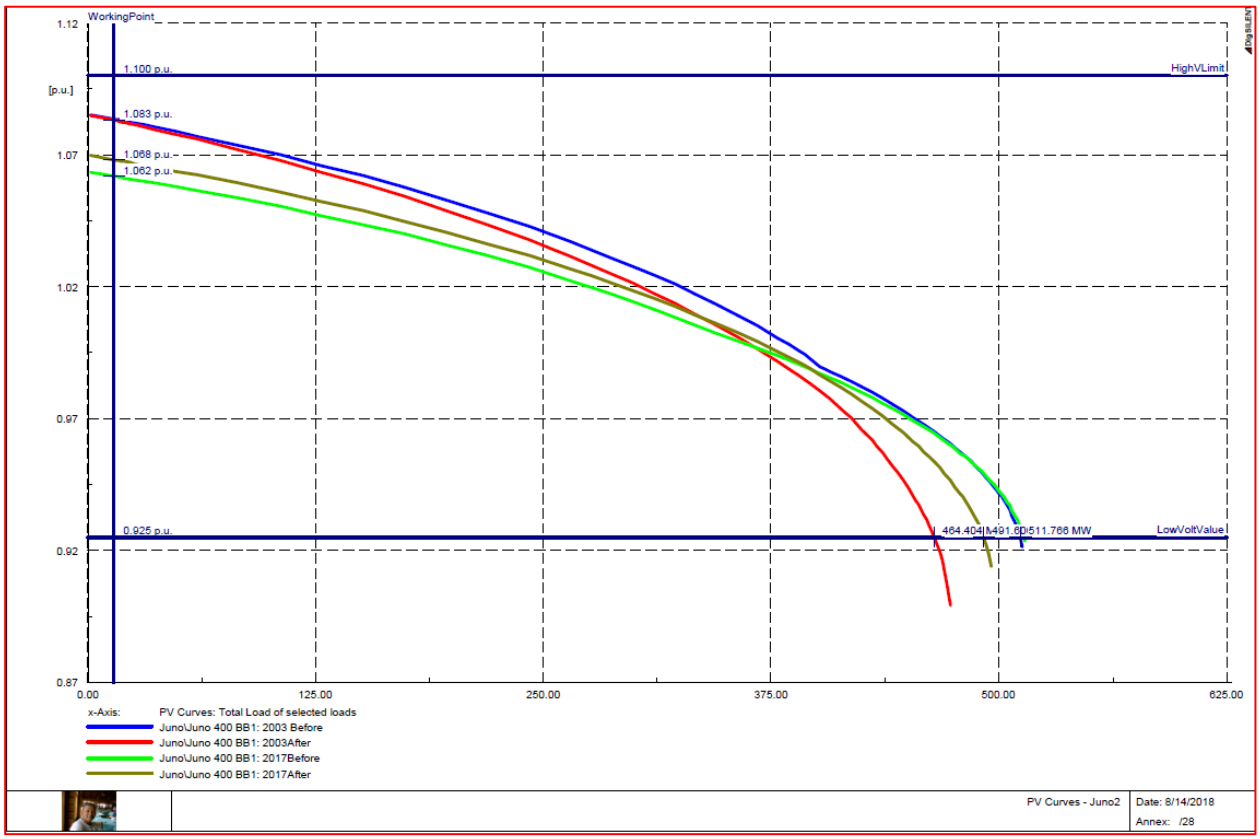

Figure C.9 : Juno 400kV BB PV Curve 2003 vs 2017 plus OneKoebergOut and TwoKoebergOut

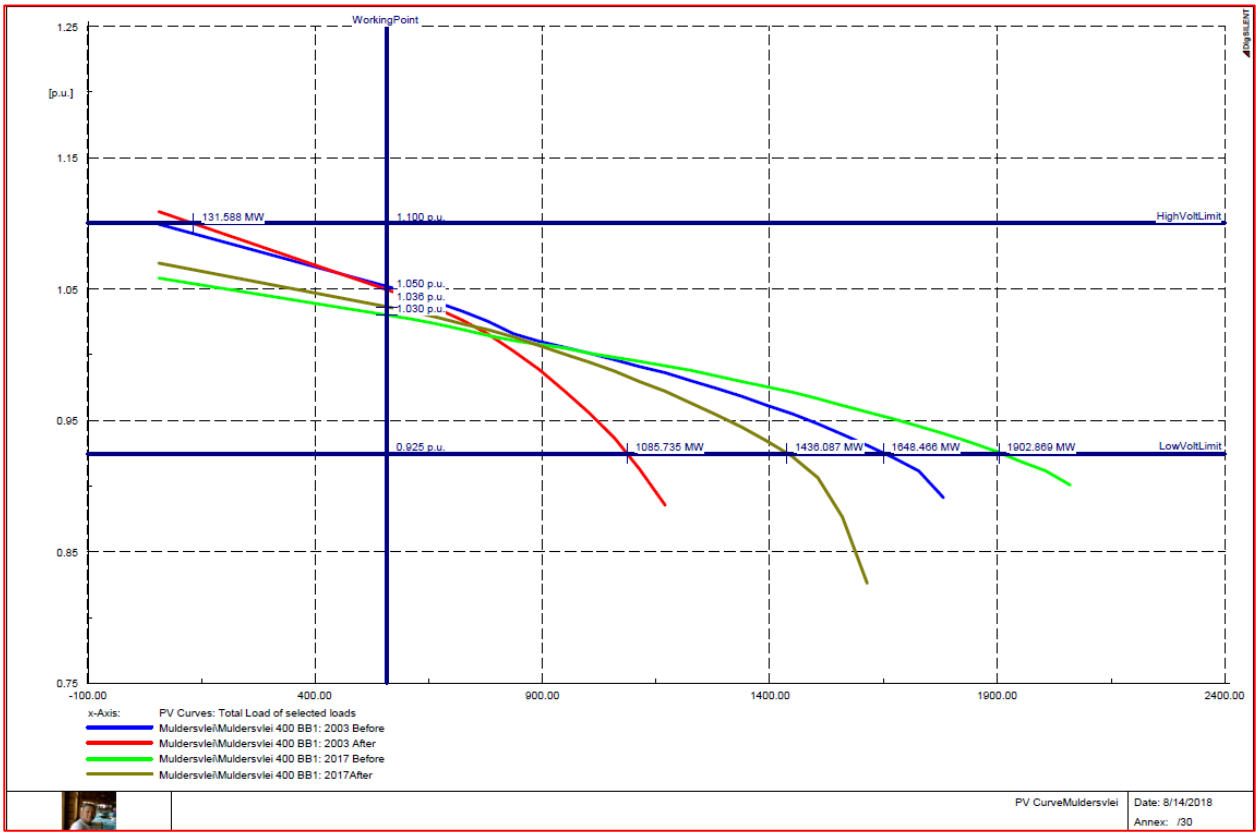

Figure C.10: Muldersvlei 400kV BB PV Curve 2003 vs 2017 plus OneKoebergOut and TwoKoebergOut

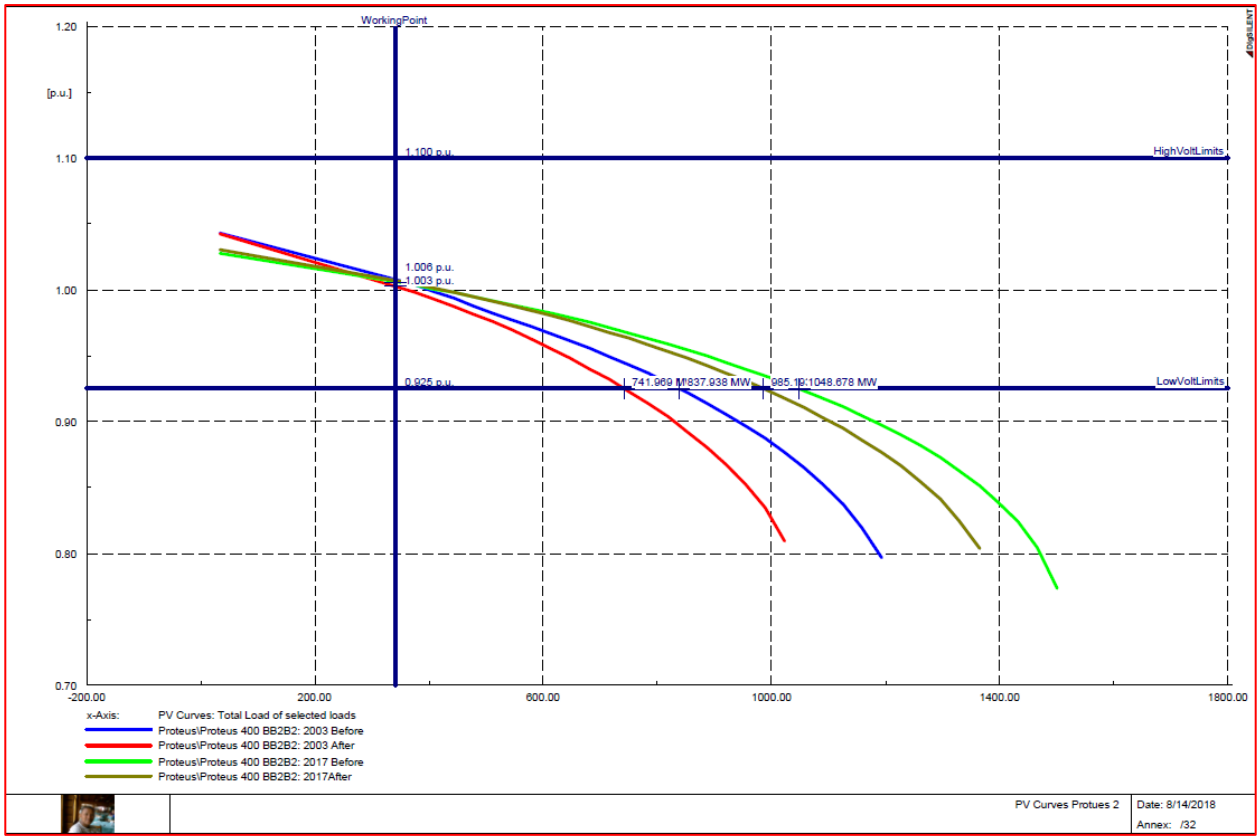

Figure C.12: Proteus 400kV BB PV Curve 2003 vs 2017 plus OneKoebergOut and TwoKoebergOut

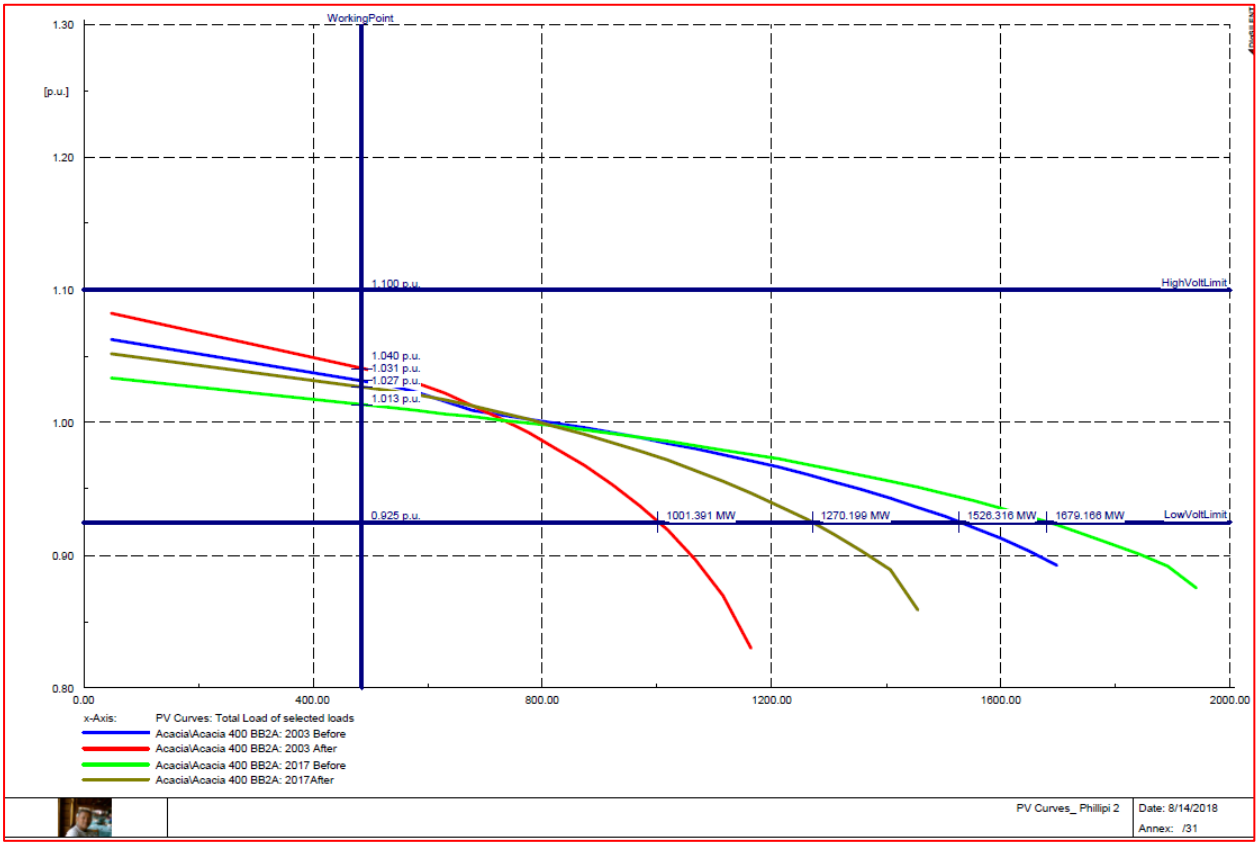

Figure C.11: Phillipi 400kV BB PV Curve 2003 vs 2017 plus OneKoebergOut and TwoKoebergOut

Appendix D. QV Curve Analysis Fundamentals

D1. QV curve analysis theory

For evaluation, the below diagram from [29] is used:

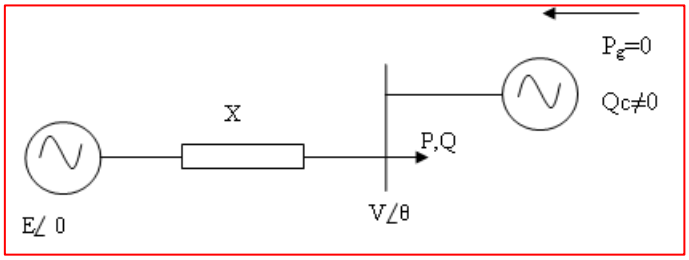

Figure D.1: Circuit used to explain the set up for performing QV curves[29]

From the diagram, the power, reactive and active, are derived as

$$P = -\frac{EV}{X}\sin\theta$$

$$Q - Q_c = \frac{V^2}{X} + \frac{EV}{X}cos\,\theta$$

In the simulation, constant power loads have been considered. Given the voltage (V) and the real power (P) from the above equations, the theta can be calculated. After this, the value Q_c can be determined from the second equation. The plots that are generated are similar to those from [30]

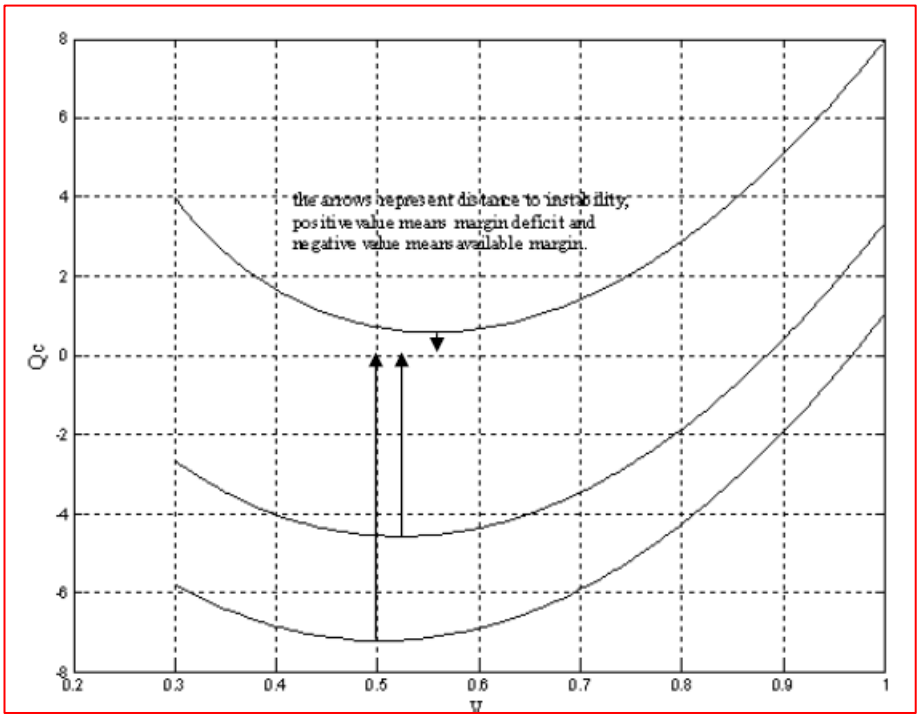

Figure D.2: QV curves produced to determine the amount of reactive power reserved or in deficit for a particular busbar [30]

Interpretation of the curves gives an indication as to what the available margins are before a voltage collapse is imminent. For these curves, the minima present the available reactive margin available before a collapse. In figure D.2, the first curve has a negative margin to the working point; this implies that a reactive support will be needed in this network to maintain a voltage within margins. Curve 2 and 3 indicate a positive margin, thus enough reactive reserve is available in these network areas and the areas are more robust to a voltage collapse [30].

An alternative explanation is given in [31] and is explained by using figure D.3

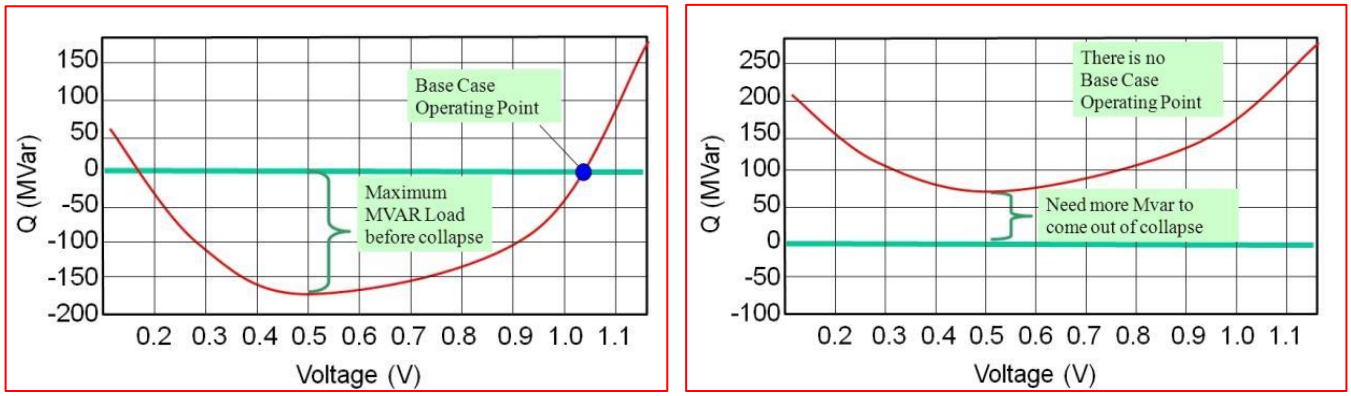

Figure D.3 : Explanation of the QV Curve[31]

A trace down the curve represents a decline in the MVar's that the fictitious static generator that is introduced can produce. The voltage required for this increase in MVar is recorded and is plotted against each other on a curve. A point will be recorded where the MVar value provided by the generator stop increasing. This is the so called critical point after which a voltage collapse is highly probable[31].

D2. QV Curve DigSilent Powerfactory® Script

The QV Curve script that was used requires a starting voltage, stepsize for voltage, and the Maximum Generation Power which relates to the transformer size connected to the bus monitored. A screen shot of the all the input parameters required is shown in figure 9.4. The description of the script as provided by DigSilent Powerfactory® is shown in figured D.4 and D.5

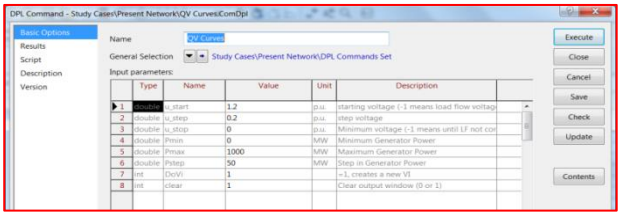

Figure D.4: Input parameters required for initiating of QV curve analysis

```
QV-Curves v1.0

This script calculates QV curves for one busbar and one generator.
A curve is created for every pre-defined active power setpoint of
the selected generator. The resulting graphs are automatically displayed.

 *Use instructions:
-Connect manually a static generator to a busbar.
-Create a DPL selection with the busbar and the static generator.
-In the Input Parameters of the script, set the start voltage, the end voltage
 and the step voltage for which load flow should be calculated.
-Set also the minimum active power, the maximum  active power and step  active
 power for the generator.
-Execute the script. QV curves are now plotted automatically.
-The result file(s) will be over-written following a subsequent
 execution of the script. To keep the results, please move the object(s)
 "*.ElmRes" within the subfolder "Fold" to the folder "Storage" and
 change its name to help you remember which results it contains.

 *Notes:
-The script will use the generator attached to the busbar.
 It will calculate loadflows for a voltage setpoint of
                    usetp = (u_start - N*u_step)
 until the loadflow does not converge any longer or usetp <= 0.
-The voltage setpoint and the reactive power flow of the generator
 are recorded in the Matrix.
-The Matrix will have a list of all QV curves for all selected
 busbar/terminals.
-Additionally, a result file is written for the first busbar/terminal.
```

Figure D.5 : QV script description as provided by DigSilent Powerfactory®

D3. QV curve generated for different critical busbars

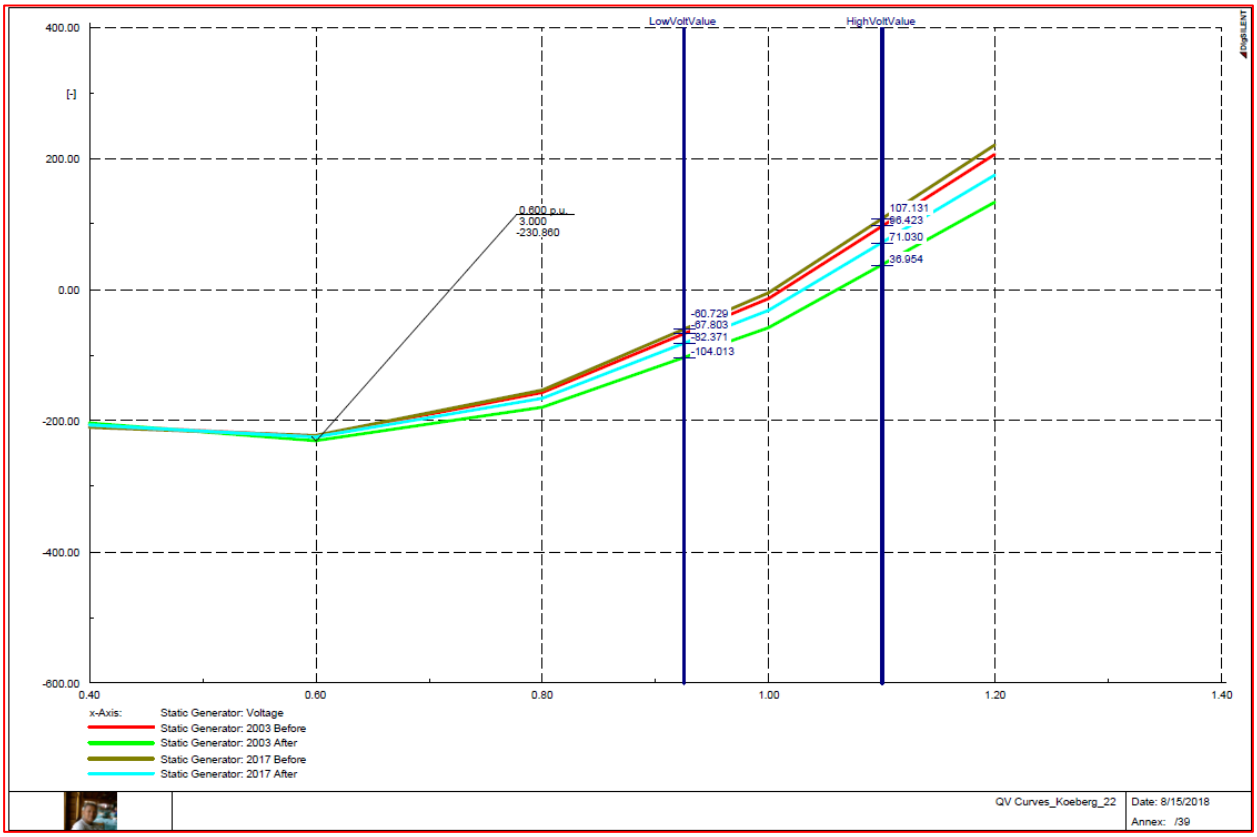

Figure D.7 : Koeberg 400kV BB PQCurve 2003 vs 2017 + OneKoebergOut and TwoKoebergOut

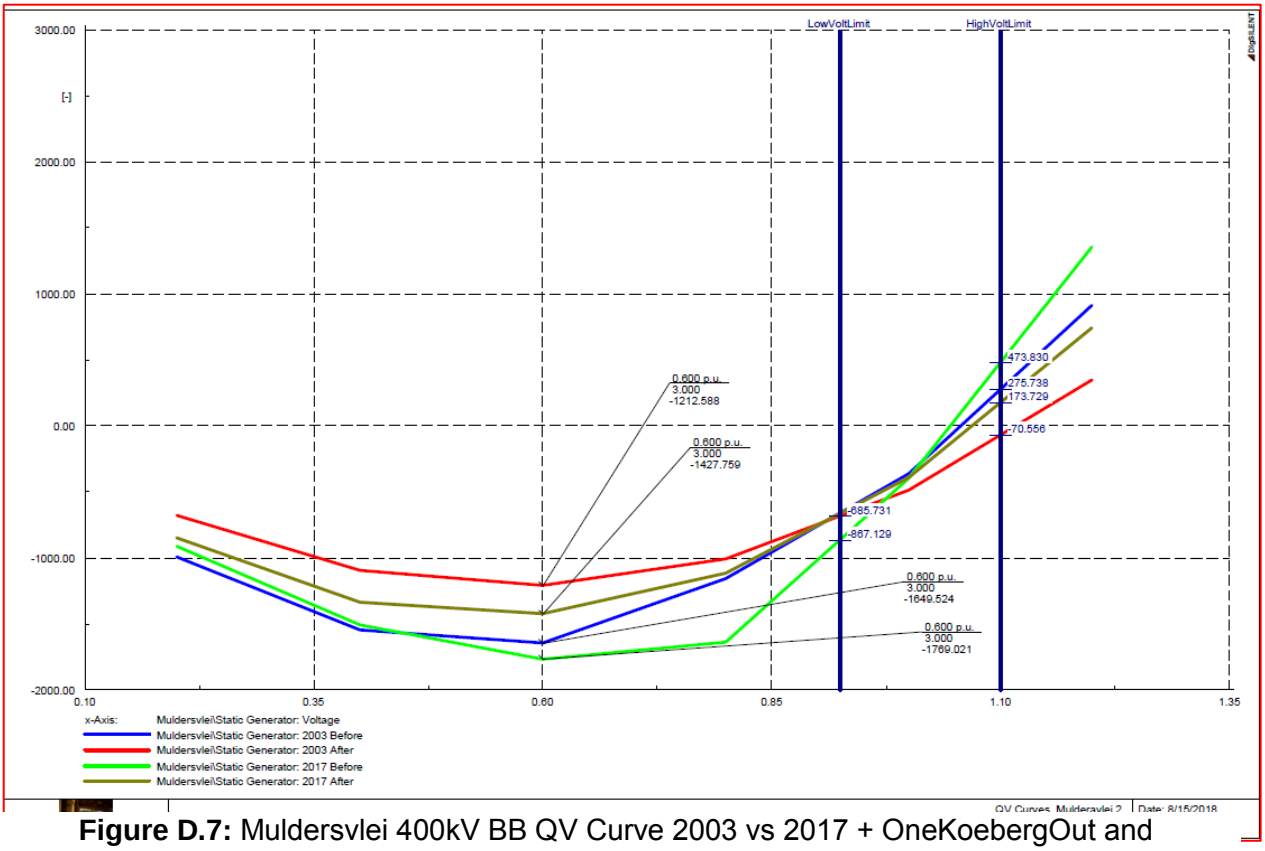

Figure D.7: Muldersvlei 400kV BB QV Curve 2003 vs 2017 + OneKoebergOut and TwoKoebergOut

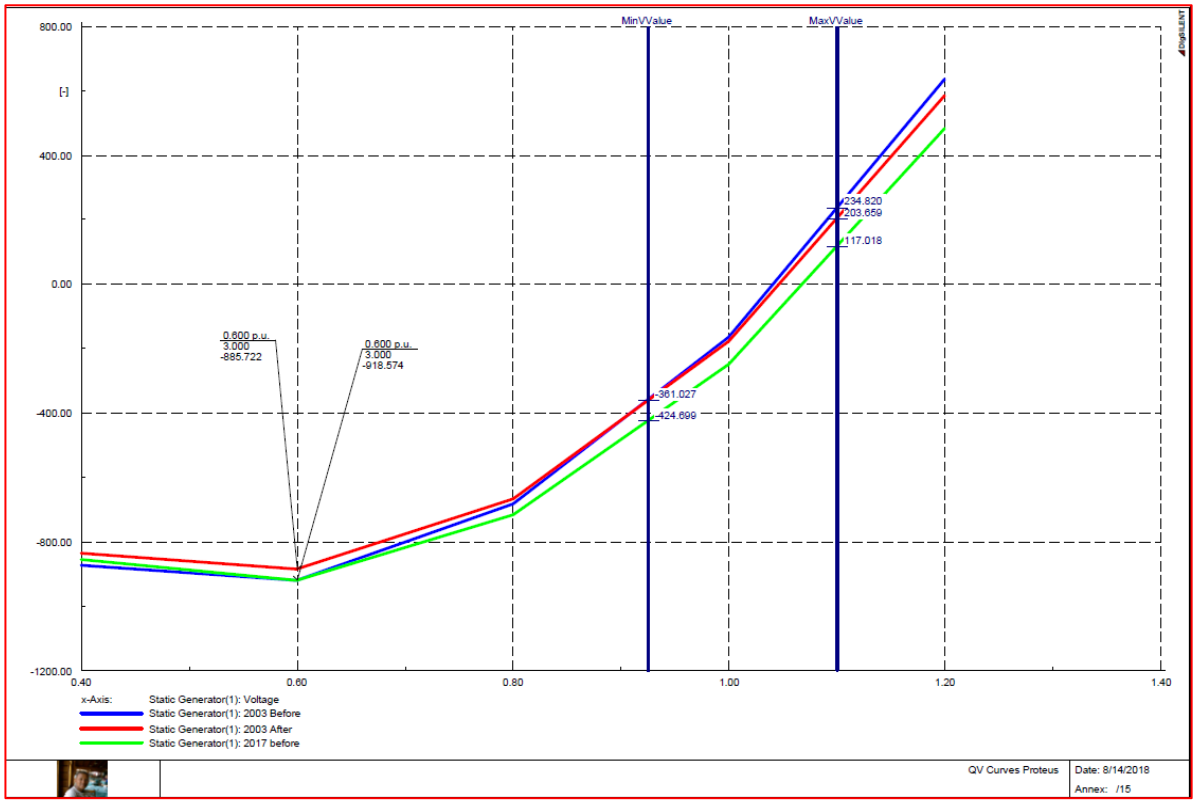

Figure D.9 : Proteus 400kV BB QV Curve 2003 vs 2017 + OneKoebergOut and TwoKoebergOut

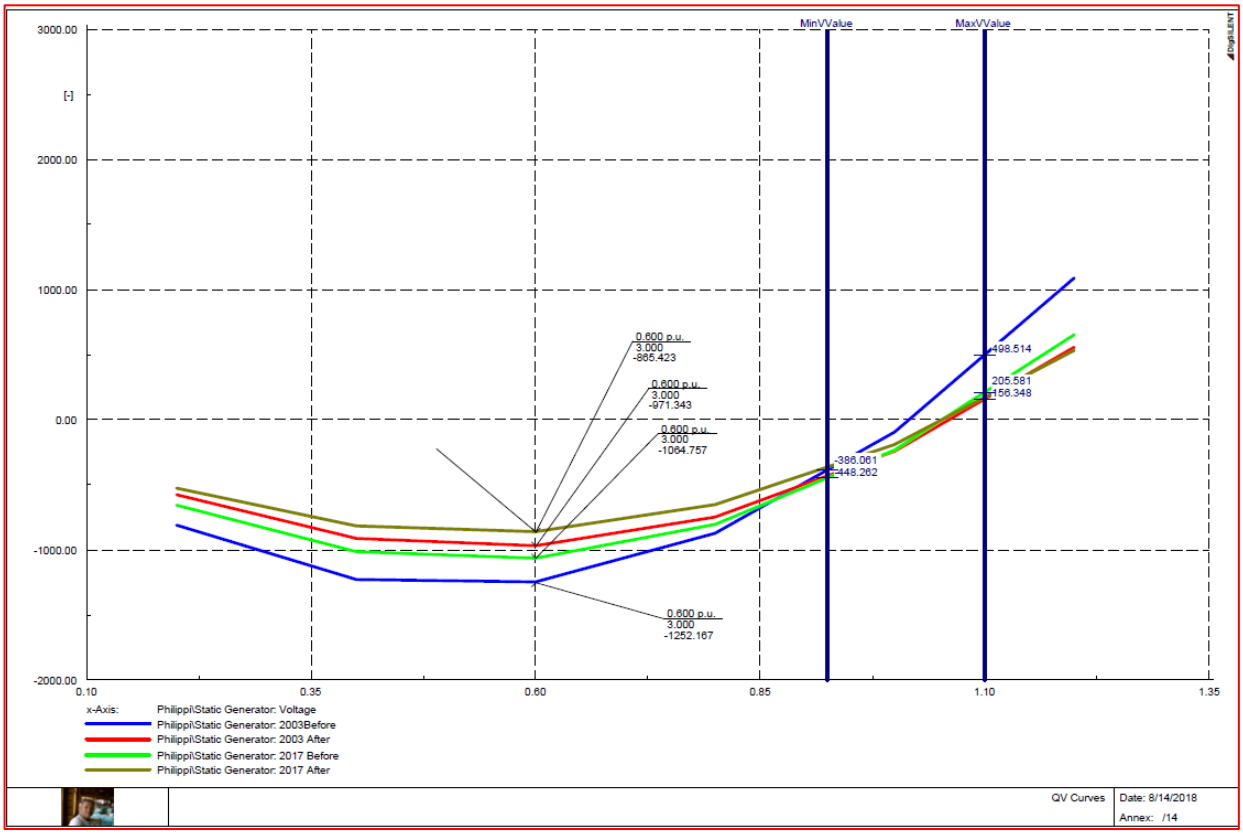

Figure D.9 : Phillipi 400kV BB QV Curve 2003 vs 2017 + OneKoebergOut and TwoKoebergOut

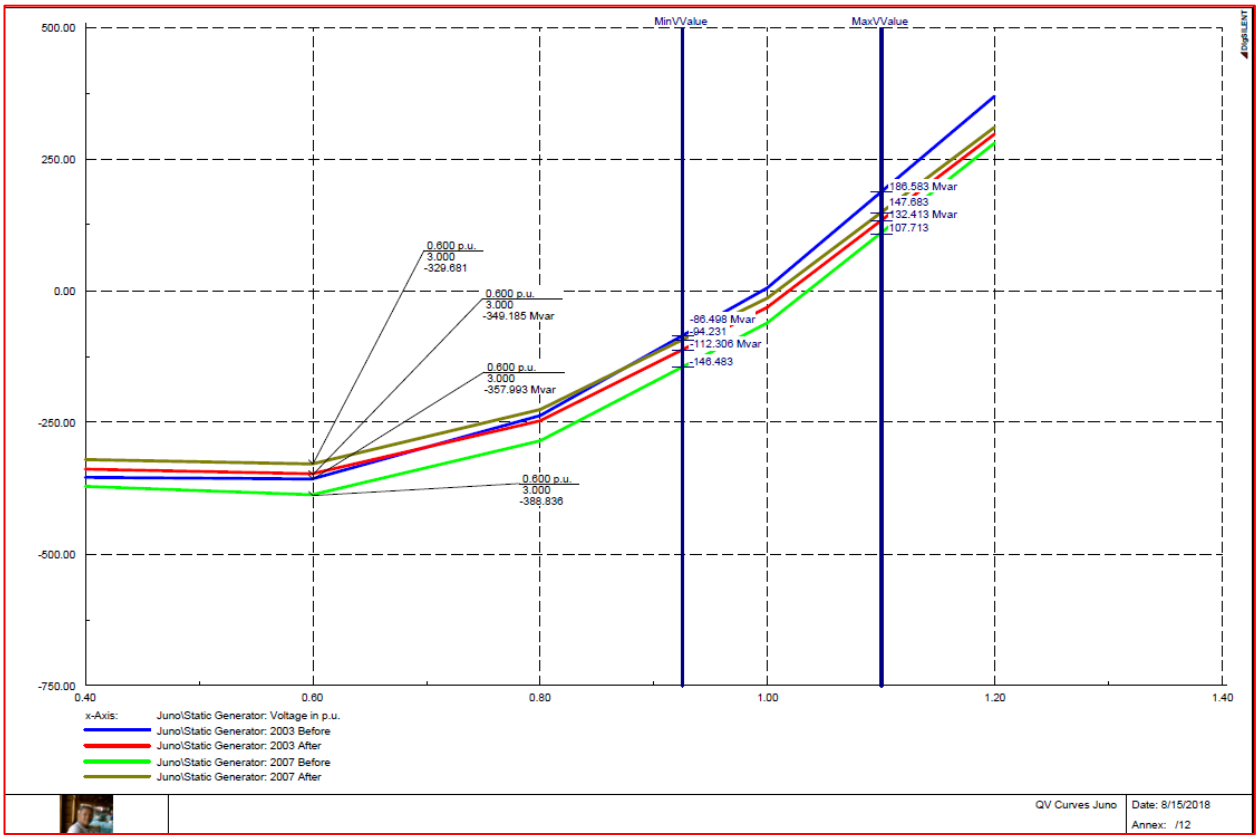

Figure D.10 : Juno 400kV BB QV Curve 2003 vs 2017 + OneKoebergOut and TwoKoebergOut

Appendix E. Configuration of Dynamic Events

E1. Load Profile configuration

Different load profiles were identified as Koeberg 132kV load, Muldersvlei 132kV load, Proteus 132kV load, Phillipi 132kV load, and

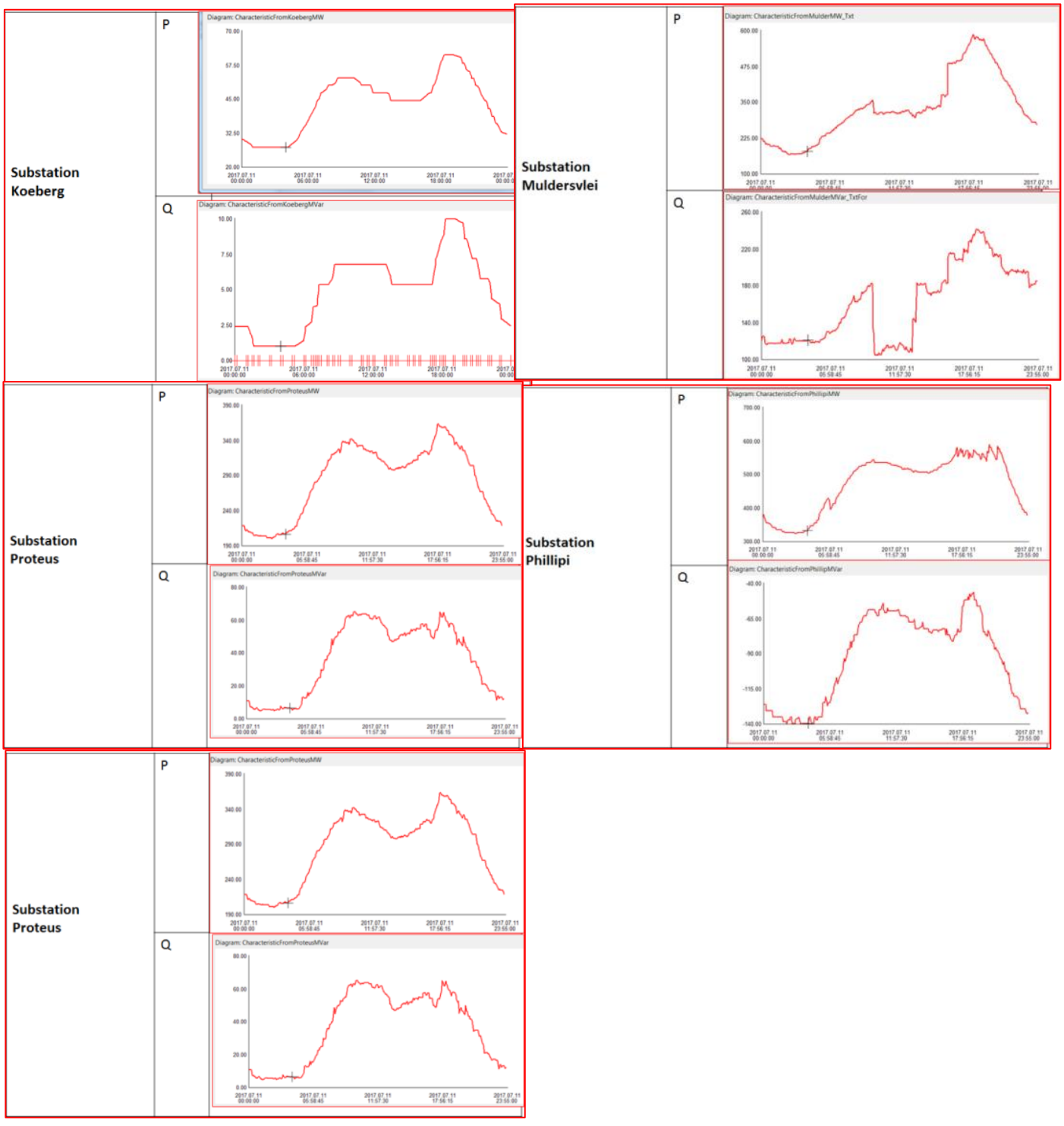

Figure E.1: MW and MVar Load Profiles programmed into DigSilent Powerfactory

Appendix F. Configuration of Dynamic Events

F1. Simulation Sequence – RMS/EMT Simulation

Name	Time	Object	Out of Service	Object modified	Object modified by
KoebergUnit2On Maintanance	0	Koeberg Gen2	1	2018/08/15 22:45	BoesakD
Outage Event	0	Koeberg Gen1	1	2018/08/15 22:45	BoesakD
KoebergUnit1Trip ped04h21	20	Koeberg Gen1 LV	0	2018/08/15 23:14	BoesakD
Load Event	22		0	2018/08/15 23:14	BoesakD
PalmietGen1TripU nderFrequency	23	Palmiet Gen1 LV	0	2018/08/15 23:14	BoesakD
PalmietGen2TripU nderFrequency	23	Palmiet Gen2 LV	0	2018/08/15 23:14	BoesakD
PalmietGen1InGe nMode-06h24	8640	Palmiet Gen1	0	2018/08/15 22:43	BoesakD
PalmietGen2InGe nMode-07h00	9540	Palmiet Gen2	0	2018/08/15 22:45	BoesakD
PalmietGen1OfGe nMode-07h25	11040	Palmiet Gen1	0	2018/08/15 22:46	BoesakD
PalmietGen2OfGe nMode-10h57	23760	Palmiet Gen2	0	2018/08/15 22:47	BoesakD

F2. Simulation Sequence – Quasi-dynamic simulation

Name	Element	Out of Service	Object modified	Object modified by
	ElmSym,ElmXnet,Elm Genstat,ElmAsm,ElmP vsys,ElmVsc*,ElmRec *			
PalmietGen1InGenMo de-06h24	Palmiet Gen1	1	2018/08/15 21:21	BoesakD
PalmietGen2InGenMo de-07h00	Palmiet Gen2	1	2018/08/15 21:21	BoesakD
Load Event		1	2018/08/15 21:21	BoesakD
KoebergUnit2OnMaint anance	Koeberg Gen2	0	2018/08/15 19:32	BoesakD
Outage Event	Koeberg Gen1	1	2018/08/15 21:21	BoesakD

PalmietGen1OfGenMode-07h25	Palmiet Gen1	1	2018/08/15 21:21	BoesakD
PalmietGen2OfGenMode-10h57	Palmiet Gen2	1	2018/08/15 21:21	BoesakD
KoebergUnit1Tripped04h21	Koeberg Gen1 LV	0	2018/08/15 20:40	BoesakD
PalmietGen1TripUnderFrequency	Palmiet Gen1 LV	1	2018/08/15 21:21	BoesakD
PalmietGen2TripUnderFrequency	Palmiet Gen2 LV	1	2018/08/15 21:21	BoesakD

F1. Extra test performed to calibrate quasi-dynamic simulations

Case 2: Perform Quasi Dynamic Simulation (run time 1 day) — Normal network configuration with 2 x Koeberg units in service and one unit in service — 2003 vs Perform quasi-dynamic simulation (run time 1 day) with events as per event on 15 October 2003, and as if the same events would have occurred in 2017

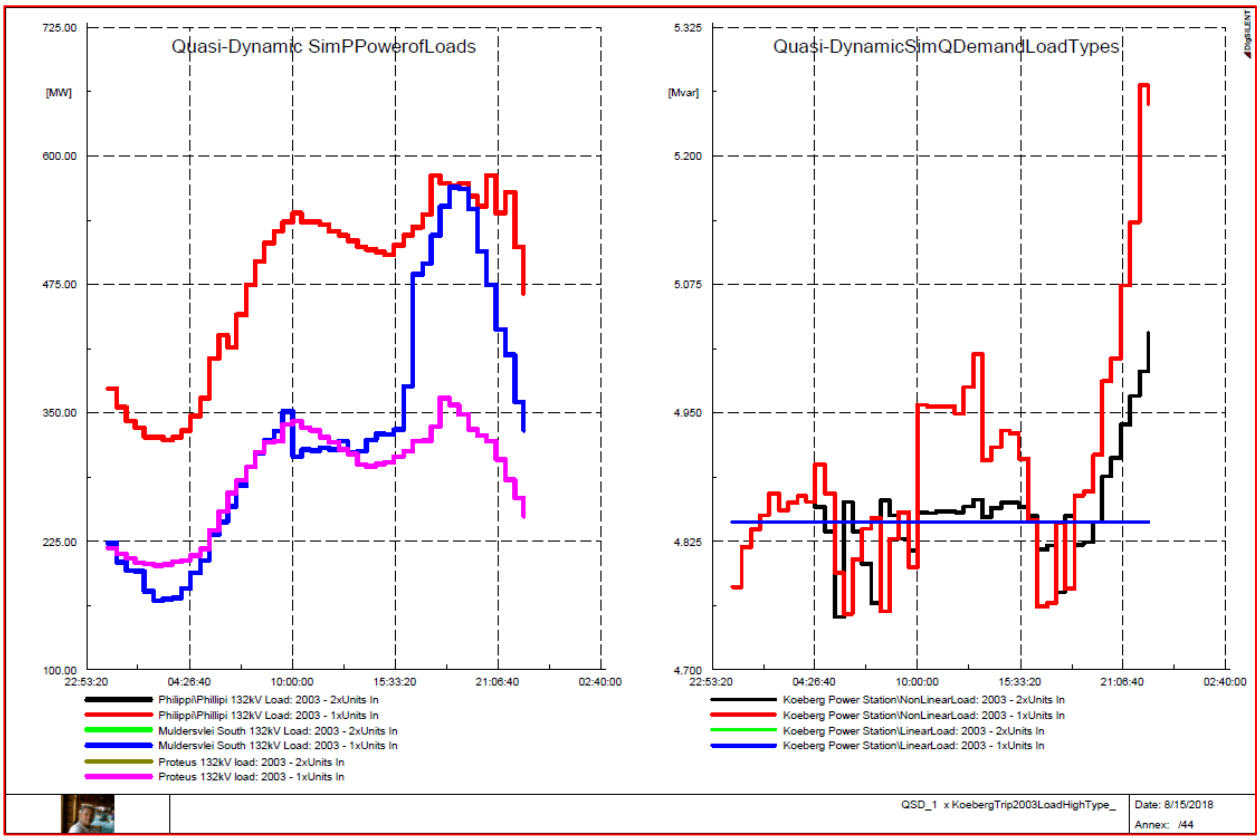

Figure F.1: P and Q of Load Types for Quasi - dynamic Study - Normal and N-1 Koeberg – 2003 Only

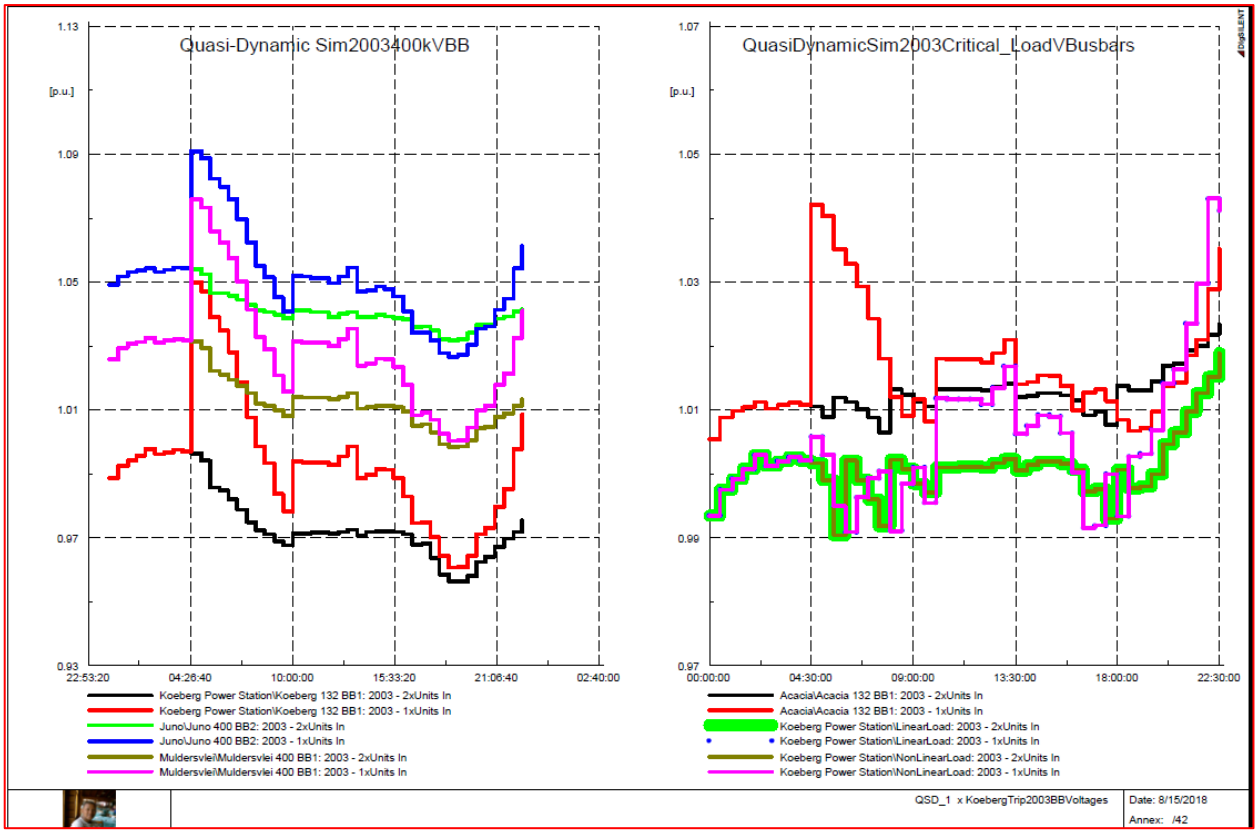

Figure F.2: Voltage at critical busbars response — normal and n-1 Koeberg quasi-dynamic studies – 2003 only

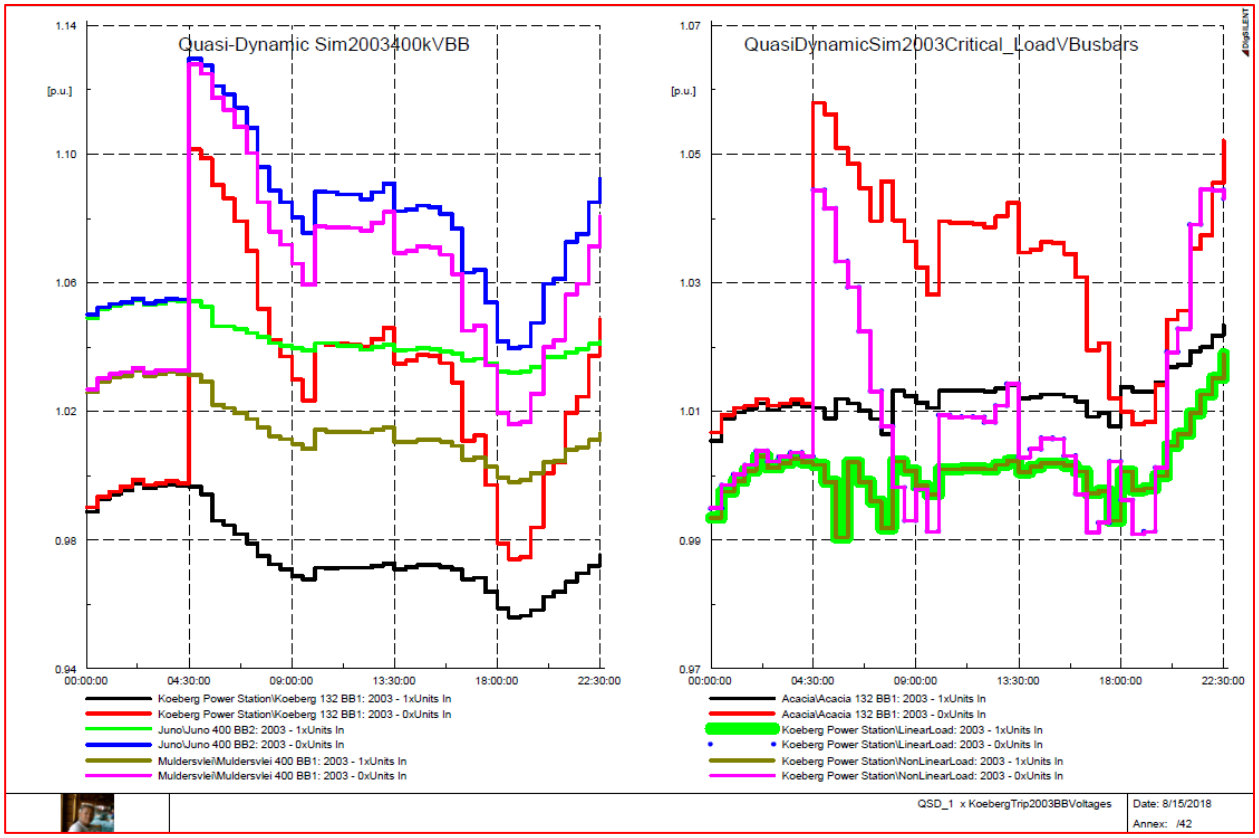

Figure F.3: Voltage at critical busbars response — N-1 and N-2 Koeberg quasi-dynamic studies

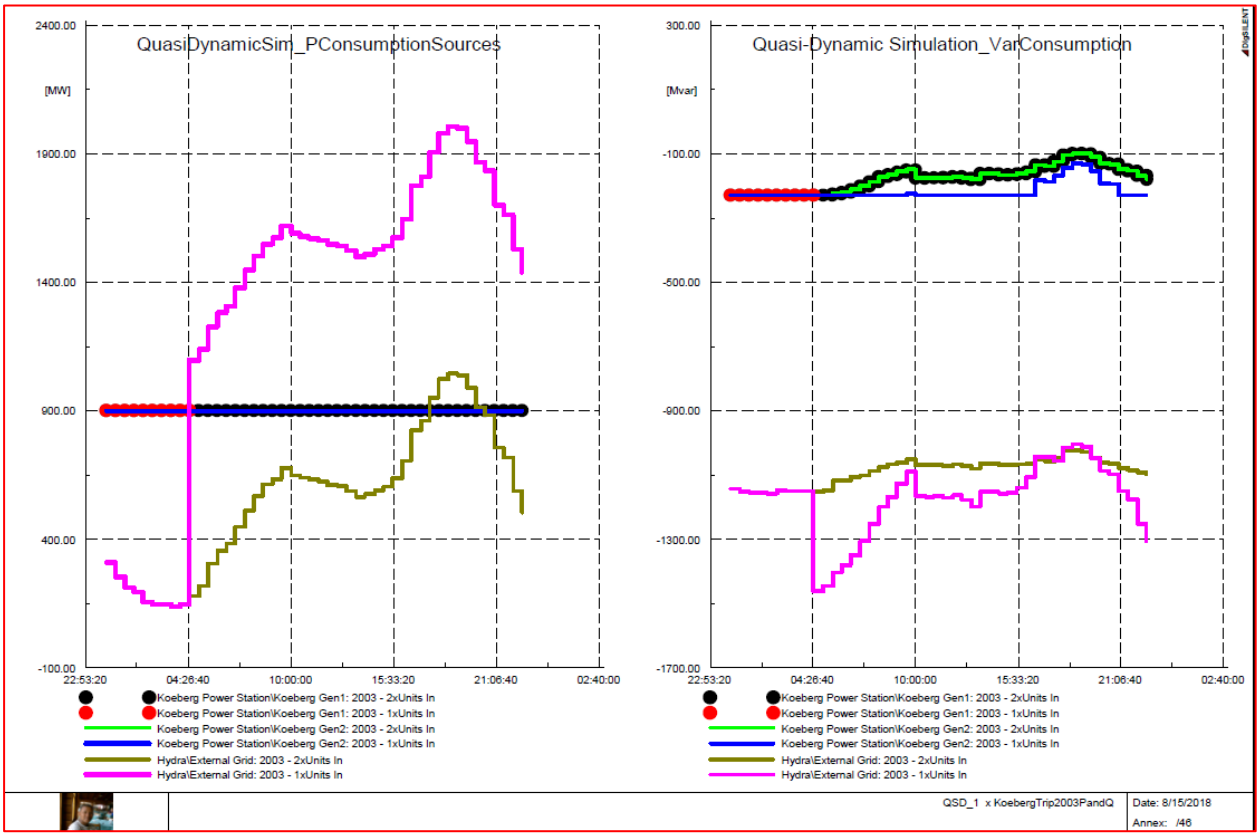

Figure F.4: Sources response – Normal and N-1 Koeberg quasi-dynamic studies – 2003 only

Appendix G. Load Characteristic Modelling

G4. Modelling of Linear and Non-linear load

The two types of loads that were modelled in this study are the linear load (constant power) and the non–linear load (constant impedance). To demonstrate the difference in response to a trip at the HV busbar, RMS/EMT was simulated using Digsilent PowerFactory® software. The model, together with the resultant real and reactive power curves are shown below in figure G.1 to G.2 and the results discussed in table 2.7:

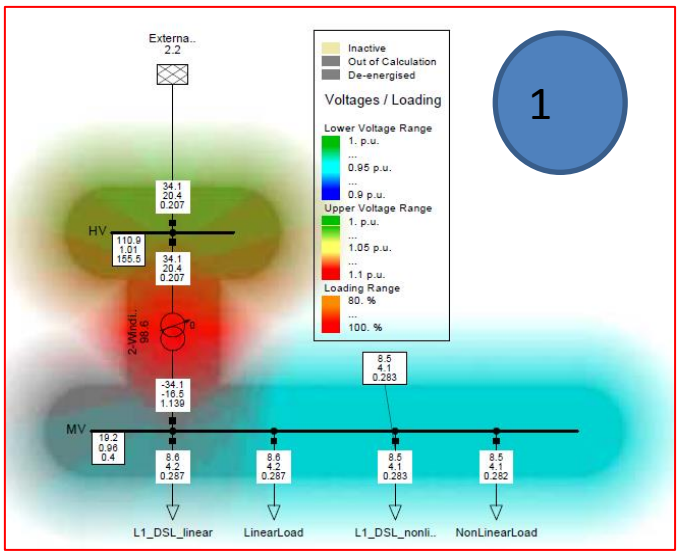

Figure G.1: Sources response – Normal and N-1 Koeberg quasi-dynamic studies – 2003 only

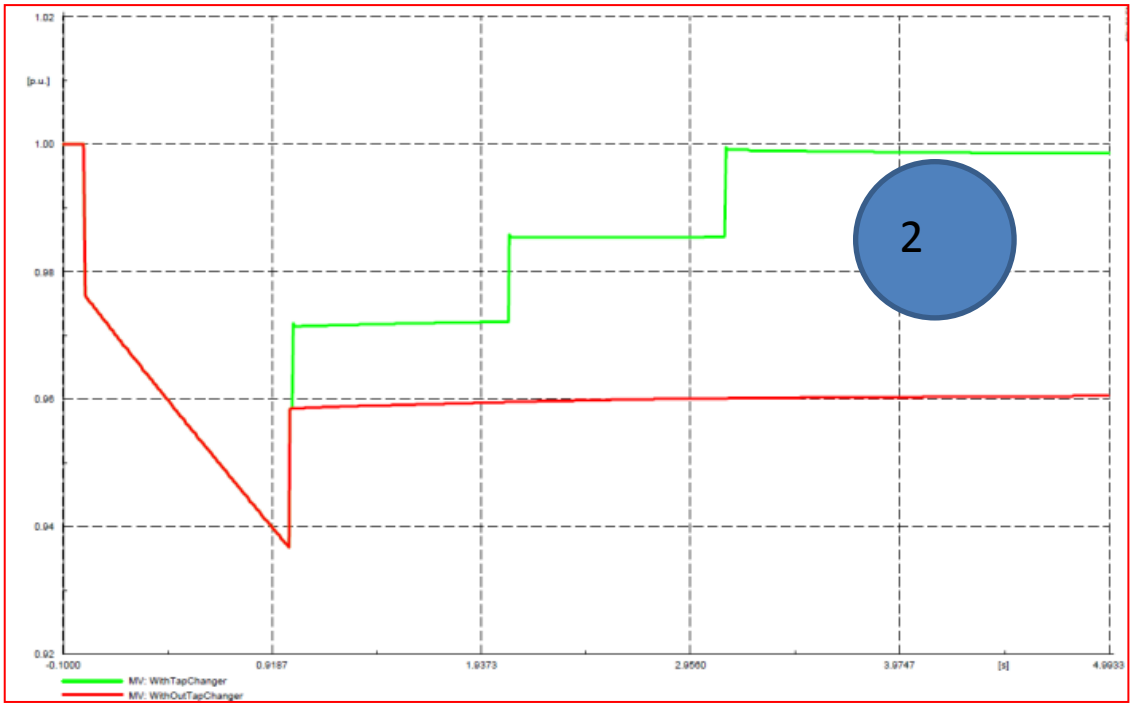

Figure G.2: Sources response – Normal and N-1 Koeberg quasi-dynamic studies – 2003 only

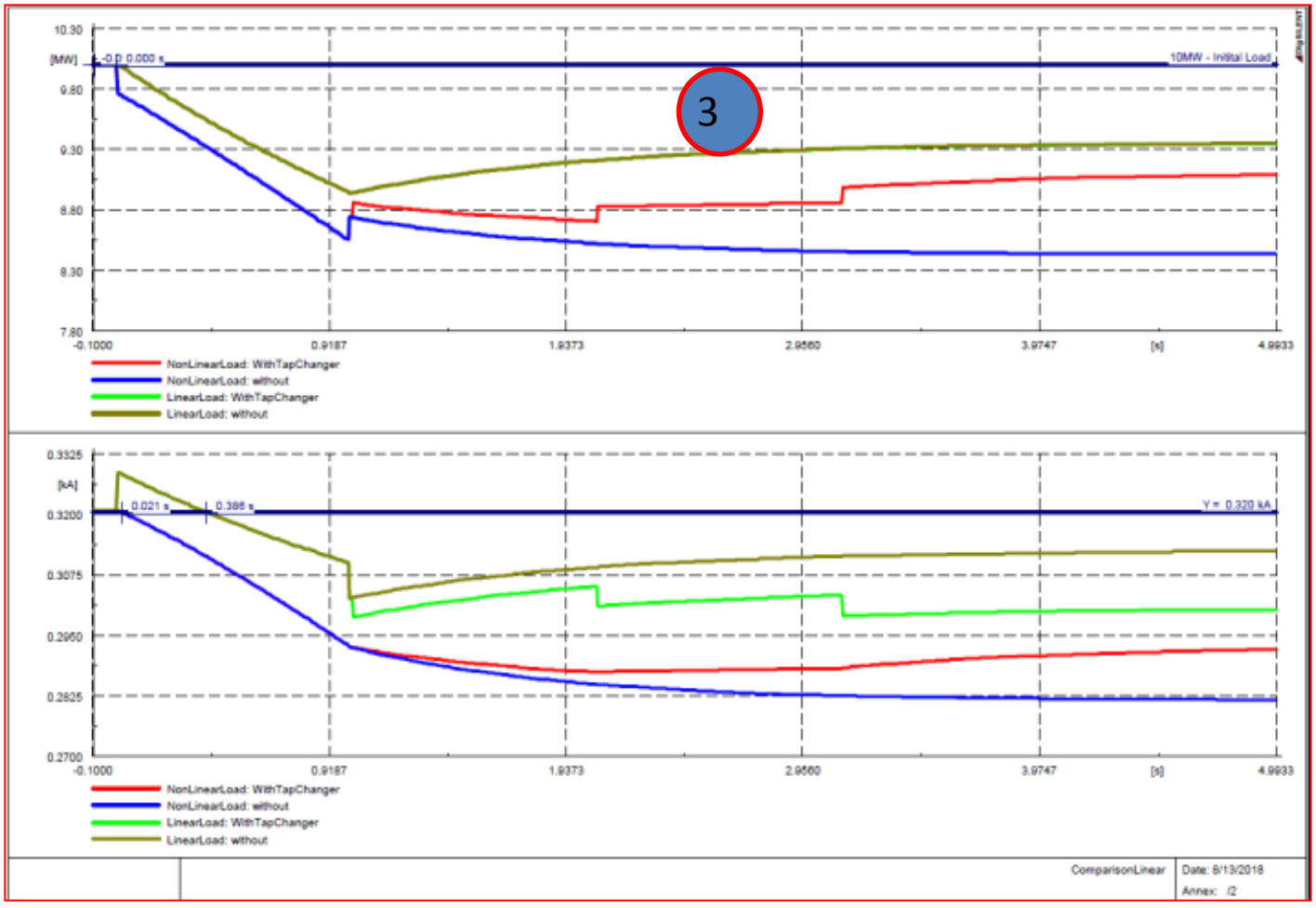

Figure G.3: Sources response – Normal and N-1 Koeberg quasi-dynamic studies – 2003 only

Based on figure G.1 – G.3, the results are discussed in table G.1.

Table G.1: Observation for different load types - constant power vs constant impedances

Figure	Presentation	No	Result Explained
1	Network overview showing linear and non-linear loads together with the transformer with under load tap changing activated (or not) depending on what is to be demonstrated	1	All load is modelled with P=10MW and 0.9 power factor. Given the load, the transformer is loaded to 34.1MW and 20.4 MVar
		2	The heat map shows that the max voltage is 1.1pu
2	MV bus bar voltage with and without tap changing	1	Without tap changing, the bus bar voltage on the MV recovers to 0.96pu
		2	With tap changing, the voltage recovers back to the initial value of 1.0pu after 3 seconds
3	The derived graphics are for the power consumption and the current for the two load types (over a time period of 5 seconds) in order to show the effect of the load being of a constant impedance (non-linear) and constant power (linear) nature	1	With tap changing, the recovery power is the same for the constant power load if one considers that tap changing occurs or not tap for both load types
		2	For the linear load, the recovery power is higher when no tap changing is present
		3	Without tap changing, the current requirement for the linear load (constant power) device is high. When the voltage drops in order to maintain the power level, this creates a worst-case scenario and requires the system imbalance to be evaluated
		4	The current requirement for constant power and constant impedance loads increase when the tap changer is not present. This again creates a worst-case analysis for dynamic studies, i.e. no tap changing present